

**PRIMARY SENSORY PROCESSING
OF VISUAL AND OLFACTORY SIGNALS
IN THE BUMBLEBEE BRAIN**

**DISSERTATION
MARCEL MERTES**

**FAKULTÄT FÜR BIOLOGIE
UNIVERSITÄT BIELEFELD**

BIELEFELD, AUGUST 2013

PRIMARY SENSORY PROCESSING
OF VISUAL AND OLFACTORY SIGNALS
IN THE BUMBLEBEE BRAIN

DISSERTATION
MARCEL MERTES

TABLE OF CONTENTS

| | |
|-----------|---|
| 9 | SUMMARY |
| 11 | GENERAL INTRODUCTION AND BACKGROUND OF THE THESIS |
| 13 | Central questions addressed in the dissertation |
| 15 | Basic navigation concepts in Hymenoptera |
| 16 | Motion vision as important source of spatial information in the context of navigation |
| 17 | Project 1: Matching saccadic fine structure between honeybees and bumblebees during navigation behavior |
| 19 | The optic lobe of the insect brain |
| 20 | Focus of interest for spatial vision in local navigation – the lobula |
| 21 | Project 2: Does the bumblebee motion vision pathway convey landmark information during a navigation task? |
| 23 | Odour processing in the hymenopteran olfactory pathway |
| 25 | Project 3: Odour coding in the bumblebee antennal lobe |
| 27 | Final considerations |
| 28 | References |

1

BUMBLEBEE HOMING: THE FINE STRUCTURE OF HEAD TURNING MOVEMENTS

| | |
|-----------|--|
| 37 | Abstract |
| 37 | Introduction |
| 39 | Material and Methods |
| 39 | General procedure |
| 40 | Experimental setup |
| 40 | Recording sessions |
| 40 | Data analysis |
| 41 | Results |
| 48 | Discussion |
| 49 | Which sensory cues do bees exploit to orient their head and how are head and body movements coordinated? |
| 49 | What is the functional advantage of the stereotypical eye movements? |
| 49 | What is the impact of morphological differences between species and within species on vision and flight performance? |
| 50 | Reasons for a partial decoupling of head and body orientation |
| 51 | Acknowledgements |
| 51 | References |

2

VISUAL MOTION-SENSITIVE NEURONS IN THE BUMBLEBEE BRAIN CONVEY INFORMATION ABOUT THE PRESENCE OF LANDMARKS DURING A NAVIGATIONAL TASK

| | |
|----|---|
| 57 | Abstract |
| 58 | Introduction |
| 59 | Material and Methods |
| 59 | Behavioural experiments |
| 59 | Reconstruction of natural optic flow |
| 60 | Electrophysiological experiments |
| 61 | Stimulus presentation and data acquisition |
| 62 | Data analysis |
| 62 | Results |
| 62 | Flight behavior of bumblebees |
| 64 | Are the landmarks represented in the neuronal response? |
| 66 | Neuronal responses to camouflaged landmarks |
| 70 | Texture effects on neuronal responses during saccadic flight phases |
| 71 | Discussion |
| 73 | Acknowledgements |
| 74 | References |

3

STRUCTURE AND ODOUR CODING PROPERTIES IN THE BUMBLEBEE ANTENNAL LOBE

| | |
|----|---|
| 79 | Abstract |
| 79 | Introduction |
| 81 | Material and Methods |
| 81 | Bumblebee preparation |
| 81 | Calcium imaging |
| 82 | Odour presentation |
| 82 | Anatomical staining |
| 82 | Data processing and analyses |
| 83 | Statistical analysis |
| 84 | Results |
| 84 | Antennal lobe anatomy |
| 87 | Intensity of odour-induced responses |
| 89 | Similarity among odour response maps |
| 93 | Comparison of honeybee and bumblebee data |

| | |
|----|---|
| 95 | Discussion |
| 95 | Body size differences within bumblebees and comparison to honeybees |
| 95 | Antennal lobe morphology |
| 97 | Functional comparison of the glomerular activity |
| 97 | Possible pheromone effects of odour stimuli |
| 98 | Conclusion |
| 98 | Acknowledgements |
| 99 | References |

105 **ERKLÄRUNG**

107 **DANKSAGUNG**

SUMMARY

Since decades honeybees are being used as an insect model system for answering scientific questions in a variety of areas. This is due to their enormous behavioural repertoire paired with their learning capabilities. Similar learning capabilities are also evident in bumblebees that are closely related to honeybees. As honeybees, they are central place foragers that commute between a reliable food source and their nest and, therefore, need to remember particular facets of their environment to reliably find back to these places.

Via their flight style that consists of fast head and body rotations (saccades) interspersed with flight segments of almost no rotational movements of the head (intersaccades) it is possible to acquire distance information about objects in the environment. Depending on the structure of the environment bumblebees as well as honeybees can use these objects as landmarks to guide their way between the nest and a particular food source. Landmark learning as a visual task depends of course on the visual input perceived by the animal's eyes. As this visual input rapidly changes during head saccades, we recorded in my first project bumblebees with high-speed cameras in an indoor flight arena, while they were solving a navigation task that required them to orient according to landmarks. First of all we tracked head orientation during whole flight periods that served to learn the spatial arrangement of the landmarks. Like this we acquired detailed data on the fine structure of their head saccades that shape the visual input they perceive. Head-saccades of bumblebees exhibit a consistent relationship between their duration, peak velocity and amplitude resembling the human so-called "saccadic main sequence" in its main characteristics. We also found the bumblebees' saccadic sequence to be highly stereotyped, similar to many other animals. This hints at a common principle of reliably reducing the time during which the eye is moved by fast and precise motor control.

In my first project I tested bumblebees with salient landmarks in front of a background covered with a random-dot pattern. In a previous study, honeybees were trained with the same landmark arrangement and were additionally tested using landmarks that were camouflaged against the background. As the pattern of the landmark textures did not seem to affect their performance in finding the goal location, it had been assumed that the way they acquire information about the spatial relationship between objects is independent of the objects texture.

Our aim for the second project of my dissertation was therefore to record the activity of motion sensitive neurons in the bumblebee to analyse in how far object information is contained in a navigation-related visual stimulus movie. Also we wanted to clarify, if object texture is represented by the neural responses. As recording from neurons in free-flying bumblebees is not possible, we used one of the recorded bumblebee trajectories to reconstruct a three-dimensional flight path including data on the head orientation. We therefore could reconstruct ego-perspective movies of a bumblebee

while solving a navigational task. These movies were presented to motion-sensitive neurons in the bumblebee lobula. We found for two different classes of neurons that object information was contained in the neuronal response traces. Furthermore, during the intersaccadic parts of flight the object's texture did not change the general response profile of these neurons, which nicely matches the behavioural findings. However, slight changes in the response profiles acquired for the saccadic parts of flight might allow to extract texture information from these neurons at later processing stages.

In the final project of my dissertation I switched from exploring coding of visual information to the coding of olfactory signals. For honeybees and bumblebees olfaction is approximately equally important for their behaviour as their vision sense. But whereas there is a solid knowledge base on honeybee olfaction with detailed studies on the single stages of olfactory information processing this knowledge was missing for the bumblebee. In the first step we conducted staining experiments and confocal microscopy to identify input tracts conveying information from the antennae to the first processing stage of olfactory information – the antennal lobe (AL). Using three-dimensional reconstruction of the AL we could further elucidate typical numbers of single spheroidal shaped subunits of the AL, which are called glomeruli. Odour molecules that the bumblebee perceives induce typical activation patterns characteristic of particular odours. By retrogradely staining the output tracts that connect the AL to higher order processing stages with a calcium indicator, we were capable of recording the odour-dependent activation patterns of the AL glomeruli and to describe their basic coding principles. Similarly as in honeybees, we could show that the odours' carbon chain length as well as their functional groups are dimensions that the antennal lobe glomeruli are coding in their spatial response pattern. Applying correlation methods underlined the strong similarity of the glomerular activity pattern between honeybees and bumblebees.

GENERAL INTRODUCTION AND BACKGROUND OF THE THESIS

In history, only three scientist doing genuine behavioural research on animals have been awarded with the Nobelprize: Konrad Lorenz, Nikolaas Tinbergen and Karl von Frisch, who influenced science with their work beginning in the first half of the 20th century. They all were pioneers in the field behavioural research, which has later on become popular under the term Ethology. In contrast to most other scientists they performed their experiments mostly under the normal living conditions of the animals they were investigating. This was in contrast to the majority of behavioural scientists, who just worked with their animals in the lab to be able to control the experimental conditions much better than is possible under the very complex natural conditions. Another reason was also to be able to influence individual parameters to understand specific mechanisms underlying behaviour. A side effect of this approach was, of course, the very artificial conditions that could also result in animal behaviour far away from their natural repertoire. The notion to look at the animals' behaviour in their natural environment and to perform experiments with the animals behaving as naturally as possible led to large achievements in behavioural research and laid an important part of the foundations of the work that is currently done in behavioural and, partly neural science.

Of those three scientists two strongly influenced my own field of research: Nikolaas Tinbergen being a pioneer in insect visual learning (Tinbergen, 1951; Graham, 2010) and Karl von Frisch. The latter did intensive research on honeybees (*Apis mellifera*) starting with behavioural experiments on their different sensory modalities to later on publishing his ground-breaking studies on their communication skills (von Frisch, 1967). Von Frisch's award-winning study however was that he could show that honeybees are able to communicate direction and distance of valuable food sources with their movement patterns so that the other bees will eventually also be able to forage at the indicated direction. As I describe this very elaborate behaviour, you get a glimpse on the honeybees' extremely rich and also complex behavioural repertoire that allows for testing a large variety of hypotheses in different fields of research making them an excellent animal for behavioural analysis.

Since these early days of modern science the honeybee has therefore been a key model organism for studying a wide range of behaviours and the underlying neural mechanisms resulting in an enormous database on honeybees. Despite this, I decided not to work on the honeybee to address my research questions, but to work on the closely related bumblebee (Michener and Grimaldi, 1988; Schultz et al., 2001; Ramírez et al., 2010), *Bombus terrestris*, that shows a very similar behavioural repertoire, as I will indicate later. In the following, I will introduce major concepts of what is known for honeybees in the research areas of motion vision, navigation, and olfaction, as these are the topics on which I focussed my research in the course of my PhD project. Based on this, I will refer to similarities or dissimilarities between honeybee and bumblebee as

far as it is relevant for the conceptual framework for my own research. Consequently, this comparison will also be a part of the three main chapters of my thesis to indicate similarities and possible differences on the behavioural level, but also on the level of the neuronal substrate linked to their behaviour.

Before starting to describe honeybee and bumblebee behaviour, I should state the reason, as to why I started working on an animal like the bumblebee, although the honeybee is already a model organism for such a long time. The reason is, that there are few practical disadvantages in doing research with honeybees, which can be avoided. Since honeybees are normally kept in outdoor hives, the animals need to willingly come out of their hive for the researcher to be able to do any experiments with them. For the honeybees to forage the weather conditions need to be relatively dry - as they don't fly during rain - and also warm enough for the foragers to be able to keep their body core temperature at a sufficiently high level allowing constant flight also on quite cold days. This minimum outside temperature is estimated to be around 7 °C (von Frisch, 1977). Consequently it is not possible to work with honeybees during wintertime, when all individuals of the hive that can consist of up to 10.000 single honeybees is gathering close to each other to loose not too much warmth and to keep their queen alive (von Frisch, 1977). And even if they are foraging during the warmer parts of the year, it takes a lot of effort to motivate honeybees to participate in behavioural experiments due to the many flowers in full blossom. They will mostly prefer foraging on the natural flowers compared to artificial food sources like sugar water solution as a replacement for natural nectar, which makes outdoor experiments rather attractive only during the late summer months. For these reasons honeybee behavioural training in outdoor environment is restricted to short periods of the year.

An alternative to the honeybee has emerged on the scientific landscape in recent years, with which it is possible to solve most of these environmental issues, and that possesses, at least as far as is known, a very similar behavioural repertoire: the bumblebee. Since the late 1980's it is possible to order single hives of bumblebees that are being bred throughout the year to supply greenhouses (Heinrich, 2004). As bumblebee colonies are much smaller (up to 500 individuals) (Goulson, 2010), they can be kept indoors, which allows behavioural experiments that are independent of weather conditions and the time of the year. This is a great advantage, if behavioural experiments can be performed while maintaining the natural behaviour of the animals' as is the case for bumblebees.

Furthermore, bumblebees are larger in size, which positively affects the robustness of single animals during physiological experiments. Additionally single individuals can survive without feeding for longer periods of time without starving to death. Also they can generally better cope with invasive treatments during an experiment, which is highly important for electrophysiological or imaging experiments as I performed during my PhD project.

Central questions addressed in the dissertation

My dissertation is divided into three projects that can be clearly separated partly by the methodological approaches, but also based on the research questions that I wanted to address. One general issue overarching all projects of my thesis are the similarities and differences between highly relevant aspects of vision and olfaction in honeybees and bumblebees. The experimental part of my study focuses on bumblebees. For a certain part of the addressed topics there is already published data in honeybees, which suggests a comparison with bumblebees. In contrast, other experiments have solely been conducted in bumblebees due to methodological advantages compared to honeybees.

In a recent study on navigation behaviour honeybees were trained to use salient objects to find a food source that was placed between the objects. Surprisingly, the honeybees were equally capable of finding the hardly visible food source also, when the objects were camouflaged (Dittmar et al., 2010) in front of the background. This finding caught my interest and led me to the question what features of objects bees are capable to perceive in a behavioural context.

Answering this question implicated that I needed to record neuronal signals in the parts of the bee's brain concerned with visual information processing. As recordings from the brain of a flying insect are hard to achieve, we decided to reconstruct a stimulus movie based on what the animal had seen before during navigation behaviour. We opted for the bumblebee as experimental animal, considering exploiting its several advantages as a model system in the long run. However, as a precondition for the analysis at the neural level I had to probe in my first project navigation behaviour of bumblebees in a similar way as was done by Dittmar and colleagues for honeybees. Moreover, to reconstruct what the bumblebee had seen during flight we had to unravel the fine temporal dynamics that are associated with bumblebee flight as well as the orientation of its view. This also implicated disentangling the coordination of head and body movements during navigation behaviour. On this basis we were also able to compare fine structure of flight and gaze control of bumblebees against the flight dynamics already being measured in the closely related honeybee (Boeddeker et al., 2010).

Based on the reconstruction of one of those recorded bumblebee flights I created in the context of my second project a set of stimulus movies that served to highlight the influence of objects that served as visual landmarks in the behavioural navigation experiments on the neuronal response of neurons that are sensitive to motion. Also, I wanted to find out in which way the texture of the objects shapes the neuronal responses, which might bring together the earlier findings in behaviour with the neuronal mechanisms.

In the third project of my dissertation I decided to change from analysing the vision sense to investigate the sense of smell, i.e. olfaction. What at the first glance might appear to mark a clear cut in my project, can be regarded a good next step to further compare honeybees with bumblebees. Although the modality is different, I continued analysing the neuronal basis of primary sensory processing. In this project I put emphasis on the representation of a set of odours that allowed determining general

coding properties that are implemented in an early processing stage of olfactory information. In contrast to the visual pathway in the bee brain, the olfactory pathway in honeybees is well characterised functionally. This is grounded on the importance of olfaction for its behaviour. As soon as meaningful olfactory cues are present the bees incorporate olfactory information to improve their navigation performance. Although the combination of visual and olfactory information in a navigation context is highly interesting, I still would like to introduce basic navigation concepts that are predominantly vision-based.

In the following I will present some more background knowledge related to the central research questions of my thesis ranging from local navigation over motion vision to the basic principles of olfaction. After reviewing key concepts that form the framework of each of my three projects, I summarise my own major conclusions that were derived from the respective experiments.

Basic navigation concepts in Hymenoptera

Bumblebees, honeybees and ants all belong to the order of Hymenoptera. They are central place foragers, which means that they frequently visit the same feeding site to collect food for the hive. To find places of especially profitable food sources they search for some time until they have found some. But to be able to really profit from the food source they need to remember where they found it to come back on the next trip. To accomplish this they employ a variety of strategies.

At first, it is important to divide navigation strategies into the ones for global homing (Collett, 2008) and local homing (Zeil et al., 1996). Local homing means navigation in the vicinity of the goal location that serves to finally pinpoint the exact goal location like a particular food source or the nest entrance. What naively seems to be an easy task is indeed quite demanding, as the entrances to nests of ants or bumblebees are often small and inconspicuous holes in the ground that are hard to find. Whereas local homing is relevant for precise orientation on a small scale, global homing mechanisms serve to robustly allow a directed flight to the area around the goal location over distances that can be as far as a few kilometres away from the starting point. For these larger distances that need to be travelled a large variety of different mechanisms could be demonstrated.

For bees and ants, it could be shown that they use obvious cues like the position of the sun or the pattern of polarized light in the sky to lead their way in global homing tasks (Collett and Collett, 2002). These allocentric cues are especially helpful in sparse environments, such as many deserts, barely containing other helpful cues, so that the animals are solely able to find their way home performing path integration. This means that they record their orientation as well as the travelled distance (egocentric cue) during a foraging trip to be later capable of calculating a home vector. This vector results in a direct path to their nest in contrast to a meandering path while they search for food (Collett and Collett, 2002). Mechanisms to record the travelled distance differ of course, if the animal is able to fly or if it is bound to the ground like ants, for instance. Whereas these have been shown to count the amount of steps during their foraging

trip (Wittlinger and Wolf, 2006), bees perceive the image flow on their eyes during flight to estimate the speed of their own forthcoming (Srinivasan et al., 1996). Both strategies – step counting or detection of image speed - serve to estimate the distance the individual animal has travelled. Of course, the longer such a foraging trip is, the larger will be the error that is accumulating if the animal would only rely on path integration. Therefore, it is no wonder that bees and ants also use visual landmarks that aid to find the correct path to the location. Landmarks themselves can be all salient objects bound to a certain position and to help the animal to guide its way. If available, ants and bees use these cues to orient along paths of visual landmarks to find their goal location, which is then called route following (Collett et al., 1992; Collett, 2010). The important role that landmarks play during navigation is also demonstrated by the fact that ants, instead of relying on path integration alone, can also navigate using landmarks, if the environment comprises objects suitable to guide their way (Wehner et al., 1996; Kohler and Wehner, 2005).

But landmarks are not only used for global homing. They also play an important role in local homing as well. Depending on their size different objects might be used as landmarks in different contexts. A tree trunk might be too small and common to serve as a landmark in global homing to indicate the direction of flight. But if the animal is already within a distance of a few metres to the goal location this tree trunk may appear unique on this small scale and will help the animal to find its way. The behavioural part of this work will be based solely on local navigation in the way it is described here.

Ants as well as honeybees and bumblebees are capable of finding back to their nest reliably, and salient features in the surrounding have been shown to help them in doing so (Cartwright and Collett, 1979; de Ibarra et al., 2009). What information about the neighbourhood of the nest do they actually store and how do they adjust their behaviour to perceive the information they need to find back to their desired goal location?

In the past, different hypotheses have been tested concerning different possibilities on what details of the environment the animals are storing to be able to return to a certain location. If the environment around the goal location is relatively sparse the shape of the skyline surrounding the goal location has been shown to help ants to find their way back to the nest (Graham and Cheng, 2009). In this case the ants learn the contours of the upper boundaries of the environment that are visible against the horizon. Skyline-based navigation also involves the extraction of possible salient features in the skyline that help gauging the correct orientation with respect to such a salient feature or object. Even a little easier for the animal is to remember the nest location, if there are landmarks close-by that can serve as a reference to indicate the precise goal location. With at least three landmarks it is possible to define the goal location unambiguously via the distance relationships or the relationship of retinal sizes of the objects on the eye of the perceiving animal.

Independent of objects in the close vicinity of the goal ants and honeybees also seem to compare the panoramic visual input while searching for the goal with a previously stored panoramic image that they acquired before leaving the goal location

(Dittmar, 2011). This method has been termed snapshot matching. Evidence exists for all these approaches to find a previously learned goal.

Motion vision as important source of spatial information in the context of navigation

Independent of the mechanism bees and ants actually use to find their goal, it is clear that their vision sense plays an important role in solving this task. To resolve the relative positions of landmarks in the surrounding of a goal it is important to have information on their three-dimensional relationships. How do insects acquire this information? For humans it is quite easy to obtain depth information using their stereovision. As both eyes are several centimetres apart from each other, the differing images that are provided by both eyes reveal the depth structure of the surroundings at least within grasp distance. Even if insects possessed stereoscopic vision this would work only on a much smaller scale, i.e. just a few millimetres, which means that it is behaviourally irrelevant at least in the context of navigation. In the context of spatial navigation and to be able to separate close objects from objects further away bees need to use optic flow (Koenderink, 1986; Lehrer et al., 1988). Now what is optic flow? Optic flow is the movement of the perceived image on the eye caused by self-motion. As soon as you start moving you will notice that objects close-by move much faster on your eyes compared to more distant objects.

Optic flow in general is separable into a translational component and a rotational component. The rotational component does not provide information on the depth structure of the environment, as during a pure rotation all objects move with exactly the same speed on the eyes, no matter in what distance they are. Depth information is only contained in the translational component, which lets the retinal images of close objects move faster and those of distant objects move slower. During normal flight these two components of optic flow are superimposed, e.g. optic flow via forward translation is perceived at the same time as optic flow via rotations around the vertical axis of the eye that might happen at the same time. To allow depth perception during flight bees, but also flies and birds have been shown to actively separate rotational from translational optic flow components (van Hateren, 1997; Eckmeier et al., 2008; Boeddeker et al., 2010). They compress the time during which they perceive rotational optic flow to very short moments of the flight that serve to adjust their flight course or gaze direction. These short turning events are called saccades. Consequently, the remaining part of the flight consists on intersaccades that just contain translational optic flow allowing depth perception (Kern et al., 2005; Egelhaaf et al., 2012).

During normal movement ants or bees perceive an enormous amount of visual information. Depending on the behavioural context where the input is perceived, it might important for the animal to remember certain places and possibly also the visual input connected to these places. To be able to find back to places of interest like their hive or a valuable food source, honeybees and bumblebees perform a stereotyped movement pattern to gather information about the environment of this place and to ensure reliable return to it. These flights typically consist of a small set of separate

manoeuvres that in sum are referred to as learning flights. They definitely need these learning flights to be able to find the learned food source or the nest as experimentally preventing learning flights has been turned out to be sufficient to suppress learning of the goal location (Lehrer, 1991). This impressively underlines the importance of a defined visual input for behavioural performance.

The required movement patterns are very similar amongst flying *Hymenoptera*. When the insect starts off from a place that it needs to remember, it immediately faces the goal at first after starting off. It then performs sideways movements and slowly backs away from the goal location. The animal is performing arcs and loops around the goal location while increasing its distance and height from the goal location (Zeil et al., 1996). During proceeding take-offs they repeat these flight manoeuvres as well, but the duration of the single segments of the learning flight decreases with growing experience in finding the goal location until it ceases completely. By changing elements in the animal's familiar environment, in which the animal does not require learning flights any more, new learning flights become necessary for the animal to be able to find its way back to the goal location (return flights).

Various studies have focussed on structural differences and similarities between learning flights and return flights to elucidate possible recapitulations of the learning flight during return flights. Different hypotheses exist on which parameters are especially important for the animal to gather the necessary information. Parameters that might play a role are viewing direction and the position of the goal location on the retina of the animal (Zeil et al., 1996; Fry and Wehner, 2005) or the compass direction of the view (Collett et al., 2013; Philippides et al., 2013). But bees also possess extensive learning capabilities in terms of visual learning of colours and shapes (Horridge, 2009) that might also be used in navigation to find a goal. However, up to now it is unclear, which of these parameters are sufficient for successful navigation of the animal. In contrast to fixed positions of the goal on the animal's eye or a certain flight angle to the goal location that the bees try to capture again while searching for a goal location, we argue differently. Instead, we hypothesize dynamic cues, i.e. translational optic flow perceived during intersaccadic flight segments, to be particularly relevant for navigation performance (Dittmar et al., 2010; Braun et al., 2012). These flight segments provide strong translational optic flow and these segments are hardly interfered by rotational components that characterise the saccadic parts of flight. Therefore the animal may acquire information about the depth structure of the goal location during intersaccadic parts of flight. To understand how this might be accomplished it is important to have a close look at the visual input of the animals during their navigation behaviour.

Project 1:

Matching saccadic fine structure between honeybees and bumblebees during navigation behaviour

As insects are not able to move their eyes independent of their head, the perceived visual input is defined by the animal's head orientation, thus critically influencing the perception of motion. For honeybees it recently has been elucidated during local

homing that the head serves to stabilize the visual input against rotational components of optic flow induced by the body (Boeddeker et al., 2010). The rotations of the honeybee head that are necessary to reorient the gaze are compressed into small turns of the head (head saccades) much faster than the turns of the body (body saccades).

In the first project of my PhD project we aimed to also reveal the fine structure of the head movements in bumblebees. We therefore recorded learning flights of freely flying bumblebees with high-speed cameras, after the bees have been trained to find an almost invisible food source that was placed between three salient landmarks. The bumblebees therefore had to learn the positional relationships of the food source to the landmarks to successfully find their goal. To be able to compare the results published for honeybees (Boeddeker et al., 2010) with the newly acquired bumblebee data we used exactly the same flight arena and visual surrounding to record the bumblebees' learning flights.

Like in flies and honeybees we could determine the body saccades to start before and to end after the head saccades, indicating a larger speed of the head during saccades. Compared to honeybees we find the speed of head saccades to exhibit a similar range with speeds between 250 °/s and 1500 °/s, which was rather surprising given the bumblebees' larger body weight at similar body size. However, the weight of the head might still be in a similar range, which also means similar inertia that the animals have to overcome, leading to similar speeds of head saccades.

In addition we also demonstrated a consistent relationship between the duration, peak velocity and amplitude of the bumblebee head saccades, which is a phenomenon that has earlier been described for vertebrates and humans in particular, but never for insects. These relations might therefore be a common principle in the animal kingdom that might serve to reduce the effect of inaccuracies of the motoric system on the final head position after a saccade has ended.

For bumblebees, we report similar search times until finding the feeder in the midst of the landmark arrangement as well as the specific pattern of flight manoeuvres typical for learning and return flights of honeybees and bumblebees. This is particularly interesting as for the reference experiment using honeybees the experimenters trained honeybees from an outdoor hive to enter the arena to solve the navigation task, whereas in this account the whole experiment was accomplished indoors. This emphasizes the possibility to perform behavioural experiments under controlled conditions in an indoor environment without altering the animals' natural behaviour.

Through this experiment we now have obtained detailed knowledge on the fine structure and the dynamics of the bumblebee flight during a navigation task. The high-speed recordings of their learning flights revealed the starting points of their characteristic head saccades in fine temporal resolution. Additionally, resolving the head orientation allows reconstruction of what the bee has seen in its visual field. This reconstruction is the key opening the door to what the bee is able to perceive of its environment and which features of the visual surrounding – like the spatial arrangement of objects or object texture - are represented in the visual system on the neuronal level.

The optic lobe of the insect brain

In insects, the brain area that is mainly involved in primary processing of visual information is the optic lobe, which exists twice in each brain, one optic lobe for each eye (see Fig. 1A for an overview). Compared to other brain components that are related to different sensory modalities the optic lobes occupy a large proportion of the overall brain volume of bees (Mares et al., 2005) indicating a prominent role in the bees everyday life that it is worth spending resources on.

The visual information is processed along a pathway through the several functional levels the optic lobe consists of. To give an impression on what kind of information is extracted from the environment, I would like to introduce the different stages briefly (retina, lamina, medulla, lobula), focussing on the stage, from which I was able to achieve electrophysiological recordings during my work: the lobula (see also Figure 1B).

The first input stage of the insect eye is the retina. Here light is being captured by the facet eye that consists of about 5400 single lenses (ommatidia) in honeybees (Seidl and Kaiser, 1981) and between 3000 to 4000 in bumblebee workers (Spaethe, 2003), depending on the body size. Within each ommatidium there are principally eight main photoreceptors (R1–R8 and an additional ninth one, R9) that are sensitive to light of a particular range of wavelengths. Whereas in a single ommatidium the receptor distribution of two of those eight photoreceptors leads to sensitivity to UV light or blue light or both (R1 and R5), there are always six receptors sensitive to green light (Wakakuwa et al., 2007). These six photoreceptors are thought to be primarily involved the processing of motion information (Kaiser and Liske, 1974; Hausen and Egelhaaf, 1989). A single axon bundle projects to single cartridges in the lamina (Sommer and Wehner, 1975) that is retinotopically arranged, meaning that neighbouring visual inputs that are perceived by the photoreceptors is also processed in neighbouring areas of the lamina. In the lamina – the first neuropile of the optic lobe - the incoming signals are processed to enhance changes in signal intensity and thereby enhancing its contrast as has been shown for *Diptera* (flies) (Laughlin, 1994). From the lamina the information is also retinotopically transferred to the medulla, which comprises of eight layers (Paulk et al., 2009a) and contains the largest number of neurons within the optic lobe. Due to a large number of physiological responses and a wide range of cell types that innervate the different layers of the medulla to a varying extent, the main task of the medulla is hard to grasp. It is known, however, that in this second neuropil of the optic lobe colour information as well as motion information are being processed and either distributed to different brain areas like the mushroom bodies (Paulk and Gronenberg, 2008), the lateral protocerebrum in the central brain (Paulk et al., 2009b), or further processed in the third visual neuropil – the lobula, where the major visual pathway is leading to.

Fig. 1

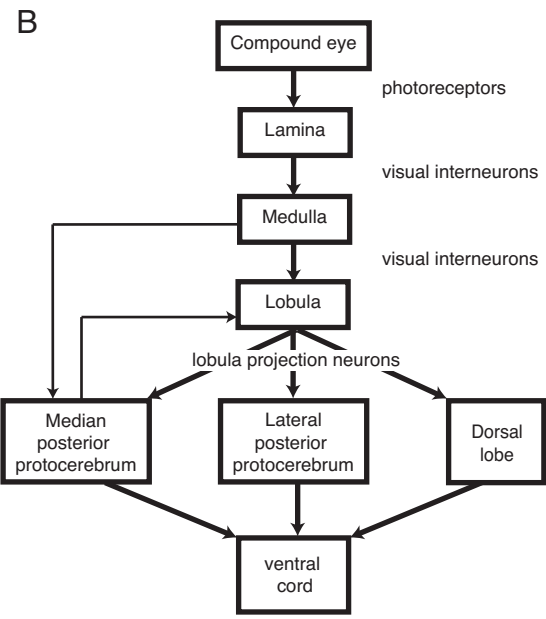
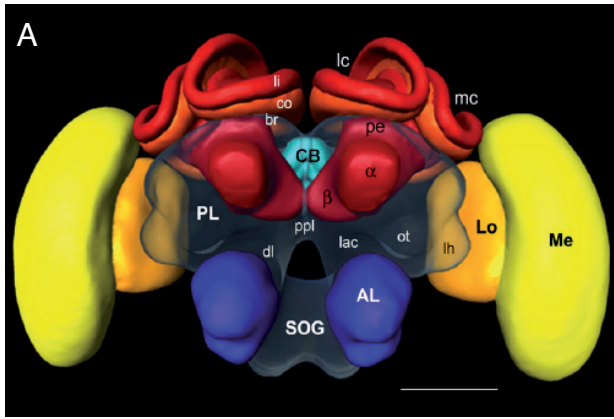


Fig. 1. Overview on the bee brain.

A: the honeybee standard brain (HSB). Neuropil areas defined in the HSB are shown in different colors. Components of the midbrain area (protocerebral lobes, PL, and subesophageal ganglion, SOG) are fused and shown in transparency. Subcompartments of the protocerebral lobe and mushroom bodies are indicated in lower case letters. Scale: 300 μ m. PL: protocerebral lobe; ppl: posterior protocerebral lobe, Lo: lobula; Me: medulla, li: lip, co: collar, br: basal ring, lh: lateral horn, ot: optic tubercle, lac: lateral accessory lobe, mc: median calyx, lc: lateral calyx, pe: peduncle, α : alpha-lobe, β : beta-lobe, SOG: subesophageal ganglion. Taken from Rybak (2010)

B: Summary diagram of visual pathways in the bee brain. The arrows indicate the direction of information flow. According to Maronde (1991)

Focus of interest for spatial vision in local navigation – the Lobula

The hymenopteran lobula consists of six layers that are perpendicularly arranged to the layers of the medulla, and which are subdivided into the distal lobula (layers 1–4) and proximal lobula that consists of two layers (layers 5,6) (Ribi and Scheel, 1981; Paulk

and Gronenberg, 2008). The lobula contains two main classes of neurons that have been studied most. Neurons with small receptive fields can be found as well as neurons with thick axons and wide arborisations that are called large-field cells as they integrate motion from a large area of the visual surroundings. These two prominent cell classes can also be found in the proximal lobula of Hymenoptera not only on the basis of their morphology (Meyer et al., 1986), but also by their typical activity profile responding to motion signals in a direction selective manner (DeVoe et al., 1982; Hertel and Maronde, 1987). These large-field (also tangential) cells are of special importance for this study as their axons are thick enough to allow reliable intracellular recording with micropipettes during visual stimulation. During test experiments we were able to reliably record from these motion-sensitive and direction-selective neurons in honeybees as well as in bumblebees. The neurons of the lobula project into different areas of the brain, for instance to the contralateral lobula (DeVoe et al., 1982; Maronde, 1991). But, as has been shown by Paulk and colleagues, about 90 % of large-field tangential neurons in the proximal lobula project into the superior lateral protocerebrum or inferior lateral protocerebrum (Paulk and Gronenberg, 2008; Paulk et al., 2009b).

These protocerebral structures serve to further process colour and visual motion information that is obtained via connections from the lobula, but also the medulla. Additionally, neurons from other sensory modalities converge here, indicating a role as a general integration stage of the posterior protocerebrum. In which way the incoming information is used or processed remains unknown up to now. In addition to this area in the central part of the brain, there are also connections between the lobula and the calyces of the mushroom body (Mobbs, 1982) that also is a multimodal integration centre in bees, which has been associated with learning and memory in insects (Giurfa, 2013). This variety of possible target areas makes wide-field neurons on the lobula especially appealing to study the representation of the close surroundings of an insect during a learning task like finding a food source between landmarks.

In my behavioural project, I took a close look at the fine temporal details of the flight manoeuvres that are necessary for the bees to acquire the information needed to solve a visual navigation task based on landmarks. So I now ask the next question: what information about the environment in general and the landmarks in particular are represented by the bee on a neuronal level, while solving a navigational task?

Project 2:

Does the bumblebee motion vision pathway convey landmark information during a navigation task?

To be able to solve its navigational tasks, i.e. relocating a barely visible goal, it is crucially important to allow the animals to perform learning flights. Otherwise they won't be able to target the goal location in later trials. This means that not only the flight in the vicinity of the goal location is sufficient to remember the place, but that also the flight motifs play a central role for local landmark-based navigation (Collett et al., 2013; Philippides et al., 2013). The flight motifs obviously seem to provide the animal with a defined pattern of visual information that it needs to find back later on. Therefore it is important to know, what bees actually perceive while performing such a learning flight.

The first project allowed measuring the exact temporal dynamics of honeybee and bumblebee flight in a local navigation task. The objects that the bees used as landmarks were either highly salient against the background or hardly visible by giving them a texture identical to that of the background and camouflaging them in this way. In a former study the search behaviour of honeybees was barely affected by these camouflaged landmarks, and the behavioural performance of the animals, i.e. the time until finding the feeder, was not affected by the camouflaged landmarks compared to the salient ones (Dittmar et al., 2010). The question now is how are the objects represented neuronally in specific sections of the learning flights and what is the influence of the object texture on the neuronal response trace?

As it is not amenable to record neuronal activity from flying insects directly, I needed to reconstruct what a bumblebee has seen during flight. This flight should also not just be any flight, but flight in a behavioural context involving landmark learning. Following an approach developed for flies (Lindemann, 2003; Kern et al., 2005; Karmeier et al., 2006), I recorded position and head orientation of the bumblebee in the vicinity of the goal with two high-speed cameras. One camera recorded from the side and one from the top. This allowed three-dimensional reconstruction of the exact flight trajectory the bumblebee flew, while leaving the feeder that was positioned between a set of three landmarks. The reconstructed flight path can be replayed as an ego-perspective movie showing what a bee has seen while performing a learning flight. In the reconstruction I also integrated the exactly same distance relations between the bumblebee and the surrounding objects as well as the distances to the borders of the flight arena. If this movie is presented to a restrained bumblebee in a panoramic LED-based stimulus device (Lindemann et al. 2003), the restrained bee perceives the same visual input as the bee has perceived during the corresponding behavioural experiment. This method depicts a major step towards recording neuronal responses that resemble those actually produced during real flight; especially as the objects that are represented are meaningful for the bee and the dynamics of the original changes in head orientation is retained.

Matched to the bees' speed of motion processing the resolution of its eyes I displayed the reconstructed learning flight in its original version, but also additional versions of that movie containing single, targeted manipulations compared to the original reconstruction. I either changed the texture of the landmarks from high contrast to camouflaged landmarks carrying the same texture as the floor and wall of the arena. But I also removed either background or the landmarks from the movie. During the presentation of the movies, I recorded intracellularly from motion sensitive and direction-selective neurons in the bee lobula, so I could unravel what details of the environment are part of the information flow that is perceived by the bee in a learning task. I could show that the objects that were acting as landmarks in the behavioural experiment are also represented in the bee visual motion pathway. Also, it was evident that the measured neuronal responses were largely independent on the objects texture. This nicely matches the findings that honeybee navigation performance was not affected by the texture of the landmarks (Dittmar et al., 2010). These data were measured during the phases of

translational optic flow (intersaccades), during which the bees are thought to be able to acquire distance information that is necessary for navigation.

Surprisingly, objects also induced responses during head saccades, although the perceived visual signals during saccadic head movements are strongly dominated by rotations. I also found that during head saccades the texture of objects seems to be represented. The animals might therefore be able to extract different information at different phases of their flight.

Odour processing in the hymenopteran olfactory pathway

It is often hard to determine what kind of information the animal uses from the band of cues in the environment to control its behaviour. Concerning the vision sense, a variety of cues including optic flow, shape, colour or polarized sunlight have been shown to be exploited by bees, depending on their availability (Horridge, 2009). However, in natural environments behavioural actions of the animal are not determined exclusively by the visual input, but a whole range of other senses provides information about the surroundings. Among these the sense of smell is very important for bees. It is used in a variety of situations also in bumblebees to pick up messages from the pheromone producing queen, for example to stimulate more workers to collect food (Granero et al., 2005; Molet et al., 2008). But also it has been shown that floral odours are shared within the hive (Molet et al., 2009) to communicate newly found target plants that are valuable food sources that other bumblebees then try to find while foraging. This is in a slight contrast to honeybees, which exchange the collected nectar to inform nest mates about the flowers that they visited and also via indirect accumulation of the nectar's odour in the hive (Wenner, 1969). Wenner could also show that bees were capable to find a new feeding site using olfaction. In addition to bees, also ants have been shown to approach valuable food sources by positioning themselves downwind to obtain olfactory cues (Wolf and Wehner, 2000). Hence, also olfactory cues can act as important cue for navigating bees.

Therefore, it is no wonder that in the honeybee a vast amount of studies concentrated on morphological aspects of the olfactory system (Flanagan and Mercer, 1989; Galizia et al., 1999; Kirschner et al., 2006; Brill et al., 2013). The different processing stages of the olfactory pathway are known in great detail (Pareto, 1972; Mobbs, 1982; Kirschner et al., 2006; Sandoz, 2011). When odour molecules arrive at the antenna the molecules bind to receptors on the membrane of specific olfactory receptor neurons (ORNs) that are particularly sensitive to a certain type of odour molecules. The olfactory information is then transmitted via four sensory tracts to the first olfactory neuropil – the antennal lobe, which is the area I focussed on during my third project (see Fig. 2 for an overview). The antennal lobe is sphere-shaped and consists of single, roundly shaped subunits that are arranged on the surface of that sphere. These subunits are called glomeruli and are the projection sites of the ORNs. Interestingly, the number of ORNs is highly correlated with the number of glomeruli of the antennal lobe. All ORNs that express the same receptor type also connect to the same glomerulus (Couto et al., 2005).

Fig. 2

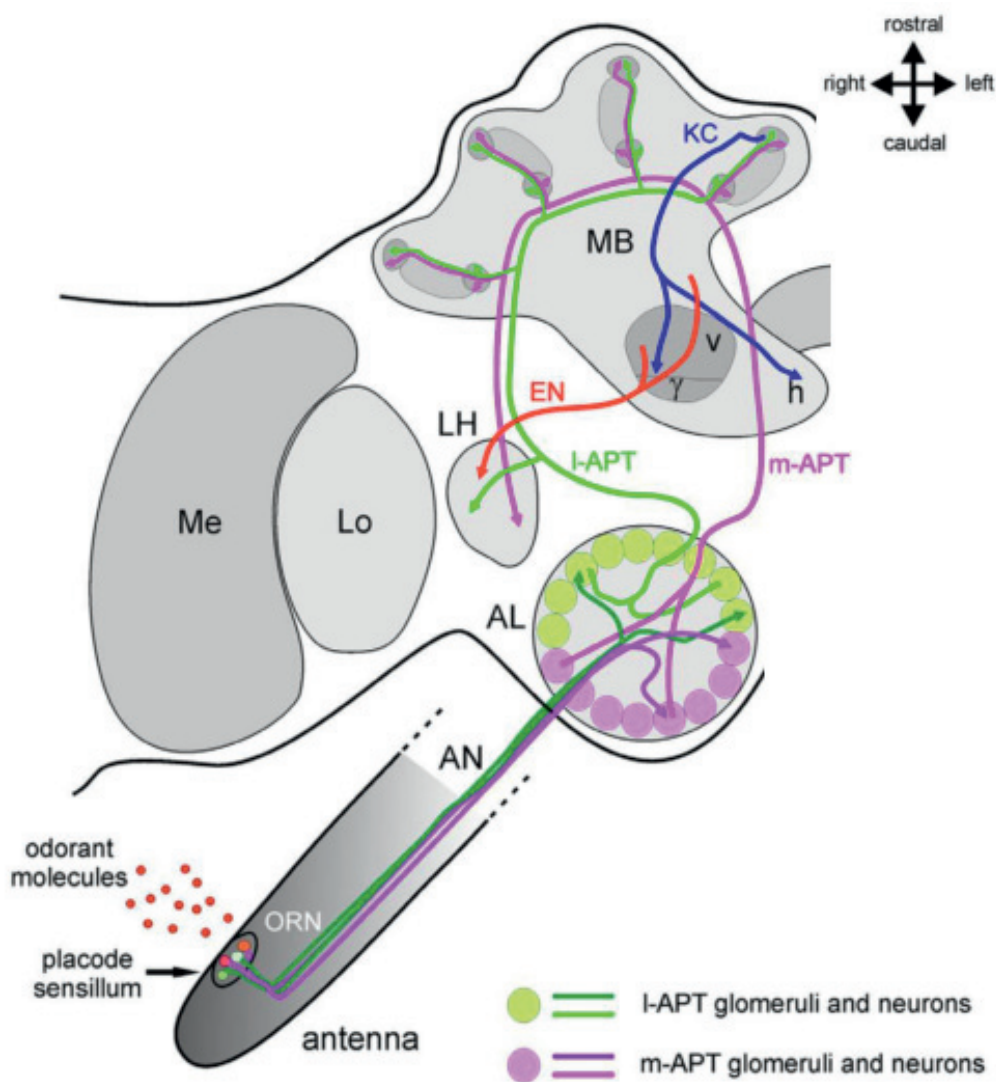


Fig. 2. The olfactory pathway of the honeybee.

The illustration shows excitatory pathways involved in the transmission of olfactory information in the brain. The antennal lobe receives input from olfactory receptor neurons (ORNs), which detect odorants within placode sensilla on the antenna. In the glomeruli of the antennal lobe, ORNs contact inhibitory local neurons (LNs) that synapse onto other glomeruli, and projection neurons, which further convey processed information via different tracts. The lateral antenno-cerebral tract (I-APT) projects first to the lateral horn (LH) and then to the mushroom body (MB) calyces. The medial tract (m-APT) projects to the same structures, but in the reverse order. These pathways depict parallel olfactory subsystems (in green and in magenta), conveying information from the antennal lobe in the periphery to higher order processing stages. Further structures indicated with abbreviations: Kenyon cells (KC), Extrinsic neurons (EN), vertical lobe (v), horizontal lobe (h), Medulla (Me), Lobula (Lo). Modified after Sandoz (2011)

The number of glomeruli in the antennal lobe differs strongly between insects (*Drosophila*: approx. 50 glomeruli) and even to a large amount within Hymenoptera with leafcutter-ants possessing up to 440 glomeruli (Kelber et al., 2010), whereas there are just about 165 in honeybees (Galizia et al., 1999). Within the glomeruli, the

incoming ORN-fibres connect to one of two classes of neurons. They either synapse in a divergent manner to the about 4000 intrinsic, mostly inhibitory, local interneurons (Flanagan and Mercer, 1989) that interconnect the different glomeruli or they synapse to projection neurons (PN). The projection neurons are mostly connected to a single glomerulus (uniglomerular) and project to the higher-order integration stages, namely the mushroom bodies and the lateral horn, via a dual olfactory pathway, i.e. the lateral antenno-protocerebral tract (l-APT) and the medial antenno-protocerebral tract (m-APT). The glomeruli of the upper part of the antennal lobe are innervated by the l-APT neurons and the lower fraction of antennal lobe glomeruli by m-APT neurons.

This pathway is unique for Hymenoptera (bees, ants, wasps) and allows transmitting signals from the glomeruli first to the mushroom bodies and afterwards to the lateral horn (m-APT, approx. 410 PN) or vice versa (l-APT, approx. 510 PN) (Rybak, 2012). Slight differences in the information transmitted by these two pathways have only recently been demonstrated at the input level of the corresponding glomerular subsystems (l-subsystem, m-subsystem), although both pathways receive similar sensory input (Carcaud et al., 2012).

The coding of olfactory information is certainly a fascinating topic. Other as visual stimuli that can be described by a distinct set of variables, such as their brightness and spectral properties, the different dimensions of odour stimuli are much more abstract (Laurent, 2002). The receptors at the antennae respond to a certain range of chemical features and get activated by them (Couto et al., 2005). As most receptors are tuned quite broadly, a certain molecule might be able to bind at different types of receptors leading to a specific activation pattern of ORNs that is also conveyed to the glomeruli of the antennal lobe. The local interneurons in the antennal lobe contribute via inhibitory connections between glomeruli to a sharpening of the overall antennal lobe activity pattern.

This activity pattern can be visualized with the help of optical imaging of calcium activity in the antennal lobe. As the concentration of intracellular calcium is an indirect indicator of neuronal activity, specific dyes that bind to calcium and then change their fluorescence properties can visualize the neuronal activity in brain areas that can be monitored using fluorescence microscopy. With this approach, much progress has been made in recent years in the honeybee with respect to understanding perception of odour stimuli and their representation in the antennal lobe (Sachse et al., 1999; Sachse and Galizia, 2002; Carcaud et al., 2012).

Whereas there is plenty of knowledge on honeybee odour processing available by now, only scarce information exists about the bumblebee olfactory system and its antennal lobe, in particular. Odour-induced calcium activity patterns in the bumblebee antennal lobe have not been visualized before. Also, an analysis of the wiring scheme of the AL input tracts by means of confocal microscopy was lacking up to the start of my third project. To be able to analyse functional properties of the bumblebee antennal lobe, I first needed to clarify the anatomical characteristics in more detail.

Project 3:
Odour coding in the bumblebee antennal lobe

On a superficial level the brain surfaces of honeybees and bumblebees look quite similar (Mares et al., 2005). Apart from that superficial view, particular knowledge on the bumblebee's sensory pathway is scarce. Especially as the bumblebee olfactory pathway has not been studied with present-day methods, we still had just a glimpse on the anatomical structure of this pathway. In an older study the structure of the antennal lobe and partly also of the different sensory input tracts has been described on the basis of cobalt stainings (Fonta and Masson, 1985). Thus, an approach using more elaborated methodology was necessary.

At first, I therefore inserted dye into the antennal nerve to stain the pathway from the ORNs to their single projection areas along the antennal lobe. Using confocal microscopy I was able to identify the major input afferent tracts to the antennal lobe that strongly resemble those described in honeybees (Kirschner et al., 2006). These antennal stainings also allowed a clear detection of the single glomeruli of the antennal lobe. Based on antennal staining we also reconstructed a complete antennal lobe with its single glomeruli. Counting the number of glomeruli of several stained antennal lobes indicated that their number is slightly lower in comparison to the honeybee antennal lobe. Nevertheless the general structure of the antennal lobe turned out to be very similar.

In a next step we applied the calcium indicator Fura-2 dextran to a position where we estimated the I-APT to reside and successfully stained this projection neuron tract. As the glomeruli projecting via the I-APT pathway are located at the top of the antennal lobe, this allowed easier access. The dye proceeded back to the synapses in the single glomeruli of the antennal lobe and allowed us therefore to present odour stimuli to explore odour representation in the bumblebee antennal lobe. To allow optimal comparison with available honeybee data we used a set of floral odours that has also been used in earlier studies (Guerrieri et al., 2005; Carcaud et al., 2012) on honeybees. The odour stimulus set consisted of highly concentrated odours that bumblebee will frequently encounter in their natural habitats. We used 16 different pure, highly concentrated odorants that differed only in the size of their carbon chain length (C6 till C9) and their functional group (4 different groups: primary alcohol, secondary alcohol, aldehyde and ketone). This permitted us to study the influence of molecule size and functional groups on the antennal lobe response pattern. Several measures can be calculated to assess the measured fluorescence signals. The most direct one is measuring the overall intensity of emitted light during olfactory stimulation compared to the non-stimulated activity. This intensity was measured for a defined section of the recorded image, which in our case was the whole antennal lobe. Similar to honeybees the intensity measure indicated a strong correlation with the single molecules vapour pressure, a measure that indicates the volatility of odour molecules at a given temperature at a given air pressure. The intensity measures of stimulus odours were found to drop with increasing carbon chain length.

To estimate the similarity of antennal lobe response patterns, I calculated the Euclidian distance between pixels of the mean fluorescence image of the camera for each odour in the stimulus set. Based on values for each pair of odours that can be compared I calculated multidimensional analyses that are used to uncover meaningful dimensions that explain the observed differences among a certain dataset. This technique revealed that the carbon chain length and the general functional group of a molecule can be distinguished on the basis of the first three dimensions that in total explain about two thirds of the overall variability of the data.

Finally, I was able to relate the measured intensities and the calculated Euclidian distances that I determined in bumblebees with the corresponding datasets that were acquired in a parallel study for honeybees (Carcaud et al, in preparation). Strong correlations further indicated a high similarity of honeybee and bumblebee odour coding. These analyses together depict a first step towards understanding primary odour coding properties in the bumblebee. Furthermore, this study depicts the first study using optical imaging in the bumblebee antennal lobe and therefore serves as a proof-of-concept. Still, a variety of still open problems bear potential for future studies in this area. Clearly, the next step would be to clarify, if single bumblebee glomeruli are responding with homologous response patterns as compared to glomeruli that are identified in the honeybee brain (Galizia et al., 1999).

Final considerations

This study combines behavioural analysis on animals navigating in a controlled laboratory environment, while showing a complex facet of their natural behaviour, with experiments at the neural level. In this respect this approach overcomes the old challenge to observe true natural behaviour while still controlling external parameters in a lab environment, but at the same time being able to unravel the underlying neural machinery. How this might be achieved best is controversial since the days of Karl von Frisch and Nikolaas Tinbergen. Their way of addressing research questions frequently comprised also comparing species that vary in certain aspects of their lifestyle and allow testing specific hypotheses that might otherwise be hard to address.

In present-day there is some pressure on behavioural and neuroscientific research to focus on so-called model systems like *Drosophila* in insects. This approach rests to some extent on the assumption that certain findings obtained in one species can be generalised to other species, at least, if no explicit evidence is speaking against this assumption. This assumption is, however, not trivial and there remains always the question of how related different species really are and, in the end, whether findings published for a certain species can be generalised.

In the context of vision honeybees and bumblebees have been found to be quite similar. This is, for instance, already obvious at the first processing step in the retina, where the spectral sensitivity functions of honeybee and bumblebee photoreceptors are almost identical (Peitsch et al., 1992). Nevertheless, within 90 million years of separate evolution major changes may have taken place. For instance, the honeybee evolved a refined communication system between individuals of the same hive, whereas

bumblebees are only regarded as primitively eusocial. Still, the navigational capacities of both species as well as basic properties of their olfactory systems are astonishingly similar as I could show in my first and third project, respectively.

Comparing both species, however, has not been the primary goal of my projects. Originally, it was rather a by-product, as the naturalistic behaviourally generated visual stimuli to be used in my electrophysiological experiments on bumblebees had to be based on bumblebee behaviour. This, however, allowed detailed comparisons between bumblebees and honeybees concerning navigation behaviour. The comparative perspective has then been extended in my third project to the olfactory system. I could show in all my projects with a broad range of methods applied, at both the behavioural as well as neural level, that bumblebees are highly versatile animals that also possess several advantages as an experimental system over honeybees. Bumblebees allow to employ a wide range of experimental approaches and are additionally quite robust, easy to keep and available throughout the year.

To sum up this line of argumentation: my account does not intend to replace the honeybee as an experimental animal, but might provide further reasons to establish the bumblebee as an interesting and fascinating experimental system on its own right in the field of neuroethological research.

REFERENCES

Boeddeker N, Dittmar L, Stürzl W, Egelhaaf M (2010) The fine structure of honeybee head and body yaw movements in a homing task. *Proc R Soc Lond B Biol Sci* 277:1899–1906.

Braun E, Dittmar L, Boeddeker N, Egelhaaf M (2012) Prototypical components of honeybee homing flight behavior depend on the visual appearance of objects surrounding the goal. *Front Behav Neurosci* 6:1–16.

Brill MF, Rosenbaum T, Reus I, Kleineidam CJ, Nawrot MP, Rössler W (2013) Parallel processing via a dual olfactory pathway in the honeybee. *J Neurosci* 33:2443–2456.

Carcaud J, Hill T, Giurfa M, Sandoz J-C (2012) Differential coding by two olfactory subsystems in the honeybee brain. *J Neurophys* 108:1106–1121.

Cartwright BA, Collett TS (1979) How honeybees know their distance from a near-by visual landmark. *J Exp Biol* 82:367–372.

Collett M (2010) How desert ants use a visual landmark for guidance along a habitual route. *Proc Natl Acad Sci* 107:11638–11643.

Collett TS (2008) Insect navigation: visual panoramas and the sky compass. *Curr Biol* 18:R1058–61.

Collett TS, Collett M (2002) Memory use in insect visual navigation. *Nature reviews Neurosci* 3:542–552.

Collett TS, Dillmann E, Giger A, Wehner R (1992) Visual landmarks and route following in desert ants. *J Comp Physiol A* 170:435–442.

Collett TS, de Ibarra NH, Riabinina O, Philippides A (2013) Coordinating compass-based and nest-based flight directions during bumblebee learning and return flights. *J Exp Biol* 216:1105–1113.

Couto A, Alenius M, Dickson BJ (2005) Molecular, anatomical, and functional organization of the *Drosophila* olfactory system. *Curr Biol* 15:1535–1547.

DeVoe RD, Kaiser W, Ohm J, Stone LS (1982) Horizontal movement detectors of honeybees: directionally-selective visual neurons in the lobula and brain. *J Comp Physiol* 147:155–170.

Dittmar L (2011) Static and dynamic snapshots for goal localization in insects? *Communicative & Integrative Biology*:1–4.

Dittmar L, Stürzl W, Baird E, Boeddeker N, Egelhaaf M (2010) Goal seeking in honeybees: matching of optic flow snapshots? *J Exp Biol* 213:2913–2923.

Eckmeier D, Geurten BRH, Kress D, Mertes M, Kern R, Egelhaaf M, Bischof H-J (2008) Gaze strategy in the free flying zebra finch (*Taeniopygia guttata*). *PloS one* 3:e3956.

Egelhaaf M, Boeddeker N, Kern R, Kurtz R, Lindemann JP (2012) Spatial vision in insects is facilitated by shaping the dynamics of visual input through behavioral action. *Front Neur Circ* 6:108.

Flanagan D, Mercer AR (1989) An atlas and 3-D reconstruction of the antennal lobes in the worker honey bee, *Apis mellifera* L. (Hymenoptera : Apidae). *International Journal of Insect Morphology and Embryology* 18:145–159.

Fonta C, Masson C (1985) Organisation neuroanatomique de la voie afférente antennaire chez les Bourdons mâles et femelles (*Bombus* sp.). *Comptes rendus des séances de l'Académie des sciences Série 3, Sciences de la vie* 300:437–442.

Von Frisch K (1967) *The dance language and orientation of bees*. London: Oxford University Press.

Von Frisch K (1977) *Aus dem Leben der Bienen*. Berlin [etc.]: Springer.

Fry SN, Wehner R (2005) Look and turn: landmark-based goal navigation in honey bees. *J Exp Biol* 208:3945–3955.

Galizia CG, Mcllwraith SL, Menzel R (1999) A digital three-dimensional atlas of the honeybee antennal lobe based on optical sections acquired by confocal microscopy. *Cell Tis Res* 295:383–394.

Giurfa M (2013) Cognition with few neurons: higher-order learning in insects. *Trends in neurosciences* 36:285–294.

Goulson D (2010) *Bumblebees - behaviour, ecology, and conservation*. New York: Oxford University Press.

Graham P (2010) Insect navigation. In: *Encyclopedia of Animal Behavior*, volume 2 (Breed MD, Moore J, eds), pp.167–175. Oxford: Oxford: Academic Press.

Graham P, Cheng K (2009) Ants use the panoramic skyline as a visual cue during navigation. *Curr Biol* 19:R935–7.

Granero AM, Sanz JMG, Gonzalez FJE, Vidal JLM, Dornhaus A, Ghani J, Serrano AR, Chittka L (2005) Chemical compounds of the foraging recruitment pheromone in bumblebees. *Die Naturwissenschaften* 92:371–374.

Guerrieri F, Schubert M, Sandoz J-C, Giurfa M (2005) Perceptual and neural olfactory similarity in honeybees. *PLoS biology* 3:e60.

Van Hateren JH (1997) Processing of natural time series of intensities by the visual system of the blowfly. *Vision research* 37:3407–3416.

Hausen K, Egelhaaf M (1989) Neural mechanisms of visual course Control in Insects. In: *Facet of Vision*, pp.391–424.

Heinrich B (2004) *Bumblebee economics*. Cambridge: Harvard University Press.

Hertel BYH, Maronde U (1987) The physiology and morphology of centrally projecting visual interneurons in the honeybee brain. *J Exp Biol* 133:301–315.

Horridge A (2009) *What Does the Honeybee See?: And How Do We Know?* Acton, ACT: ANU E Press.

De Ibarra NH, Philippides A, Riabinina O, Collett TS (2009) Preferred viewing directions of bumblebees (*Bombus terrestris* L.) when learning and approaching their nest site. *J Exp Biol* 212:3193–3204.

- Kaiser W, Liske E (1974) Die optomotorischen Reaktionen von fixiert fliegenden Bienen bei Reizung mit Spektrallichtern. *J Comp Physiol* 89:391–408.
- Karmeier K, van Hateren JH, Kern R, Egelhaaf M (2006) Encoding of naturalistic optic flow by a population of blowfly motion-sensitive neurons. *J Neurophys* 96:1602–1614.
- Kelber C, Rössler W, Kleineidam CJ (2010) Phenotypic plasticity in number of glomeruli and sensory innervation of the antennal lobe in leaf-cutting ant workers (*A. vollenweideri*). *Developmental neurobiology* 70:222–234.
- Kern R, van Hateren JH, Michaelis C, Lindemann JP, Egelhaaf M (2005) Function of a fly motion-sensitive neuron matches eye movements during free flight. *PLoS Biol* 3:1130–1138.
- Kirschner S, Kleineidam CJ, Rybak R, Gru B, Zube C (2006) Dual olfactory pathway in the honeybee, *Apis mellifera*. *Comparative and General Pharmacology*:933–952.
- Koenderink JJ (1986) Optic flow. *Vision Research* 26:161–179.
- Kohler M, Wehner R (2005) Idiosyncratic route-based memories in desert ants, *Melophorus bagoti*: how do they interact with path-integration vectors? *Neurobiology of learning and memory* 83:1–12.
- Laughlin SB (1994) Matching coding, circuits, cells, and molecules to signals: general principles of retinal design in the fly's eye. In: *Progress in retinal and eye research*, pp.165–196.
- Laurent G (2002) Olfactory network dynamics and the coding of multidimensional signals. *Nature reviews Neurosci* 3:884–895.
- Lehrer M (1991) Bees which turn back and look. *Naturwissenschaften* 78:274–276.
- Lehrer M, Srinivasan M V, Zhang SW (1988) Motion cues provide the bee's visual world with a third dimension. *Nature* 332:356–357.
- Lindemann J (2003) FliMax, a novel stimulus device for panoramic and highspeed presentation of behaviourally generated optic flow. *Vision Research* 43:779–791.
- Mares S, Ash L, Gronenberg W (2005) Brain allometry in bumblebee and honey bee workers. *Brain, behavior and evolution* 66:50–61.
- Maronde U (1991) Common projection areas of antennal and visual pathways in the honeybee brain, *Apis mellifera*. *J Comp Neurol* 309:328–340.

- Meyer EP, Matute C, Streit P, Nässel DR (1986) Insect optic lobe neurons identifiable with monoclonal antibodies to GABA. *Histochemistry* 84:207–216.
- Michener CD, Grimaldi D a (1988) The oldest fossil bee: Apoid history, evolutionary stasis, and antiquity of social behavior. *Proc Natl Acad Sci* 85:6424–6426.
- Mobbs PG (1982) The brain of the honeybee *Apis mellifera* I. the connections and spatial organization of the mushroom bodies. *Phil Trans R Soc Lond B* 298:309–354.
- Molet M, Chittka L, Raine NE (2009) How floral odours are learned inside the bumblebee (*Bombus terrestris*) nest. *Die Naturwissenschaften* 96:213–219.
- Molet M, Chittka L, Stelzer RJ, Streit S, Raine NE (2008) Colony nutritional status modulates worker responses to foraging recruitment pheromone in the bumblebee *Bombus terrestris*. *Behavioral Ecology and Sociobiology* 62:1919–1926.
- Pareto A (1972) Die zentrale Verteilung der Fühlerafferenz bei Arbeiterinnen der Honigbiene, *Apis mellifera* L. *Zellforschung* 131:109–140.
- Paulk AC, Dacks AM, Gronenberg W (2009a) Color processing in the medulla of the bumblebee (Apidae: *Bombus impatiens*). *J Comp Neurol* 513:441–456.
- Paulk AC, Dacks AM, Phillips-Portillo J, Fellous J-M, Gronenberg W (2009b) Visual processing in the central bee brain. *J Neurosci* 29:9987–9999.
- Paulk AC, Gronenberg W (2008) Higher order visual input to the mushroom bodies in the bee, *Bombus impatiens*. *Arthropod Struct Dev* 37:443–458.
- Peitsch D, Fietz a, Hertel H, de Souza J, Ventura DF, Menzel R (1992) The spectral input systems of hymenopteran insects and their receptor-based colour vision. *J Comp Physiol A* 170:23–40.
- Philippides A, de Ibarra NH, Riabinina O, Collett TS (2013) Bumblebee calligraphy: the design and control of flight motifs in the learning and return flights of *Bombus terrestris*. *J Exp Biol* 216:1093–1104.
- Ramírez SR, Nieh JC, Quental TB, Roubik DW, Imperatriz-Fonseca VL, Pierce NE (2010) A molecular phylogeny of the stingless bee genus *Melipona* (Hymenoptera: Apidae). *Molecular phylogenetics and evolution* 56:519–525.
- Ribi WA, Scheel M (1981) The second and third optic ganglia of the worker bee. *Cell Tissue Res* 221:17–43.

Rybak J (2012) The digital honey bee brain atlas. In: Honeybee neurobiology and behaviour (Galizia CG, Eisenhardt D, Giurfa M, eds), pp.125–140. Dordrecht, Netherlands: Springer Netherlands.

Rybak, J., Kuß, A., Lamecker, H., Zachow, S., Hege, H.-C., Lienhard, M., ... Menzel, R. (2010). The digital bee brain: Integrating and managing neurons in a common 3D reference system. *Front Sys Neurosci* 4:1–15.

Sachse S, Galizia CG (2002) Role of inhibition for temporal and spatial odor representation in olfactory output neurons: A calcium imaging study. *J Neurophys* 87:1106–1117.

Sachse S, Rappert A, Galizia CG (1999) The spatial representation of chemical structures in the antennal lobe of honeybees : steps towards the olfactory code. *EJN* 11:3970–3982.

Sandoz JC (2011) Behavioral and neurophysiological study of olfactory perception and learning in honeybees. *Front Sys Neurosci* 5:1–20.

Schultz TR., Engel MS., Aschier JS. (2001) Evidence for the origin of eusociality in the corbiculate bees (Hymenoptera : Apidae). *Journal of the Kansas Entomological Society* 74:10–16.

Seidl R, Kaiser W (1981) Visual field size, binocular domain and the ommatidial array of the compound eyes in worker honey bees. *J Comp Physiol A* 143:17–26.

Sommer EW, Wehner R (1975) The retina-lamina projection in the visual system of the bee, *Apis mellifera*. *Cell Tis Res* 163:45–61.

Spaethe J (2003) Interindividual variation of eye optics and single object resolution in bumblebees. *J Exp Biol* 206:3447–3453.

Srinivasan M, Zhang S, Lehrer M, Collett T (1996) Honeybee navigation en route to the goal: visual flight control and odometry. *J Exp Biol* 199:237–244.

Tinbergen N (1951) *The study of instinct*. Oxford: Clarendon Press.

Wakakuwa M, Stavenga DG, Arikawa K (2007) Spectral organization of ommatidia in flower-visiting insects. *Photochemistry and photobiology* 83:27–34.

Wehner R, Michel B, Antonsen P (1996) Visual navigation in insects: coupling of egocentric and geocentric information. *J Exp Biol* 199:129–140.

Wenner AM (1969) Honey bee recruitment to food sources: olfaction or language? *Science* 164:84–86.

Wittlinger M, Wolf H (2006) The ant odometer : stepping on stilts and stumps. *Science* 312:1965–1967.

Wolf H, Wehner R (2000) Pinpointing food sources: olfactory and anemotactic orientation in desert ants, *Cataglyphis fortis*. *J Exp Biol* 203:857–868.

Zeil J, Kelber A, Voss R (1996) Structure and function of learning flights in bees and wasps. *J Exp Biol* 199:245–252.

1

BUMBLEBEE HOMING: THE FINE STRUCTURE OF HEAD TURNING MOVEMENTS

The content of this chapter is submitted for publication as: N Boeddeker, M Mertes, L Dittmar, M Egelhaaf: **BUMBLEBEE HOMING: THE FINE STRUCTURE OF HEAD TURNING MOVEMENTS**

ABSTRACT

Flying insects change their flight direction by combinations of roll, yaw and pitch rotations of their body. By turning the orientation of their flight motor they are able not only to change flight direction, but even to fly sideways and backwards. Many insects employ head movements that are independent of their body movements to stabilise gaze. Here we use high-speed video equipment to record head- and body-movements of the bumblebee *Bombus terrestris* approaching and departing from a food source that was located between three landmarks in an indoor flight-arena. During these navigation flights the flight paths consist of straight flight segments combined with rapid turns. These short and fast yaw turns (“saccades”) are in most cases accompanied by even faster head yaw turns. Between saccades gaze stabilization leads to a behavioural elimination of rotational components from the optical flow pattern, which facilitates depth perception from motion parallax. The time course of single head saccades is very stereotypical. We find a consistent relationship between the duration, peak velocity and amplitude of saccadic head movements, which resembles in its main characteristics the so-called “saccadic main sequence” in humans. Saccades in bumblebees – like in many animals – are highly stereotyped, which hints at a common principle that reliably reduces the time during which the eye moves by fast and precise motor control.

INTRODUCTION

Insects such as bees, wasps and ants, use salient objects as landmarks to accurately find their way back to newly discovered food sources (Collett and Collett, 2002; Zeil, 2012). The basic design of behavioural experiments aimed at finding out *what* features

the homing insects actually use, is to allow them to become accustomed to distinct visual features close to a place of interest, i.e. their feeding site, and then displacing or modifying these cues with the aim of observing where and how they would search for the goal. From such experiments it is clear that insects use the retinal size and position, the colour, distance and texture of landmarks (Cartwright and Collett 1983, Cartwright and Collett 1979, Cheng et al. 1986, Lehrer and Collett 1994, Fry and Wehner 2005, Dittmar et al. 2011) as well as skyline elevations (Graham and Cheng 2009) for homing. Recent experiments with landmarks that are camouflaged by carrying the same texture as the background, suggest that honeybees can also exploit dynamic cues like the optic flow pattern to pinpoint the goal location (Dittmar et al. 2010).

To understand *how* the insects find home, i.e. to unravel the behavioural mechanisms with which bees extract spatial information from their retinal input and how they use this information to guide their learning and return flights, it is crucial to analyse the organization of their behaviour (Zeil et al. 2008). In the past years, research has increasingly focussed on bumblebees to study hymenopteran flight. One important reason for using bumblebees instead of honeybees is the possibility to house them indoors, which allows experiments throughout the year (Riveros and Gronenberg, 2009). Bumblebees are also, compared to honeybees, more robust, which makes them suitable for several neurobiological approaches like calcium imaging (Pfeiffer and Kinoshita, 2011) or single cell intracellular recording (Paulk et al., 2008, 2009a, 2009b). Additionally, bumblebees show a very similar behavioural repertoire and learning ability as honeybees do. Therefore, similar experimental paradigms can be used for honeybees and bumblebees e.g. in pattern discrimination experiments (Dyer and Chittka, 2004a; Morawetz and Spaethe, 2012), or conditioning studies exploiting the proboscis extension response (Dyer and Chittka, 2004b). But in particular, they are exquisitely capable to solve navigational tasks (Hempel de Ibarra et al., 2009; Lihoreau et al., 2012)

Bumblebees like honeybees and wasps have evolved highly structured flight patterns for place learning, often called learning or turn-back-and-look-flights (Lehrer, 1991, 1993). They perform turn-back-and-look (TBL) flights when leaving their nest for the first time or when leaving a newly discovered food source. These learning routines are crucial for subsequent successful homing (reviewed in Zeil, Boeddeker and Stürzl 2009) and indicate an active vision strategy that helps bees to navigate by utilizing translational optic flow (Dittmar et al. 2010). The specific pattern of optic flow moving animals experience is determined by both the layout of the environment and by the animal's behaviour (Gibson 1950; Lappe 2000). Depending on their flight style bees can, like other flying animals, experience two basic types of image motion patterns, one is due to rotations of the eyes (rotational optic flow) and one is due to translations – translational optic flow (Koenderink and Doorn, 1987). The rotational optic flow component is generated by orientation changes of the eye; image displacements have uniform directions across the visual field and amplitudes are independent of the distance to objects. In contrast, optic flow generated by a pure translation depends on the direction and speed of the movements and on the distance of objects in the world. The pattern of optic flow during translational movements therefore contains range information

as images of close objects move faster across the retina than those of more distant objects. Optic flow is therefore shaped by the organisation of behaviour, and there are several examples that suggest that the specific mode and pattern of movement facilitates visual information processing, creating favourable conditions for image analysis (Zeil and Boeddeker, 2008; Egelhaaf et al., 2012).

Head and eye movements can shape and reduce the complexity of optic flow. During view-based homing the bees' flight style facilitates depth perception from motion parallax (Boeddeker et al., 2010; Dittmar et al., 2010; Braun et al., 2012): the bees' trajectories consist of straight flight segments combined with rapid turns about the vertical axis of the bee. By analogy with human eye movements, these rapid changes of gaze direction have been called saccades (Collett and Land, 1975). Between saccades gaze direction is mostly constant since head stabilizing movements largely keep the head stable with respect to rotation, eliminating rotational optic flow. As a result, head orientation in free flight is stabilized around all three rotational axes for most of the time except for fast changes in the horizontal gaze direction that serve to compress the visual system's exposure to rotational optic flow into very brief moments in time. Gaze changes involve coordinated head- and body movements, whereby head saccades are faster and shorter than body saccades (de Ibarra et al., 2009, Boeddeker and Hemmi 2010). A seminal study shows how precisely blowflies compensate rotations of the thorax in flight by counter rotations of the head relative to the thorax (Schilstra & van Hateren 1998; van Hateren & Schilstra 1999). If the fly's or bee's head were fixed to its thorax such fast rotations would have great impact on vision, as the reference coordinate system of the visual system would keep changing rapidly and frequently. In locusts and blowflies it has been shown that the processing of depth information from motion parallax crucially depends on a precise gaze stabilisation against rotations (Kern et al. 2006; Collett 1978).

Here, we analyse the fine structure of bumblebees' horizontal head and body turns in the context of local spatial navigation. In bees and other insects, the direction of gaze is determined by the orientation of the head; they cannot move their eyes relative to the head capsule. We recorded eye- and body-movements of bumblebees during a homing task to investigate how they shift gaze during their TBL and return flights and discuss the impact of structured gaze movements on visual motion processing.

MATERIAL AND METHODS

General procedure

We obtained commercial bumblebee hives from Koppert (Berkel en Rodenrijs, The Netherlands). The bumblebees were taken from their original carton box and then housed in custom-built Perspex boxes (300 mm × 200 mm × 300 mm) that were connected to the experimental apparatus by a plastic tube (length of 500 mm, diameter of 30 mm). The sidewall of the circular flight arena (diameter of 1.95 m) was 500 mm high and covered with the same red-white Gaussian blurred random dot pattern as the

arena floor. We used only bumblebee workers for the experiments. Bumblebees were trained to collect sugar solution from a transparent feeder in a circular flight arena. Bees that continued to visit the feeder regularly were individually marked with acrylic paint on thorax and abdomen. These bees were then trained to associate the food reward with a constellation of three cylinders we will refer to as landmarks. The whole setup, the training and the recording procedures were similar to those used in a study, where the performance of honeybees in locating the feeder was probed by targeted modifications of landmark texture and the landmark-feeder arrangement (Dittmar et al., 2010). The data for the search duration of honeybees (fig. 1B) was also taken from the study by Dittmar et al. (2010).

Experimental setup

Landmarks had a height of 250 mm and a diameter of 50 mm and were covered with homogeneously red paper. They were placed at different distances (100, 200, 400 mm) around the feeder, at angles of 120° to each other with the feeder in their centre (fig. 1). A drop of sugar solution was provided on the feeder, which was made of an upright Perspex cylinder (100 mm high, 20 mm diameter) carrying a Perspex disc (5 mm high, 40 mm diameter) on top. A dome of white cloth surrounded and covered the upper part of the flight arena to prevent the bees from seeing external visual cues. Indirect illumination was provided by eight Dedo-Lights (DLH4; 150 W each) placed outside the cloth around the arena and by nine 50 W halogen lamps from above. All lights ran on DC power and were positioned symmetrically with respect to the arena centre.

Recording sessions

Departing and approach flights were recorded from a distance of about 2 m above the flight arena with a high-speed digital stereo camera system. Two synchronised video cameras (Redlake MotionPro500) were positioned above the arena and allowed us to measure the position and orientation of the body length axis at 250 frames/sec with a resolution of 1024×1024 pixels in each view. The optical axis of one of the two stereo cameras was levelled with respect to gravity and pointed straight down. The visual field of the cameras covered an area of about 1 m^2 around the landmark arrangement. Video sequences were stored as uncompressed 8-Bit image files in tiff format on computer hard disk for off-line processing. With these parameter settings the maximum recording time was restricted by the onboard memory of our video cameras to 16 s.

Data analysis

The position of the bee and the orientation of its body length axis were automatically determined in each video frame by custom-built software in some image sequences (<https://opensource.cit-ec.de/projects/ivtools>). This was done for both cameras of the stereo video camera system. We determined the bee's body yaw angle from the levelled camera that viewed the flight arena from above (Top View). For camera calibration and 3D stereo triangulation we used the Camera Calibration Toolbox for Matlab by Bouquet (1999). 3D coordinates and the yaw body orientation of the bee were then low-pass filtered (second-order Butterworth filter) with a cut-off frequency of 20 Hz.

We also used our custom-built computer program to measure the bee's head position and yaw orientation in the image sequences. The centre of the bee's head was manually marked by clicking on it in every frame of the sequence. A region of interest (ROI, size 90 × 90 pixels) was then automatically defined around the centre of the head. A new image was generated on the computer screen from this ROI and rotated by moving the computer mouse until the bee's head appeared straight on the computer monitor. The inverse of the angle, which was used to straighten the image, then gave the yaw orientation of the bee's head relative to the orientation of the camera. Orientation measurements were greatly facilitated by this method and tracking errors were easy to detect this way. We checked the positional precision of our methods using markers with known positions in the flight arena. We analysed differences of orientation measurements of the bee's head that were done by two different observers in a given image sequence. These differences were on average smaller than 1°. We also compared manual and automatic measurements of the bee's body orientation and found that differences were also smaller than 1°. These operations, the statistical testing and all further calculations, e.g. the quantification of saccades amplitudes, velocities and durations were done in Matlab (The Mathworks, Natick, MA, USA).

RESULTS

After some training bees travelled regularly through the plastic tubing between hive box and flight arena. They entered the arena via a hole in its sidewall, where, in the early training phase, they immediately encountered the feeder. During this early training phase at the beginning of the experiment, they were made to find the feeder in a stepwise manner, starting with a Perspex feeder that was conspicuously marked by coloured rubber tape, located directly at the entrance, so that they could walk to the feeder. Later in training they flew towards the feeder (F in fig. 1A) that was then placed between three landmarks and made less conspicuous by removing the tape. The bees often performed learning flights both, at the entrance of the flight arena and also at the feeder during departure. This was especially the case when we had changed the position or the appearance of the feeder. These flights are thought to enable bees to store and reacquire similar nest-focused views during learning and return flights (Lehrer, 1993; Collett et al., 2013). We recorded their flight trajectories in the vicinity of the landmark arrangement using two high-speed cameras and measured the time needed to land on the feeder after entering the flight arena ($n = 4$; 33 flights). Trained bumblebees needed only about ten seconds to find the feeder in this experiment, demonstrating their extraordinary homing capabilities. For comparison we plot honeybee search times ($n = 14$; 68 flights; Dittmar et al.), which seem to take a little longer to find the feeder, most likely because we focussed on a few highly trained bumblebees (Fig. 1B).

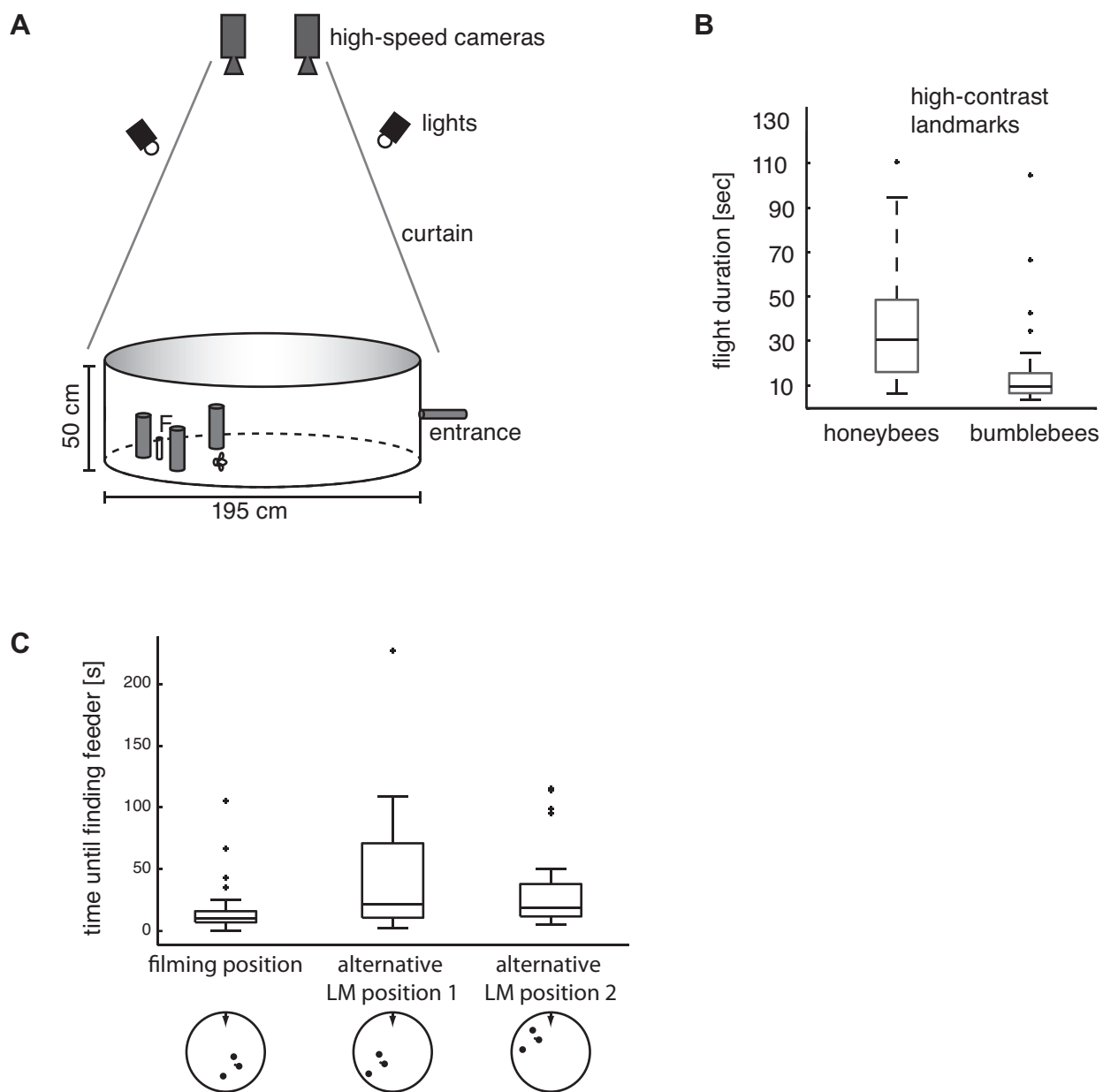


Fig. 1

Fig. 1. Flight arena and behavioural performance in the arena.

A: We trained honeybees and bumblebees to enter the arena via a hole in the sidewall. They were required to find a perspex feeder F between three landmarks placed around the feeder at different distances. Under indirect, uniform light conditions we recorded flight trajectories in the vicinity of the landmark arrangement using two high-speed cameras.

B: Boxplots of the time required for honeybees ($n = 14$; 68 flights) and bumblebees ($n = 4$; 33 flights) to land on the feeder. Time was stopped when touching the feeder during landing. Box symbols: central horizontal line within the box – median; box edges represent 25th and 75th percentiles; whiskers – most extreme data points that are not outliers ($> 75^{\text{th}}$ percentile $+ 1.5 \cdot$ box size or $< 25^{\text{th}}$ percentile $- 1.5 \cdot$ box size).

C: Histogram of bumblebee flight times when changing the position of the landmark arrangement within the arena, while maintaining the geometry of the landmark arrangement ($n = 74$ flights). Boxplot legend same as in B. Pictograms below the boxplot indicate the position of the landmark arrangement in the flight-arena. The arrow at the top of each pictogram denotes the entrance to the flight-arena.

To test whether the bumblebees really learned the landmark arrangement or rather relied on additional navigational mechanisms like path integration, we changed the position of the landmark arrangement within the arena, while maintaining the geometry of the landmark arrangement ($n = 74$ flights) constant. This did not drastically change the search times (fig. 1C). The search times are significantly different for the two alternative locations compared to the main training and filming site (Kruskal-Wallis test; $p = 0.02$), but well within the range of honeybee search times. The search time for the two alternative locations are not significantly different from each other, even though bees had to fly a much shorter path to one of the two feeder locations (Kruskal-Wallis test; $p = 0.8$). It is therefore unlikely that the bees were predominantly using path integration or other visual cues available in the circular flight arena to find the feeder and mostly relied on using the three cylinders as landmarks.

Bumblebees performed a “turn-back-and-look” (TBL) learning flight on leaving the feeder the first few times (fig. 2A). We analysed high-speed recordings of such learning flights and the following return flights to assess the visual input bumblebees perceive and to relate commonalities between learning and return flights that might improve the bees' local navigation performance. During these flights, the bee's body yaw direction is kept nearly constant except for brief periods when yaw orientation changes quickly (fig. 2B). These yaw body turns ('body saccades') are often accompanied by even faster head yaw turns ('head saccades'). The body saccade starts slightly earlier compared to the head saccade and also ends later compared to the shorter head saccades. The time course of body and head yaw orientation is very similar, with the difference that the head orientation is more constant than body yaw orientation between saccades and angle changes of the head are performed in a more step-like manner. Maximum head yaw velocities are therefore higher for the head than for the bee's body, since the times with only little rotations are longer between saccades for the head (fig. 2C). This flight pattern of bumblebees is very similar to that of honeybees (Boeddeker et al. 2010). Since the bee's head position and orientation determine the visual input, we will focus only on head coordinates in the following.

We divided the data of learning and return flights into the two characteristic phases: 'saccades', when angular velocities of the head reach up to 1500 °/sec (fig. 2C), and 'intersaccades', when the yaw orientation of the head is kept virtually constant. For detecting saccades we used a yaw angular velocity threshold criterion and a criterion that was sensitive to the direction of movement; this procedure was derived from the method used in (van Hateren & Schilstra 1998). Only if the absolute value of saccade velocity exceeded 200 °/sec, and the head moved in this direction for at least five frames ($= 20$ ms) a turn was classified as saccade. Once saccades were detected this way, we determined the maximum angular velocity and went 70 ms back and 70 ms forth in time to also capture the rising and falling phase of the angular velocity. We then searched again for the start and end points of every single saccade as defined by the yaw angular velocity threshold criterion (> 200 °/sec) and a duration criterion (same direction for at least four frames). To compare the characteristics of head saccades during learning and return flights, we calculated histograms of the amplitudes, velocities and durations of head saccades (fig. 3).

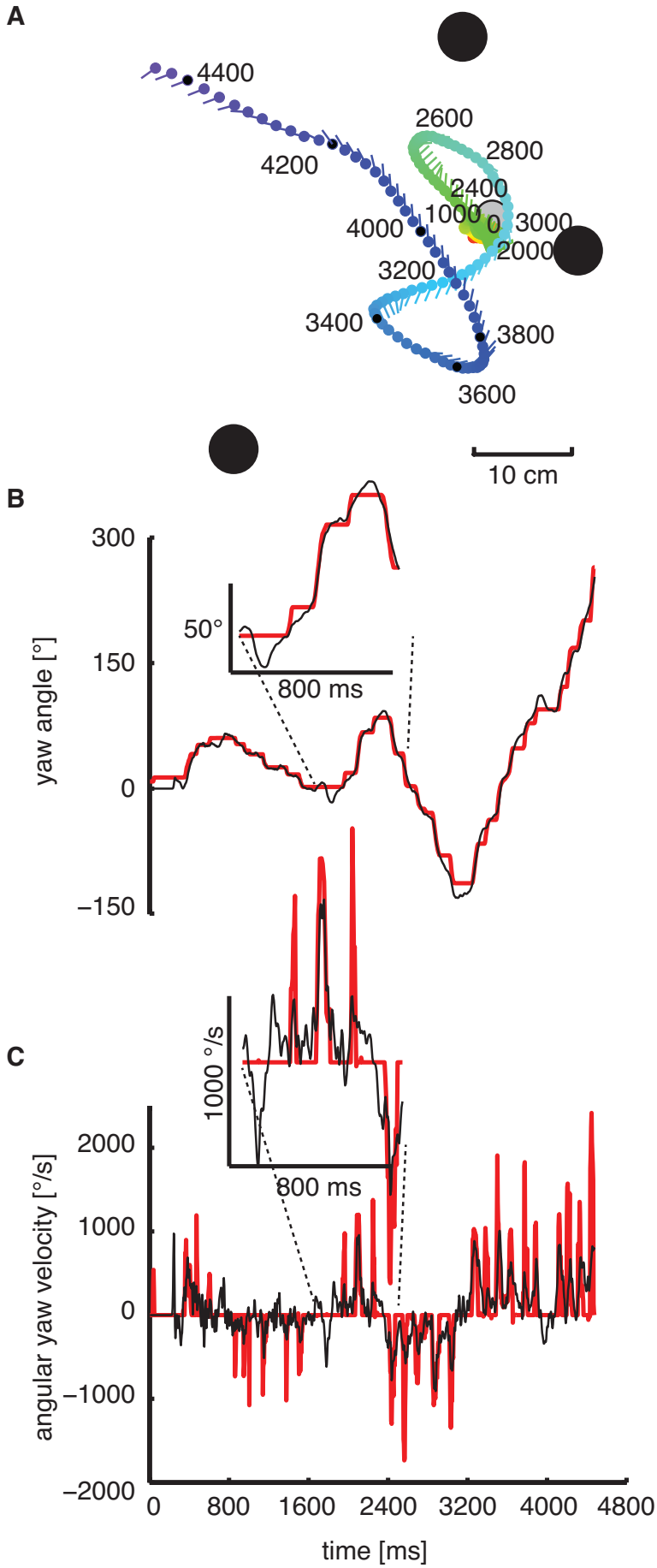


Fig. 2. Example of turn-back-and-look flight (TBL).

A: Top view of the typical flight trajectory of a bumblebee departing from the feeder (light grey circle). The position of the bee's head is shown every 16 ms. During the initial sections of this "turn-back-and-look" (TBL) flight the bee is facing the goal while backing away from it. The three landmarks are drawn in dark grey.

B: Head yaw angle (red) and body yaw angle (black) for the flight shown in A. It illustrates that the bee's head orientation (black) can deviate considerably from the yaw orientation of its body. The head usually turns with the thorax but at a higher angular speed, starting and finishing slightly earlier.

C: Head (red) and body (black) yaw angular velocity for the same flight. Head saccades partially coincide with body saccades, but not each body saccade leads to a head saccade. Inset: magnification of the yaw velocities illustrating the coincidence of saccadic head and body saccades.

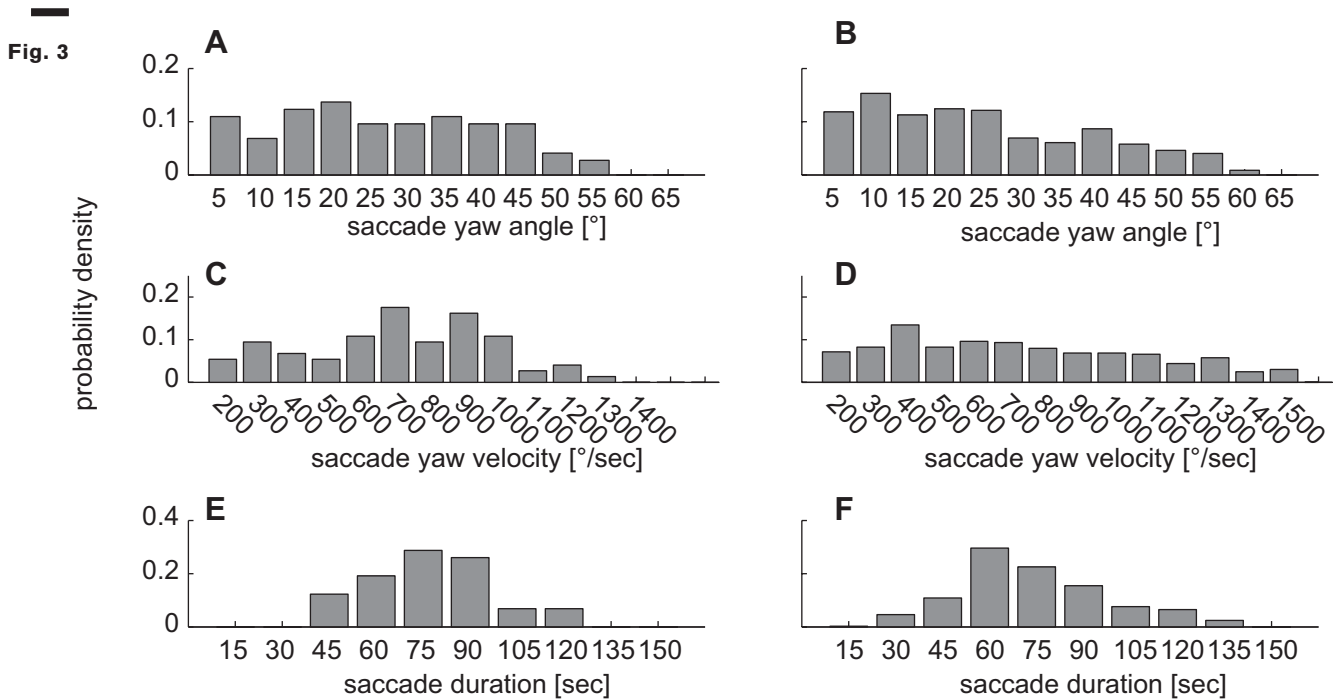


Fig. 3. Angular velocity and amplitude distributions.

Histograms for the amplitude, velocity and duration of head saccades are calculated from a total of 443 saccadic head movements for different head saccade size classes. Saccades were detected as peaks in yaw angular velocity. Each data plot is normalized to sum up to one. A, C, E: TBL flight saccade size, saccade velocity and saccade duration (n = 74). B, D, F: Angular velocity and amplitude distributions for return flights (n = 443).

It turned out that these are fairly similar for the two types of flights, with broadly distributed data in head yaw angles between 5° and about 60° (fig. 3A, B), but also – to a lesser degree - for the saccade duration that typically last for between 45 ms to 135 ms (fig. 3E, F). A small difference between learning flights and return flights is visible in the data of saccade yaw velocities: saccades with high angular velocity appear to occur slightly more often during return flights (fig. 3C, D). This could be due to the stereotypical flight choreography of learning flights, where the animal moves in loops and arcs in short straight flight segments during which gaze direction is kept constant. These segments are linked by saccadic head movements against the direction of the pivoting arc around the goal location. The saccadic head movements during learning flights seem to be part of an inherent motor programme that is present and very similar in all flying hymenopteran insects that have been analysed in detail (Boeddeker et al. 2010; Zeil et al 2012). Saccades during search flights appear to be distributed less regularly and less stereotypical in their sequence although they also share many similarities or 'motifs' with learning flights (Philippides et al. 2013). The occurrence of larger saccades during return flights than during learning flights might facilitate faster scanning of a larger part of the surroundings of the goal.

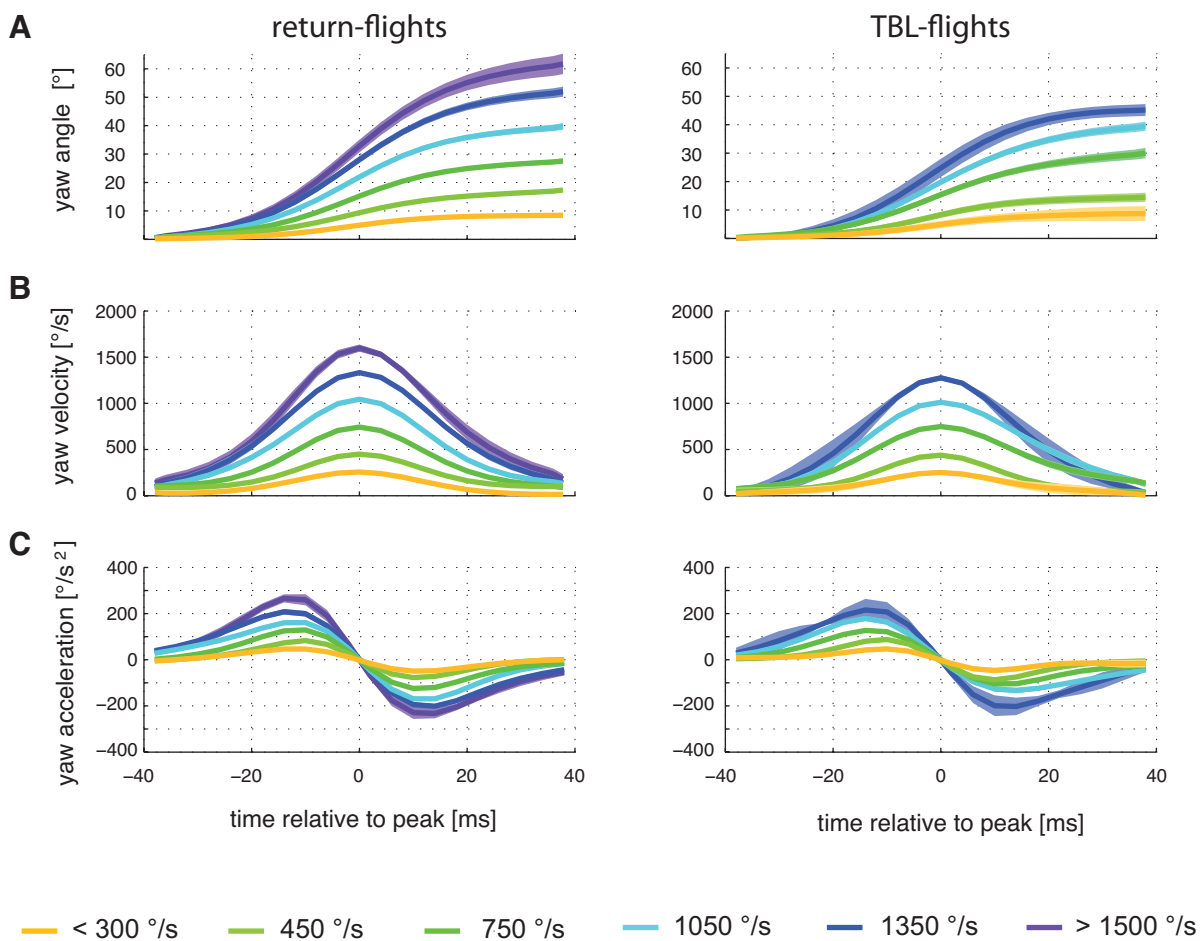


Fig. 4

Fig. 4. Average saccade amplitude, velocity and acceleration profiles.

Saccade-triggered averages of head yaw orientation (*A*), velocity (*B*) and acceleration (*C*) for all return (left) and TBL flights (right) around the peak velocity of each saccade from all saccades that fall within one of the velocity classes. All but the smallest and the largest velocity classes have a width of 300°/s and the numbers give the mean of the respective class (see legend). The shaded areas around the average lines (mean) depict the standard error of the mean. The angular velocity profile of saccadic head movements is very similar for different head saccade size classes and also for the two types of flights.

Resolving saccades at a finer time scale we see that all saccades show a similar pattern following a stereotyped time course that does not much change with saccade velocity (fig. 4). Although the distribution of measured saccade parameters is quite broad, we find a tight relationship between the angular velocity and the angular amplitude of saccadic head yaw turns during TBL flights (Pearson's $r = 0.81$ for all head saccades; see also fig. 5A). Although saccade peak velocities range from below 250 to 1500 °/sec, the angular velocity profile of saccadic head movements is very similar for different head saccade sizes (fig. 2A). The time course of saccades is symmetrical, which can be best seen in the yaw acceleration profiles. These acceleration profiles are symmetrical with respect to the maximum yaw velocity (0 ms relative to the peak of the saccade). Only the profiles of the two largest saccade amplitude classes (1200 °/s–1500 °/s and < 1500 °/s, which is only present during return flights) are significantly asymmetrical. For quantification of this finding we took the integral of the acceleration profile from -38 ms to 0 ms and subtracted the second half of this profile for every saccade (0 ms to 38 ms). If there is an asymmetry this value should differ from zero. Only the two large saccade classes proved to be significantly different from the others (Kruskal-Wallis test; $p < 0.01$). Thus, from the saccade velocity profiles, large saccades appear to be magnified versions of small saccades. To quantify this, we fitted Gaussian velocity profiles to all saccades within the different size classes using the 'fminsearch' function in Matlab to fit an 80 ms long Gaussian curve to the yaw velocity profile of every single saccade. The fitting parameters were the location of the mean, sigma (standard deviation), the offset value, and the gain value). We find that the scaling (gain) is indeed the main factor that determines the difference between small and large saccades since. Saccade width, estimated by the Gaussian fit to be in the range of 10 ms to 15 ms, is similar for all saccades independent of their size (Kruskal Wallis Test, $p = 0.27$). The kinematics of the different sized saccades seems to be determined by a tightly controlled and stereotypical motor programme.

As another characteristic feature of bumblebee head saccades we can identify the tight relationship between the velocity with which the head moves and the saccade amplitude. Saccade amplitude and velocity are closely related (fig. 5A; $r = 0.84$). Saccadic duration, as determined with the algorithm described above, increases in a non-linear manner as the amplitudes (size) of saccades increase from about 30 ms for the smallest to over 100 ms for the largest saccades (fig. 5B). Even though the

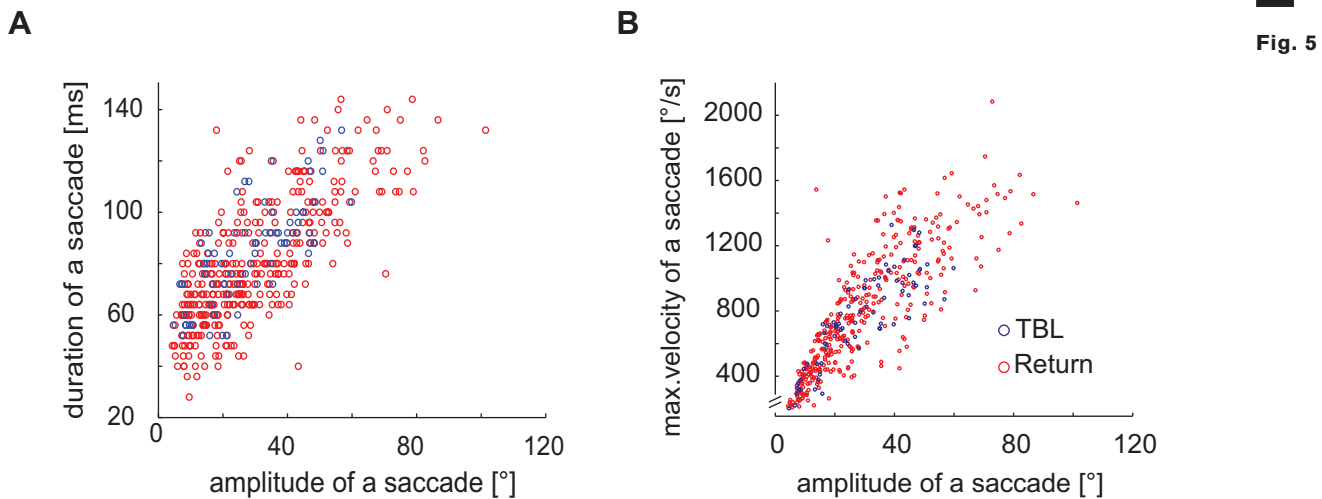


Fig. 5 Correlation between saccade duration, peak velocity and amplitude of saccadic head movements.

The saccade duration was calculated from the start and end points as determined with the saccade finding algorithm that uses a combined velocity threshold and slope criterion (see results section). Saccades from the two kinds of flight both follow a strict pattern and show very similar characteristics on the fine time scale analysed here. For this reason we take the two types together for the correlation analysis. Figure A shows a strong relationship between saccade amplitude and velocity (Pearson's $r = 0.84$) and B also demonstrates that saccades are highly stereotypical movements with the duration and saccade amplitude being closely related ($r = 0.74$). Please note that the pattern that is visible in B is due to the sampling interval of our high-speed video system (4ms).

underlying motor programme might be very similar for the different sized saccades, the durations are different. This might seem slightly paradoxical in the first place, but is mainly a consequence that the saccade-defining threshold is earlier reached due to the higher velocity of large saccades than in small saccades through a stronger acceleration. The strong relationship between saccade duration and saccade amplitude (fig. 5B; $r = 0.74$) further indicates that saccades follow a strict pattern and again demonstrates that saccades are highly stereotypical movements that mainly differ in their velocity.

DISCUSSION

Why is it so important for flying animals to control the orientation of the optic flow field? We assume that the facilitation of depth perception from motion parallax is one important reason, because visual mechanisms that exploit the translational components of optic flow for odometry or depth perception are likely to break down, if contaminated by strong rotational optic flow.

Which sensory cues do bees exploit to orient their head and how are head and body movements coordinated?

A recent study shows that flying honeybees stabilise head roll orientation visually (Boeddeker & Hemmi 2009), and that vision dominantly controls head roll rotations. However, many details of the mechanisms controlling the bees' head and body rotations remain to be determined. Also the question what other sensory and neuronal mechanisms might assist in stabilising gaze against roll and yaw rotations during flight remains unsolved. A possible role may be attributed to hard-wired motor programs that might assist head-body coordination in both bees and flies. In vertebrates, similar forward models were proposed to predict the sensory consequences of actions and are thought to play a crucial role for understanding motor control (Wolpert & Ghahramani 2000). Moreover, there is recent evidence from invertebrates for the predictive modulation of sensory processes by motor output (Webb, 2004; Huston and Jayaraman, 2011). Information on saccade timing and rotational optic flow might be conveyed to neck muscles to keep the head levelled except for the brief periods of saccadic head orientation changes.

What is the functional advantage of the stereotypical eye movements?

Saccadic head movements in bumblebees share many similarities with saccades in other insects and even vertebrates like humans or monkeys. The consistent relationship between the duration, peak velocity and amplitude of human saccadic eye movements is known as the 'main sequence'. The reason why such a stereotypical relationships evolved is unknown (Harris and Wolpert, 2009). It was shown that the stereotypical durations and trajectories are optimal for minimizing the variability in saccade endpoints that is caused by motor noise (van Beers, 2008).

What is the impact of morphological differences between species and within species on vision and flight performance?

Head saccades in bees with their maximal yaw velocities around 1500 °/s are slower than head saccades in flies where yaw velocities above 2500 °/s have been measured (van Hateren & Schilstra 1999). Experiments by Hengstenberg (1993) and Sherman & Dickinson (2003, 2004) show that the fly's visual system is tuned to relatively slow rotation, whereas the haltere-mediated response to mechanical rotation increases with increasing angular velocity. Up to now it is not yet clear, whether honeybees or bumblebees possess specialised inertial sensors. The advantage of specialised inertial sensors would be their much shorter response delay than that of a motion vision system. The latency measured in neck motor neurones from haltere deflection is only about 3 ms in blowflies (Sandeman & Markl 1980), whereas visual motion stimuli evoke neural activity in the brain of flies with a delay of about 30 ms (Warzecha & Egelhaaf 2000). These findings indicate that fast haltere-mediated reflexes help flies to control their fast head-body coordination and thus enable them to perform very rapid flight manoeuvres. Rapid flight manoeuvres are the harder to perform the larger the animal's body weight is, and

the further the centre of mass is shifted away from the wingbases, which increases the moment of inertia (Cooper, 1993; Ellington, 1999). As the bumblebees' centre of mass is shifted strongly to the abdomen, these restrictions make it even more important for the bumblebee to cancel out rotational optic flow via head-body coordination.

Individual bumblebees also differ largely in size, which has certain implications for their visual system. For instance larger bumblebees have been shown to be more precise in single target detection (Spaethe, 2003) than smaller specimens. The same study revealed that the number of ommatidia involved in object detection correlates with body size. Since we did not want to address the complex issue of a potential size dependence of the fine structure of homing flights, we used only medium-sized bumblebees in our study.

Even between the closely related honeybees and bumblebees a number of differences could be found that might influence their navigational performance. Compared to honeybees bumblebees possess a resolution that is approximately 25% higher than that of honeybees since they can resolve gratings with higher spatial frequencies, indicating a larger visual acuity (Srinivasan and Lehrer, 1988; Macuda et al., 2001). And even though both honeybees and bumblebees have almost identical photoreceptor sensitivity spectra (Peitsch et al., 1992), colour discrimination performance of bumblebees is not as good as that of honeybees (Dyer et al., 2008). Despite these differences in the peripheral visual system we found honeybees and bumblebees to exhibit a very similar performance in their performance in navigation according to visual landmarks.

Reasons for a partial decoupling of head and body orientation

We find here that in bumblebees (fig. 3C) the general relationship between head and body orientation is very similar to honeybees (Boeddeker et al., 2010). In a recent study on bumblebees employing high-speed recordings de Ibarra et al. (2009) concluded that the bumblebees' body orientation allows a reasonable estimate of gaze direction. However the same authors also find a substantial deviation of the head orientation compared to its body orientation. As the dynamics of the bees' optical input depend crucially on the orientation of its head rather than its body we considered the exact measurement of head orientation on a fine time scale necessary. Using high-speed cameras we were capable to reveal fine temporal details on the coordination of head and body saccades that most likely will have an impact on optic flow processing neurones in the bumblebees' brain. For blowflies, Kern and colleagues could show in this context that the temporal differences in head and body rotations of blowflies are relevant for motion processing in the fly's visual system (Kern et al. 2006). More specifically, they indicated that if the fly's head were tightly coupled to the body, the resulting optic flow during intersaccades would not contain behaviourally relevant information about the spatial layout of the environment. Losing this information would heavily impair the bees' ability to navigate on a local scale using visual landmarks via optic flow as a relevant cue helping to find the goal location (Dittmar et al., 2010; Kapustjansky et al., 2010). The detailed knowledge on the behavioural dynamics of eye movements presented here, thus provides the fundament for future experiments on the coding

properties of visual motion sensitive neurones in the bumblebee brain, since the dynamics of the visual input perceived by a homing bee crucially depends on the dynamics of its behaviour.

ACKNOWLEDGEMENTS

We thank Tim Siesenop for analysing part of the video sequences. The study was supported by the Deutsche Forschungsgemeinschaft (DFG). L.D. was funded by the Studienstiftung des deutschen Volkes.

REFERENCES

Van Beers RJ (2008) Saccadic eye movements minimize the consequences of motor noise. *PloS one* 3:e2070.

Bender, J. A. & Dickinson, M. H. (2006) A comparison of visual and haltere-mediated feedback in the control of body saccades in *Drosophila melanogaster*. *J Exp Biol* 209: 4597–4606.

Boeddeker N, Dittmar L, Stürzl W, Egelhaaf M (2010) The fine structure of honeybee head and body yaw movements in a homing task. *Proc R Soc Lond B* 277:1899–1906.

Boeddeker, N., & Hemmi, J. M. (2009) Visual gaze control during peering flight manoeuvres in honeybees. *Proc R Soc Lond B* 1685:1209–1217

Boeddeker, N., Lindemann, J., Egelhaaf, M., & Zeil, J. (2005) Responses of blowfly motion-sensitive neurons to reconstructed optic flow along outdoor flight paths. *J Comp Physiol A* 191:1–13.

Bouquet, J. (1999) Visual methods for three-dimensional modeling. California Institute of Technology.

Braun E, Dittmar L, Boeddeker N, Egelhaaf M (2012) Prototypical components of honeybee homing flight behavior depend on the visual appearance of objects surrounding the goal. *Front Behav Neurosci* 6:1–16.

Collett TS, Collett M (2002) Memory use in insect visual navigation. *Nature reviews Neuroscience* 3:542–552.

Collett, T. S. Graham, P. Harris, R. A. Hempel-De-Ibarra, N. (2006) Navigational memories in ants and bees: Memory retrieval when selecting and following routes. *Adv Stud Behav* 36:123–172.

- Collett TS, de Ibarra NH, Riabinina O, Philippides A (2013) Coordinating compass-based and nest-based flight directions during bumblebee learning and return flights. *J Exp Biol* 216: 1105–1113.
- Collett, T. S. & Land, M.F. (1975) Visual spatial memory in a hoverfly. *J Comp Physiol A* 100: 59–84.
- Collett, T. S., & Paterson, C. J. (1991) Relative motion parallax and target localisation in the locust, *Schistocerca gregaria*. *J Comp Physiol A* 169:615–621.
- Collett, T. S., (1978) Peering - A locust behavior pattern for obtaining motion parallax information. *J Exp Biol* 76:237–241.
- Collett, T. S. (1988) How ladybirds approach nearby stalks: a study of visual selectivity and attention. *J Comp Physiol A* 163:355–363.
- Cooper AJ (1993) Limitations of bumblebee flight performance, 222p.
- Dickinson, M. (1999) Haltere-mediated equilibrium reflexes of the fruit fly, *Drosophila melanogaster*. *Philos Trans R Soc Lond B* 354:903–916.
- Dittmar L, Stürzl W, Baird E, Boeddeker N, Egelhaaf M (2010) Goal seeking in honeybees: matching of optic flow snapshots? *J Exp Biol* 213:2913–2923.
- Dyer AG, Chittka L (2004a) Bumblebees (*Bombus terrestris*) sacrifice foraging speed to solve difficult colour discrimination tasks. *J Comp Physiol A* 190:759–763.
- Dyer AG, Chittka L (2004b) Fine colour discrimination requires differential conditioning in bumblebees. *Die Naturwissenschaften* 91:224–227.
- Dyer AG, Spaethe J, Prack S (2008) Comparative psychophysics of bumblebee and honeybee colour discrimination and object detection. *J Comp Physiol A* 194:617–627.
- Egelhaaf M, Boeddeker N, Kern R, Kurtz R, Lindemann JP (2012) Spatial vision in insects is facilitated by shaping the dynamics of visual input through behavioral action. *Front neur circ* 6:108.
- Ellington CP (1999) The novel aerodynamics of insect flight: applications to micro-air vehicles. *J. Exp Biol* 202:3439–3448.
- Gibson, J. J. (1950) *The perception of the visual world*. Oxford, England: Houghton Mifflin.
- Hardie, R. C. (1986) The photoreceptor array of the dipteran retina. *Trends Neurosci.* 9:419–423.

- Harris CM, Wolpert DM (2009) The main sequence of saccades optimizes speed-accuracy trade-off. *Biol Cybernetics* 95:21–29.
- Hedrick, T.L., Cheng, B. & Deng, X. (2009) Wingbeat time and the scaling of passive rotational damping in flapping flight. *Science* 324:252–255.
- Hempel de Ibarra, N., Philippides, A., Riabinina, O., & Collett, T. S. (2009) Preferred viewing directions of bumblebees (*Bombus terrestris* L.) when learning and approaching their nest site. *J Exp Biol* 212:3193–3204.
- Hengstenberg, R. (1988) Mechanosensory control of compensatory head roll during flight in the blowfly *Calliphora erythrocephala* Meig. *J Comp Physiol A* 163, 151–165.
- Hengstenberg, R. (1993) Multisensory control in insect oculomotor systems. In *Visual motion and its role in the stabilization of gaze* F. A. Miles & J. Wallman (eds.), Amsterdam, The Netherlands: Elsevier, 285–298.
- Huston SJ, Jayaraman V (2011) Studying sensorimotor integration in insects. *Current Opinion in Neurobiology* 21:527–534.
- Kapustjansky A, Chittka L, Spaethe J (2010) Bees use three-dimensional information to improve target detection. *Die Naturwissenschaften* 97:229–233.
- Kern, R., van Hateren, J. & Egelhaaf, M. (2006) Representation of behaviourally relevant information by blowfly motion-sensitive visual interneurons requires precise compensatory head movements. *J Exp Biol* 209:1251–60.
- Kern, R., van Hateren, J., Michaelis, C., Lindemann, J., & Egelhaaf, M. (2005) Function of a fly motion-sensitive neuron matches eye movements during free flight. *PLoS Biol.* 3(6) e171.
- Kimmerle, B., Egelhaaf, M., & Srinivasan, M. V. (1996) Object detection by relative motion in freely flying flies. *Naturwissenschaften* 83:380–381.
- Koenderink JJ, Doorn AJ Van (1987) Facts on optic flow. *Biol Cybernetics* 254:247–254.
- Kral, K., & Poteser, M. (1997) Motion parallax as a source of distance information in locusts and mantids. *J Insect Behav* 10:145–163.
- Land, M.F. (1973) Head movement of flies during visually guided flight. *Nature* 243:299–300.
- Land, M. (1999) Motion and vision: why animals move their eyes. *J Comp Physiol A* 185:341:352.
- Lappe, M. (2000) *Neuronal processing of optic flow*. New York, NY: Academic Press.

- Lehrer, M., (1991) Bees which turn back and look. *Naturwissenschaften* 78:274–276.
- Lehrer, M. (1996) Small-scale navigation in the honeybee: active acquisition of visual information about the goal. *J Exp Biol* 199:253–261.
- Lehrer M (1993) Why do bees turn back and look? *J Comp Physiol A* 172:549–563.
- Lehrer, M., & Campan, R. (2005) Generalization of convex shapes by bees: what are shapes made of? *J Exp Biol* 208:3233–3247.
- Lihoreau M, Chittka L, Le Comber SC, Raine NE (2012) Bees do not use nearest-neighbour rules for optimization of multi-location routes. *Biology letters* 8:13–16.
- Macuda T, Gegear RJ, Laverty TM, Timney B (2001) Behavioral assessment of visual acuity in bumblebees (*Bombus impatiens*). *J Exp Biol* 204:559–564.
- Morawetz L, Spaethe J (2012) Visual attention in a complex search task differs between honeybees and bumblebees. *J Exp Biol* 215:2515–2523.
- Nalbach, G. (1993) The halteres of the blowfly *Calliphora* 1. Kinematics and dynamics. *J Comp Physiol A* 173:293–300.
- Paulk AC, Dacks AM, Gronenberg W (2009a) Color processing in the medulla of the bumblebee (Apidae: *Bombus impatiens*). *J Comp Neurol* 513:441–456.
- Paulk AC, Dacks AM, Phillips-Portillo J, Fellous J-M, Gronenberg W (2009b) Visual processing in the central bee brain. *J Neurosci* 29:9987–9999.
- Paulk AC, Phillips-Portillo J, Dacks AM, Fellous J-M, Gronenberg W (2008) The processing of color, motion, and stimulus timing are anatomically segregated in the bumblebee brain. *J Neurosci* 28:6319–6332.
- Peitsch D, Fietz a, Hertel H, de Souza J, Ventura DF, Menzel R (1992) The spectral input systems of hymenopteran insects and their receptor-based colour vision. *J Comp Physiol A* 170:23–40.
- Pfeiffer K, Kinoshita M (2011) Segregation of visual inputs from different regions of the compound eye in two parallel pathways through the anterior optic tubercle of the bumblebee (*Bombus ignitus*). *J Comp Neurol* 229:212–229.
- Philippides, A., de Ibarra, N. H., Riabinina, O., & Collett, T. S. (2013) Bumblebee calligraphy: the design and control of flight motifs in the learning and return flights of *Bombus terrestris*. *J Exp Biol* 216:1093–104.

- Pringle, J.W.S., (1948) The gyroscopic mechanism of the halteres of diptera. Phil Trans R Soc Lond B 233:347–384.
- Riveros AJ, Gronenberg W (2009) Learning from learning and memory in bumblebees. Naturwissenschaften 96:437–440.
- Sandeman, D. & Markl, H., (1980) Head movements in flies (*Calliphora*) produced by deflexion of the halteres. J Exp Biol 85:43–60.
- Schilstra, C. & van Hateren, J.H. (1998) Stabilizing gaze in flying blowflies. Nature 395:654.
- Schilstra, C., & van Hateren, J. H. (1999) Blowfly flight and optic flow. I. Thorax kinematics and flight dynamics. J Exp Biol 202:1481–1490.
- Sherman, A., & Dickinson, M. (2003) A comparison of visual and haltere-mediated equilibrium reflexes in the fruit fly *Drosophila melanogaster*. J Exp Biol 206:295–302.
- Sherman, A., & Dickinson, M. (2004) Summation of visual and mechanosensory feedback in *Drosophila* flight control. J Exp Biol 207:133–142.
- Spaethe J (2003) Interindividual variation of eye optics and single object resolution in bumblebees. J Exp Biol 206:3447–3453.
- Srinivasan M V., Lehrer M (1988) Spatial acuity of honeybee vision and its spectral properties. J Comp Physiol A 162:159–172.
- Srinivasan, M. V. & Zhang, S. (2004) Visual motor computations in insects. Annu. Rev. Neurosci. 27:679–696.
- Taylor, G. K. & Krapp, H. G. (2007) Sensory systems and flight stability: what do insects measure and why? Adv. Insect Physiol. 34:231–316.
- van Hateren J. H. & Schilstra, C. (1999) Blowfly flight and optic flow. II. Head movements during flight. J Exp Biol 202:1491–1500.
- Warzecha, A.-K. & Egelhaaf, M. (2000) Response latency of a motion-sensitive neuron in the fly visual system: dependence on stimulus parameters and physiological conditions. Vis. Res. 40:2973–2983.
- Webb, B. (2004) Neural mechanisms for prediction: do insects have forward models? Trends Neurosci 27:278–82.
- Wehner, R. & Flatt, I. (1977) Visual fixation in freely flying bees. Z Naturforsch 32:469–471.

Wolpert, D. M., & Ghahramani, Z. (2000) Computational principles of movement neuroscience. *Nature Neurosci* 3:1212–1217.

Zeil J (2012) Visual homing: an insect perspective. *Current opinion in neurobiology* 22:285–293.

Zeil J., Boeddeker N., Hemmi J.M. & Stürzl W. (2007) Going wild: Toward an ecology of visual information processing. In: *Invertebrate Neurobiology*, North G. & Greenspan R. (eds.), New York: Cold Spring Harbor Press, 381–403.

Zeil, J., Boeddeker, N., & Hemmi, J. M. (2008) Vision and the organization of behaviour. *Curr Biol* 18:320–323.

Zeil J, Boeddeker N, Stürzl W (2009) Visual homing in insects and robots. In: *Flying Insects and Robots*, Floreano D et al (eds), Berlin Heidelberg, New York: Springer Verlag, 87–100.

Zhang, S. W., Srinivasan, M. V. & Collett, T. (1995) Convergent processing in honeybee vision: multiple channels for the recognition of shape. *Proc Natl Acad Sci USA* 92:3029–3031.

2

VISUAL MOTION-SENSITIVE NEURONS IN THE BUMBLEBEE BRAIN CONVEY INFORMATION ABOUT THE PRESENCE OF LANDMARKS DURING A NAVIGATIONAL TASK

The content of this chapter is submitted for publication as: M Mertes, L Dittmar, M Egelhaaf, N Boeddeker: **VISUAL MOTION-SENSITIVE NEURONS IN THE BUMBLEBEE BRAIN CONVEY INFORMATION ABOUT THE PRESENCE OF LANDMARKS DURING A NAVIGATIONAL TASK.**

ABSTRACT

Bees use visual memories to learn the spatial location of their food sites. Characteristic learning flights help acquiring these memories at newly discovered foraging locations where landmarks - salient objects in the vicinity of the goal location - can play an important role in guiding the animal's homing behaviour. Although behavioural experiments have shown that bees can use a variety of visual cues to distinguish objects as landmarks, the question of how these landmark features are encoded by the visual system is still open.

To tackle this question, we tracked learning flights of free-flying bumblebees (*Bombus terrestris*) in an arena with distinct visual landmarks, reconstructed the visual input during these flights, and replayed ego-perspective movies to tethered bumblebees while recording the activity of direction-selective wide-field neurons in their optic lobe.

By comparing neuronal responses during a typical learning flight and targeted modifications of landmark properties in this movie we demonstrate that these objects are indeed represented in the bee's visual motion pathway. We find that object-induced responses vary little with object texture, which is in agreement with behavioural evidence. These neurons thus convey information about landmark properties that are useful for navigation.

INTRODUCTION

Bees, ants, and wasps are exquisitely able to find back to important places like their nest or valuable food sources using different navigational strategies including path integration, route following and landmark navigation (Menzel et al., 1996; Collett et al., 2006; Zeil et al., 2009). Landmarks are salient objects that provide reliable information about the goal location (Gillner et al., 2008), and honeybees are even able to find a goal between camouflaged landmarks that carry the same texture as the background. For this reason, it has been proposed that they memorize the motion pattern on their eyes (“optic flow”) generated during translational movements (“optic flow snapshot matching”; Boeddeker et al., 2010; Dittmar et al., 2010).

During translational movements, close objects move faster on the retina than objects further away, allowing the bee to potentially use these motion parallax cues to determine the spatial relation of the goal and the landmarks. In contrast, during rotations of the animal the perceived optic flow is independent of object distance, and all objects move with the same speed on the retina. Therefore, it has been suggested that the processing of depth information from motion parallax depends crucially on the saccadic flight strategy largely separating rotational movements from translation and that has been described in a variety of insects, such as blowflies and (Egelhaaf et al., 2012). These insects minimize the time of flight during which rotations occur by performing fast body and head rotations (“saccades”)(Hateren and Schilstra, 1999; Kern et al., 2005; Boeddeker and Hemmi, 2010; Boeddeker et al., 2010). Within the longer segments of flight, the intersaccades, they move on a straight course and, therefore, perceive almost purely translational optic flow.

This gaze strategy, thus, appears to facilitate gathering spatial information by the nervous system (Kern et al., 2005, 2006; Karmeier et al., 2006). Processing of depth information from translational optic flow depends heavily on precise gaze stabilization against rotations, which has been demonstrated in locusts and blowflies (Collett, 1978; Kern et al., 2006). Gaze stabilization can thus be regarded as an important prerequisite for successful navigation.

To navigate back to a goal location a bee gathers information about the landmark constellation around the goal. This information is presumably acquired and stored during learning flights where the bees face the goal and perform highly stereotyped arcs and loops at and around the goal location (Lehrer, 1993; Zeil et al., 1996; Hempel de Ibarra et al., 2009; Collett et al., 2013; Philippides et al., 2013).

To better understand the neuronal mechanisms bees and other insects use to relate the current visual input to the previously learned input, we need to know how the environment is represented in the animal’s visual system during navigation. Landmark detection by relative motion cues is highly relevant, in particular, if the landmarks are textured with a camouflaging pattern. Therefore, the influence of landmarks on neuronal responses in the visual motion pathway is a relevant issue. This issue has not been addressed so far, although important groundwork was provided by studies successfully

characterizing neurons in the relevant brain areas (Ribi, 1976; Ribi and Scheel, 1981; DeVoe et al., 1982; Paulk et al., 2008). Thus, we analysed the responses of motion sensitive neurons in the optic lobe of bumblebees to retinal motion sequences as were seen by the bee during a learning flight. Combining behaviour and physiology in this way, we find that the responses of visual motion-sensitive wide-field neurons also provide information about the spatial layout of the landmark arrangement, and that the texture of landmarks has no major impact on the neuronal responses. Object-induced response components in motion sensitive cells are also strong during the saccadic turns, although during such fast turns the perceived optic flow is dominated by rotational optic flow components.

MATERIAL AND METHODS

Koppert (Berkel en Rodenrijs, The Netherlands) provided commercial bumblebee hives that we kept in custom-built perspex boxes at a day / night cycle of 12 hrs. for both phases. The temperature was kept between 23 ± 2 °C at 50 % relative humidity. Exclusively bumblebee workers were used for the experiments.

Behavioural experiments

We let bumblebees (*Bombus terrestris*) enter a circular flight arena (diameter: 1.95 m) that was lined with a Gaussian-blurred red/white random dot texture on walls (height: 50 cm) and floor. The bees were trained to find a see-through Perspex feeder (height: 10 cm) providing a sugar solution between three homogeneously textured cylinders that acted as landmarks (red, height: 25 cm, diameter: 5 cm). To test whether the bumblebees used the landmarks to solve the task, we placed the feeder outside the landmark arrangement in control trials. In these cases the bumblebees did not find the feeder, which underlines the role of the cylinders as landmarks.

We filmed learning flights at 250 images per second with two high-speed cameras (Redlake Motion Pro 500). One camera viewed the flight arena from the side, the other from above, enabling us to reconstruct a 3D flight trajectory afterwards.

The complete setup and experimental procedure of the behavioural experiment are described in greater detail in (Dittmar et al., 2010) where a similar methodology was used.

Reconstruction of natural optic flow

We reconstructed the movies with a custom-built software (Braun and Lindemann, 2011) and used the Camera Calibration Toolbox (Bouget, Jean, 1999) in Matlab (The Mathworks) to compose a 3D head and body trajectory out of the two 2D trajectories (for details see Kern et al., 2005; Dittmar et al., 2010).

We assumed a constant head roll angle of 0° and a pitch angle of the bee's head of 24° shifted up relative to the horizontal. These assumptions are based on head angle

measurements obtained from the side camera and close-up pictures of the bumblebee head anatomy.

We fed the 3D-trajectory of a learning flight into a virtual model of the flight arena using custom-built software (Braun and Lindemann, 2011) and determined a panoramic image sequence of what the bumblebee had seen from all the reconstructed positions during this flight [condition 2]. When generating the image sequences, the flight arena was manipulated virtually in four different ways leading to five different image sequences of nearly 4.5 s duration: we either left out the objects [condition 1], changed the texture of the objects [condition 3], or changed the texture of the background (walls and floor changed to grey, conditions 4 and 5). Apart from these manipulations the flight trajectory used for generating the movie was the same. The ceiling of the flight arena was always grey (half-maximum brightness). In stimulus condition 6 we presented a homogeneously grey screen to the bee. This condition was employed to measure spontaneous neuronal activity. For an overview on the stimulus conditions see figure 2.

The head yaw orientation used for stimulus calculation was determined for each frame by the top camera. This was done manually, because automatic tracking of head orientation turned out to be hard to achieve. To validate this manual tracking, we obtained image sequences based on a second, independent measurement of the head trajectory performed by another person and found that it did not noticeably affect the neuronal responses. Thus, we combined the data based on both trajectory versions to a single dataset.

Additional to the reconstructed natural image sequences, we also presented bars (10° by 20°) moving horizontally and vertically in both directions at a speed of $100^\circ/\text{s}$, to coarsely measure the size and location of the cells' receptive fields.

Electrophysiological experiments

We used bumblebees of body length 1.5 ± 0.3 cm. With bee wax we glued the back of the thorax onto a small piece of glass, removed the legs and bent the head backwards. Then we glued the bee's head to the edge of the glass without restricting the field of view, but covered the ocelli. Afterwards, we opened the left hemisphere of the head capsule and exposed the lobula.

To ensure the correct placement of the bumblebee within the stimulus device throughout the experiments, we oriented the long axis of the bee's eyes vertically, compensated for roll around the body long axis and centred the animal's head with the antenna bases as points of reference.

We pulled microelectrodes with a Sutter P-1000 puller from aluminosilicate glass pipettes (Harvard Apparatus, UK) and inserted them into the lobula of the left brain hemisphere. Filled with 1 mol/l KCl they typically had a resistance range of 40 ± 20 M Ω . As reference electrode a chlorinated silver wire was inserted into a small cut on the other side of the head capsule. The temperature range during the recordings was $30 \pm 3^\circ\text{C}$. In this temperature range a cross-covariance analysis indicated that the time lag between visual input and neuronal response changes was between 21 ms to 36 ms in different bees.

We recorded from motion-sensitive and direction-selective wide-field neurons. They reacted strongest to wide-field stimulation, but were also responsive to horizontally moving small bars. Visual stimulation in their preferred direction of motion resulted in graded membrane potential changes partly superimposed by spikes (Fig.1). The resting membrane potential was typically around -50 mV with a modulation depth of up to 11 mV. Spike-like depolarisations superimposed on the graded response component with up to 35 mV in amplitude similar as has been described for several types of fly motion sensitive neurons (Hausen, 1982; Haag and Borst, 1997). The horizontal extent of the cells' receptive fields ranged from approximately -10° to 100° , with zero being in front of the animal, and negative/positive values corresponding to the left and right half of the visual field, respectively. All neurons were sensitive to motion between 0° and 40° horizontal extent of the visual field.

Based on this functional characterization it was hard to further distinguish the cells into different subclasses without the use of neuroanatomical techniques or an extended presentation of more sophisticated classification stimuli, so we grouped these neurons as one functional class of cells. As the recording time was often limited to a few minutes, we decided to favour a larger number of stimulus repetitions to characterize the cells functionally at the expense of anatomical staining. Therefore, we were able to present five to twenty repetitions of each of the five stimulus conditions.

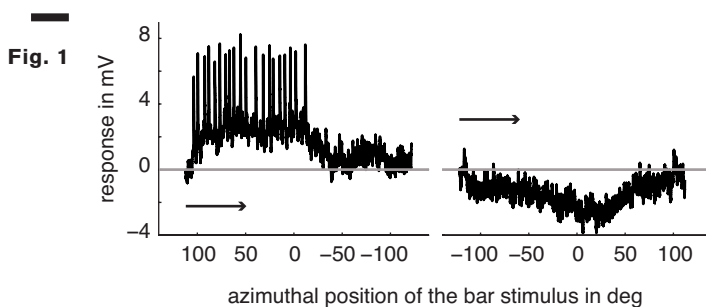


Fig. 1. Example of a single trace recording of a typical LWC sensitive to regressive motion.

Here, we presented a bar moving horizontally through the center of the cell's receptive field (elevation: $+20^{\circ}$ above horizon) from right to left and vice versa. The x-axis denotes the position of the first (of two) edges of the bar stimulus depending on the direction of movement. As indicated in the methods section the extent of the bar is 10° in azimuth and 20° in elevation and moves with $100^{\circ}/s$. The arrows indicate the direction of movement of the bar.

Stimulus presentation and data acquisition

For stimulus presentation we used an icosahedral, panoramic LED stimulus device (FliMax) covering most of the visual field of the bee. It employs a spatial resolution of 2.3° and thus matches the spatial resolution of the bee's eye quite well (for details see Lindemann et al., 2003). Stimuli were presented with 8 bits per pixel, allowing

256 different intensities. We up-sampled the bees' flight trajectory by linear interpolation in time, to be able to replay stimulus movies at 370 Hz, and presented them in pseudo-random order and with an inter-stimulus-interval of 4-6 s. Before each movie started all LEDs were lit for 1 s at half-maximum brightness followed by 0.5 s fading from grey into the first image of the stimulus movie. Due to the animal being mounted upside down, we flipped the stimulus movies along the horizontal axis and shifted the horizon slightly to account for the orientation of the long axis of the bumblebee's eye during flight.

The low-pass filtered response signal (2400 Hz cut-off frequency) was sampled at 8,192 Hz with a custom build amplifier, digitized (DT 3001, Data Translation, Marlboro, MA, USA) and stored for offline analysis using Matlab (The Mathworks, Natick, MA, USA).

Data analysis

Before further analysis, we subtracted the baseline membrane potential from all response traces. As a quality criterion for recordings used for further analysis, we set the minimum range of membrane potential changes to be at least 2 mV. To account for varying overall response amplitudes of different cells, we normalized the responses of each individual cell independently for saccadic and intersaccadic flight phases. To accomplish this, we averaged the neuronal responses to the stimulus sequence corresponding to the original behavioural experiments over the length of 27 intersaccades and 26 saccades and used the corresponding peak responses for normalization of the responses to all other stimulus conditions.

Correlation values (= R) were calculated with Matlab using the implemented calculation of the correlation coefficient (Matlab, n.d.).

RESULTS

Flight behaviour of bumblebees

To reconstruct the visual image sequences that are available to the bees during a learning flight we first analysed the bumblebees' behaviour in a local navigation paradigm. We trained them to find a see-through Perspex feeder between three salient objects that acted as landmarks in a textured flight arena. It took trained bumblebees between 4 and 229 seconds (mean = 40 s, s.d. = 49 s, n = 4, 53 flights in total) to find the feeder, which is in a similar range as for honeybees in the same experimental setup (Dittmar et al., 2010).

The structure of the bumblebees' flight manoeuvres was also very similar to that seen in honeybees (Dittmar et al., 2010) when searching for the (hardly visible) food source between the three landmarks (Fig. 3A). In the sample trace shown in Fig. 3A the bumblebee started at the feeder and hovered at first in front of it. Then it turned to the left, flew two arcs and finally to the exit of the arena. The fine structure of such flight manoeuvres is characterized by a pronounced saccadic separation of translatory and rotatory movements, similar to honeybees (Boeddeker et al., 2010). The corresponding

time course of the angular velocity around the yaw axis consists of relatively long phases with only small changes in head orientation (intersaccades), meaning that almost pure translational optic flow is perceived (Fig. 3C). These phases are interspersed by saccades with fast rotations of head and body around the yaw axis. This gaze strategy facilitates the acquisition of motion cues for distance estimation (Collett, 1978; Kern et al., 2006).

Based on these behavioural data we ask whether information about the spatial constellation of the landmarks that is used to find the feeder is reflected in neuronal responses of motion sensitive visual interneurons.

Fig. 2







| condition # | background texture | landmarks inserted | landmark texture | comment |
|-------------|---|--------------------|------------------|--|
| 1 |  random dots | - | - | to record background responses without objects |
| 2 |  random dots | yes | homogeneous | same stimulus as in navigational task |
| 3 |  random dots | yes | random dot | textured (camouflaged) objects |
| 4 |  gray | yes | homogeneous | pure influence of high contrast objects without background texture |
| 5 |  gray | yes | random dot | pure influence of textured objects without background texture |
| 6 |  gray | - | - | to record spontaneous neuronal activity |

Fig. 2. Overview on the used stimulus conditions.

The inserted pictures show one inserted landmark with the corresponding background texture (arena floor and wall) behind it. The ceiling was kept gray constantly. For more details see methods section. Throughout the main text, we refer to this figure using squared brackets containing numbers that indicate the stimulus condition that was presented, e.g. [cond. 2] or [1].

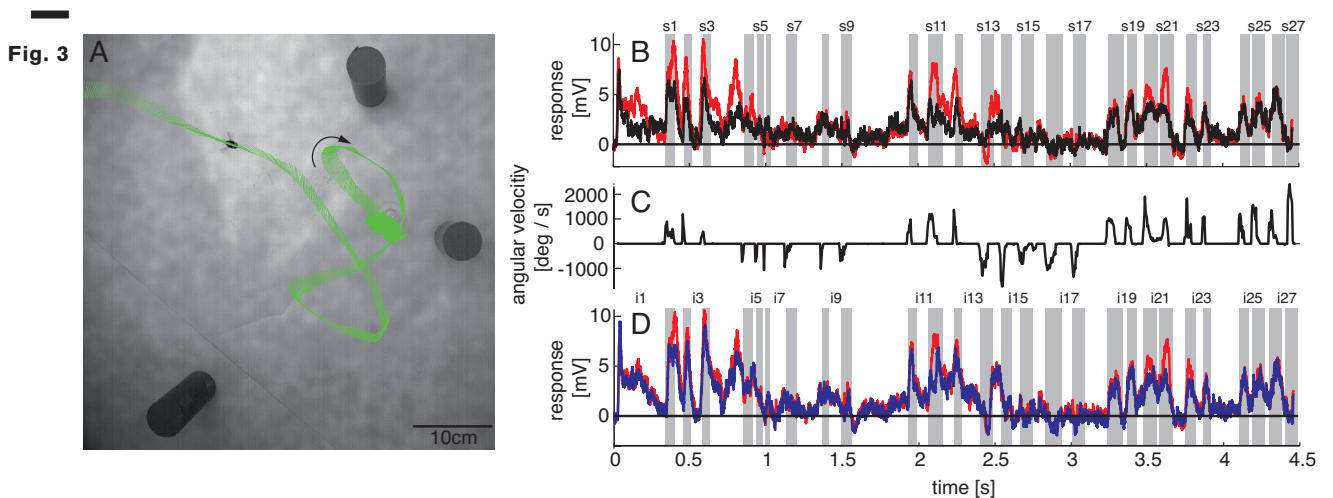


Fig. 3. Bumblebee flight trajectory and corresponding neuronal response traces of a single neuron with preferred direction of motion from back-to-front.

A: trajectory of a typical learning flight during the navigational task involving landmarks. Each green line indicates a point in space and the corresponding viewing direction of the bee's head each 4 ms. The arrow indicates the direction of flight. *B*: mean response traces of a single neuron recorded during presentation of two different stimulus conditions. Baseline membrane potential is subtracted. Red trace: homogeneous landmark condition ([cond.2]; 9 repetitions), black trace: no landmark condition ([cond.1]; 7 repetitions). Responses are subdivided into intersaccades and saccades (gray shadings). *C*: changes of head orientation. Positive/negative values denote turns to the left and right, respectively. *D*: response traces of the same neuron as in *B*. Red trace: as described above. Blue trace: random pattern landmark condition i.e. camouflaged landmarks ([cond.3]; 7 repetitions).

Are the landmarks represented in the neuronal responses?

To investigate the influence of the landmarks on the neuronal response of motion sensitive cells in the lobula we reconstructed the visual input during a typical learning flight of a bumblebee (Fig. 3A). We presented this ego-perspective movie, while the bee was tethered in the centre of our panoramic LED stimulus device. Additionally to the original optic flow sequence we presented several systematic alterations of it to study how different landmark properties are reflected in the neuronal responses (see methods section).

How is this naturalistic visual input reflected in the neuronal responses? Motion sensitive neurons in the bee lobula are known to respond in a direction-selective way to visual motion (DeVoe et al., 1982; Ibbotson, 1991; Paulk et al., 2008). In our account we focus on one class of lobula wide-field cells (LWC) that is direction-selective to horizontal motion, with a preferred direction from back-to-front. These cells respond to visual stimulation with graded membrane potential changes partly superimposed by spikes (Fig. 1), similar as depicted in DeVoe et al. (1982, Fig. 7). This response mode is also typical for visual interneurons in the fly (Hausen, 1982; Haag and Borst, 1997; Egelhaaf, 2006).

To assess how objects affect neuronal activity we compared the responses elicited by the original stimulus movie [cond. 2] to responses elicited by the same movie, but without landmarks [cond. 1]. The original movie corresponds to the visual input that is experienced by the freely flying bumblebee during a learning flight. In the 11 neurons that we recorded we find a strong object influence in the neuronal response in some sections of the flight (Fig. 3B). This object influence seems to be largely independent of object texture during intersaccades (Fig. 3D, non-shaded area). To determine the differences between neuronal response traces recorded under different stimulus conditions we averaged, for both saccades and intersaccades, the normalized difference of the responses to the stimulus conditions without objects [cond.1] and with objects that carry a different texture [cond.2 and cond.3]. Values that substantially deviate from zero indicate response changes due to the objects. Depending on the stimulus condition we were able to record from 7 and 11 neurons (the same 7 neurons plus 4 additional neurons). We see a characteristic temporal pattern in the profile of object-induced

response changes that is similar between intersaccades (Fig. 4, left side) and saccades (Fig. 4, right side). This pattern also remains when we artificially removed the background pattern to exclude background effects, and to just let the objects influence the neuronal responses (Figs. 4B, 4D). These general similarities of the intersaccadic and saccadic object-induced response profiles underline that the neuronal responses are shaped by the spatial layout of the environment. Therefore, LWCs not only perceive wide-field motion, but their responses also convey information about the spatial constellation of the landmarks, which are important for bees to be able to find their goal during local navigation.

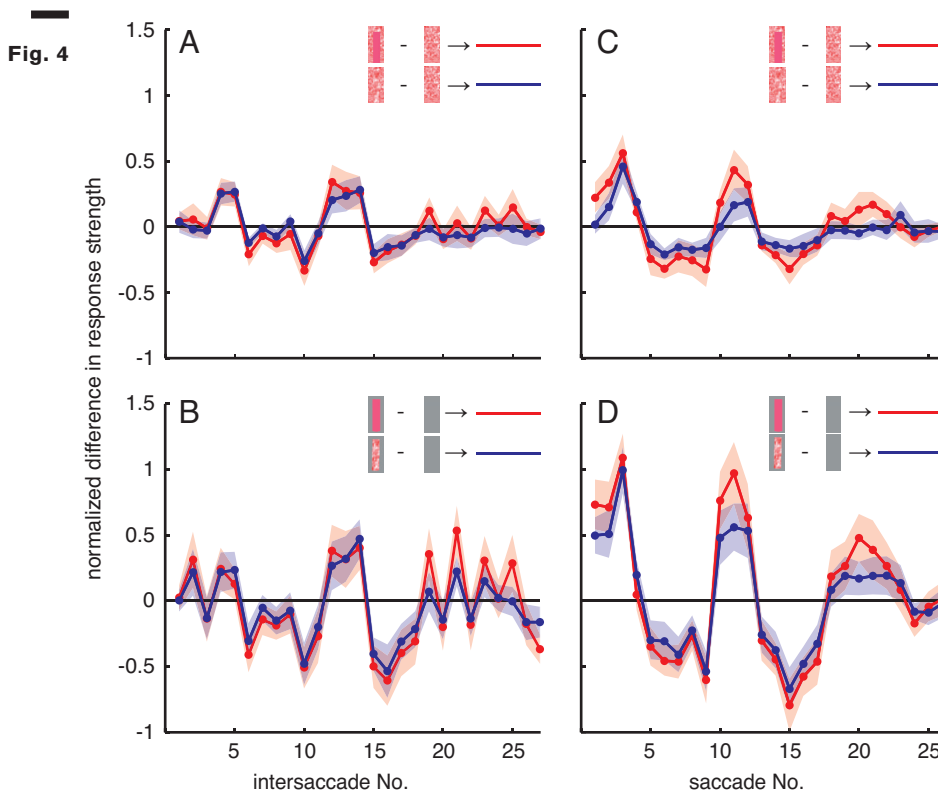


Fig. 4. Response profiles of mean, normalized differences between pairs of stimulus conditions for consecutive intersaccades.

A, B and saccades *C, D* during the learning flight of LWCs with a preferred direction from back-to-front. *A, C*: mean normalized difference of responses to one stimulus condition with object and one without ('object-induced response changes'). Red traces: object-induced response change for 'homogeneous landmark' [2] and 'no landmark' condition [1]. Blue traces: object-induced response change for 'random pattern landmark' condition [3] and 'no landmark' condition [1]. For *A* and *C* the number of included cells is $n = 11$. *B, D*: traces have the same meaning as in *A* and *C*, but object-induced response changes were induced by stimulus conditions with the random background being replaced by a uniform gray background. For *B, D*, $n = 7$. Shadings indicate SEM. For details on normalization procedure see Material and Methods.

Neuronal responses to camouflaged landmarks

Bees can use camouflaged landmarks that carry the same texture as the background for homing, and the search time for such objects is similar to that seen for high-contrast landmarks (Dittmar et al., 2010). Since these camouflaged landmarks are hard to detect in stationary images, it was suggested that bees might use relative motion cues, present in optic flow during flight, to perceive them (Dittmar et al., 2010). To test whether landmarks that can be discriminated only by relative motion cues are reflected in the neuronal responses of LWCs, we camouflaged the objects by using the same random dot texture for the objects and the background [cond. 3], i.e. floor and walls.

In accordance with the characteristics of goal-finding behaviour (Dittmar et al., 2010) the object-induced intersaccadic responses do not differ much between objects with random dot texture and homogeneously red texture (Fig. 4A). To confirm the object influence on the neuronal responses with a less complex stimulus, we also presented stimuli with both versions of object texture, but with arena wall and floor being plain grey [cond. 4 and 5]. This way the background does not have any influence on the neural responses, leaving just the objects to shape them. Under these conditions the profile of object-induced response changes is similar to those profiles obtained with a textured background (compare Figs. 4A and 4B). The only prominent difference is the larger modulation depth of the profile under the conditions without background (Fig. 4B). This can potentially be attributed to different contrast values between background and object. The similarity of the intersaccadic profiles of object-induced response changes obtained with different object and background textures corroborates the above conclusion that during learning flights the intersaccadic neural responses provide information about the spatial layout of landmarks in the vicinity of the goal. We obtained similar results also for a second class of LWCs, which we recorded less often and that had a preferred direction of motion from front-to-back (Fig. 5). These cells showed general properties that were very similar to back-to-front LWCs. Only the preferred direction of motion was opposite.

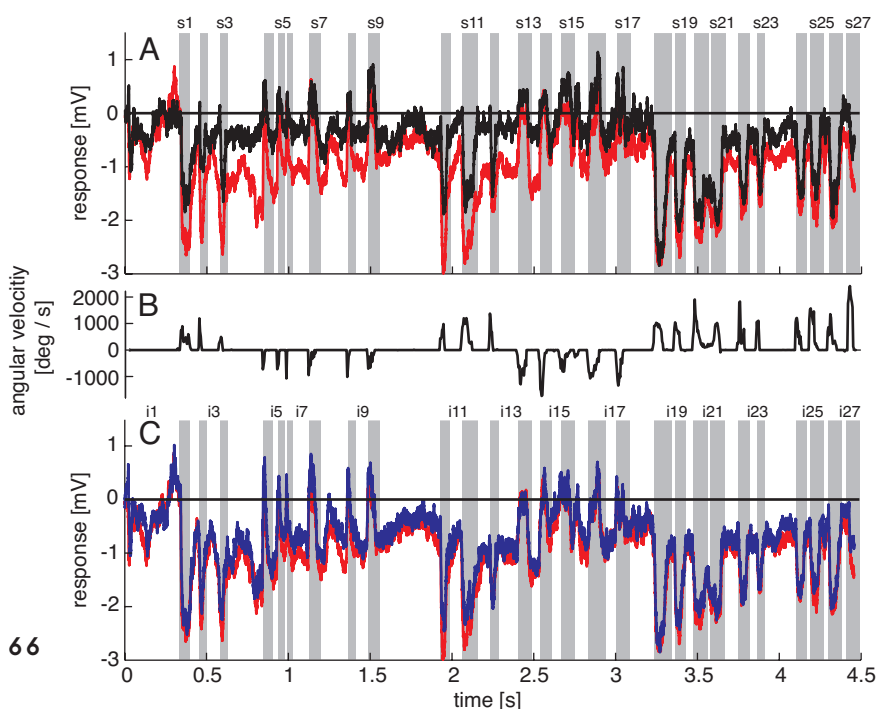


Fig. 5

Fig. 5. Response traces of a single LWC sensitive to front-to-back motion during presentation of different stimulus conditions.

A: response traces of one neuron recorded during visual stimulation. Baseline membrane potential is subtracted. For the evaluation we calculated the mean responses over many trials (also Fig.1B). Black trace: no landmark condition ([cond. 1]; 6 repetitions), red trace: homogeneous landmark condition ([cond. 2]; 9 repetitions). Neuronal response is subdivided into intersaccades and saccades (gray shadings; light gray shading is a saccade to the right, dark gray a saccade to the left). B: response traces of the same neuron as in A. Red trace: homogeneous landmark condition ([cond. 1]; 9 repetitions), Blue trace: random pattern landmark condition i.e. camouflaged landmarks ([cond. 3]; 7 repetitions).

Also the profiles of object-induced response changes are similar between these two classes of cells for landmarks with different textures (Fig. 6). Depending on the cells' preferred direction of motion, the deviations from zero are approximately phase-inverted to those obtained in LWCs with back-to-front motion as preferred direction.

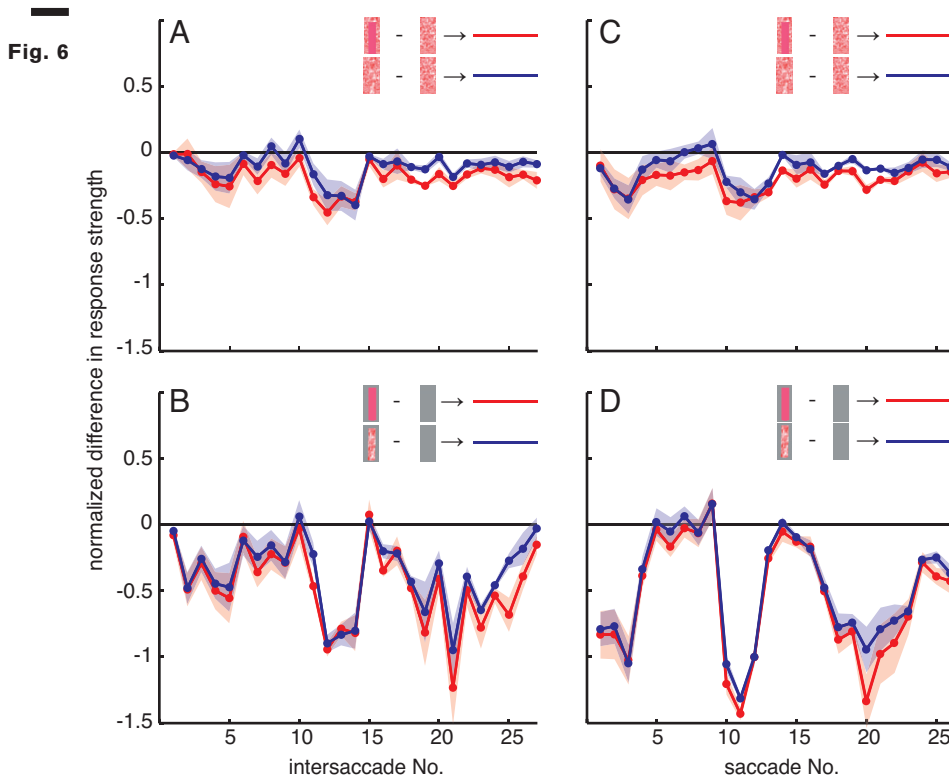


Fig. 6. Response profiles of LWCs with front-to-back as preferred direction of movement.

Plots show object-induced response changes as the mean, normalized differences between two stimulus conditions for intersaccades A, B and saccades C, D. For A and C traces indicate object-induced response changes for subsequent intersaccadic A or saccadic C intervals. Red traces: object-induced response changes during 'no landmark' condition [1] subtracted from those during 'homogenous landmark' condition [2]. This indicates the influence of homogeneously textured objects. Blue traces: object-induced response changes during 'no landmark' condition [1] subtracted from those during 'random pattern landmark' condition [3]. This indicates influence of objects that were randomly patterned. For B, D traces have same meaning, but responses were obtained during stimulus conditions with a gray background. Number of cells included in this figure is $n = 3$. Shadings indicate SEM. All responses were normalized to the cells' maximum mean response during intersaccades or saccades respectively during the stimulus condition identical to behavioral situation (homogeneous landmark condition, [1]). For more details see methods section.

So far, we have seen that objects change the neuronal responses during different parts of the flight. To get an idea of what kind of manoeuvres during the learning flight led to prominent object-induced response changes, we averaged the intersaccadic object-induced response level and plot the mean colour-coded response along the original flight trajectory. We compared the “no landmark”-condition [cond. 1] with the “homogeneous red landmark” condition [cond. 2] (see also Fig. 4A; red trace) for our larger dataset, which is based on LWCs with preferred direction of motion from back-to-front ($n = 11$).

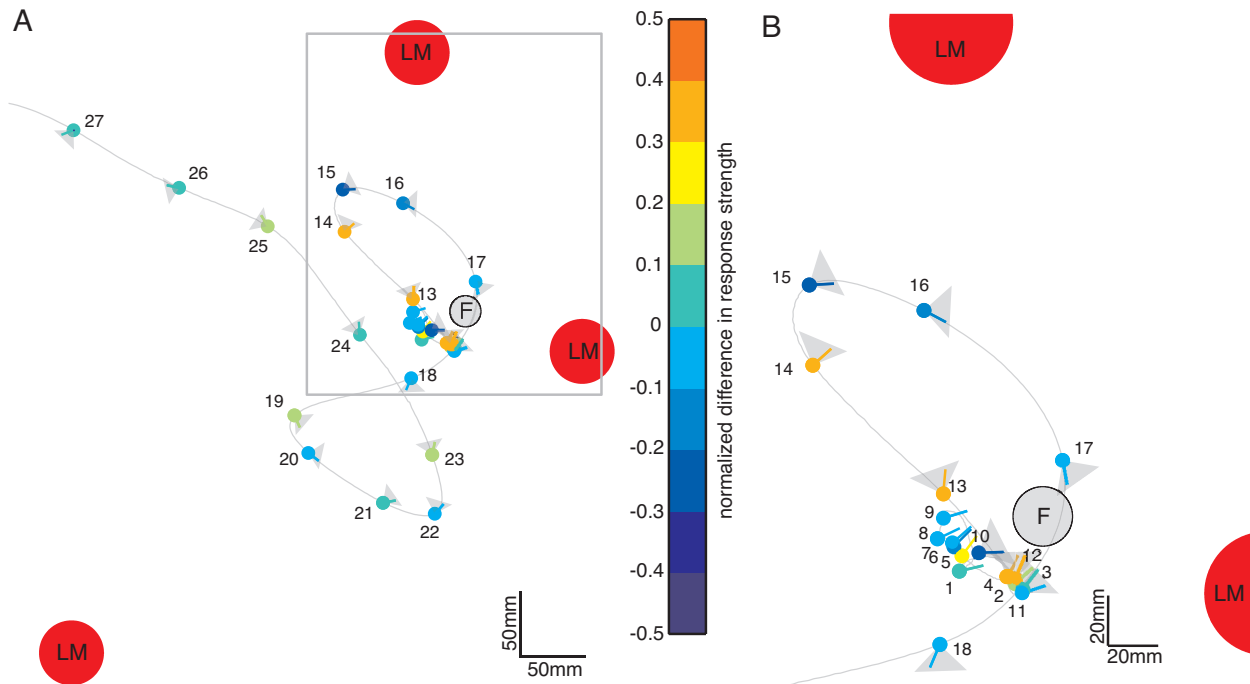


Fig. 7

Fig. 7. Object-induced intersaccadic response changes of a LWC with a preferred direction from back-to-front plotted along the flight trajectory of the replayed ego-perspective flight sequence (compare to Fig. 2A).

This example indicates the difference between the no-landmark condition [cond. 1] and the homogeneous landmark condition [cond. 2]. Red circles denote landmarks (LM) and the gray circle the see-through feeder (F). The color-coded dots represent the position of the bee in the middle of each intersaccade; the corresponding line shows the direction of view. Warm colors indicate response increments, and cold colors response decrements induced by objects in the receptive field of the cell. The gray triangles attached to each dot illustrate the typical horizontal extent of the receptive field of the analyzed cells ($n = 11$). A: overview on entire learning flight. B: enlarged view on the intersaccades during the beginning of the learning flight. For sake of clarity the receptive field areas are not indicated for intersaccades 1 to 9.

During forward flight the object response does not deviate much from zero most of the time, with only a slight negative shift (Fig. 6, e.g. intersaccades 23 to 27). This negative shift is the consequence of the objects moving through the receptive field (Fig. 7, grey triangles) from front-to-back, i.e. in the anti-preferred direction of the cells. Strong

deviations from zero occur when the bee translates with a larger sideways than forward velocity (e.g. intersaccades 12 to 14). Accordingly, we find a positive correlation between the intersaccadic neuronal responses and the angle α between flight direction and body orientation (27 data points each). Here, we find correlation values of $R = 0.38$ ($p < 0.05$) for the responses recorded with homogeneous textured landmarks [cond. 2] and even $R = 0.52$ ($p < 0.01$) between the neuronal response and α , when we compare the stimulus condition with random dot textured landmarks [cond. 3] with the stimulus condition without landmarks inserted. These correlation values are similar when correlating the α angle with the intersaccadic responses to the stimulus conditions with grey background ([cond. 2] vs. [cond. 1]: $R = 0.41$, $p < 0.05$; [cond. 3] vs. [cond. 1]: $R = 0.52$, $p < 0.01$). The large sideways movements cause a specific optic flow pattern on the retina: landmarks close to the animal appear to move faster than the background, leading to enhanced neural responses during stimulus conditions with objects ([cond. 2 and 3] compared to [cond. 1 and cond. 4] and [cond. 5] compared to pure grey screen [cond. 6]) that elicits no response difference from spontaneous neuronal activity.

For other stimulus parameters we did not find correlations with the intersaccadic neural responses. The retinal size of the landmarks within the cell's receptive field was not correlated with the normalized object-induced intersaccadic response changes (random dot pattern background: $R = -0.10$; $R = -0.14$; grey background: $R = -0.19$; $R = 0.20$). Similarly weak correlations are obtained when we only take the largest landmark in the visual field into account or sum the size of all landmarks within the receptive field. Also, the distance to the landmarks in the receptive field does not influence the intersaccadic neural response significantly ($R = -0.09$ to 0.09), despite the distance dependence of the retinal velocity. This finding, thus, is the likely consequence of more than one stimulus parameter, such as the velocity of retinal pattern displacements or the direction of motion and pattern contrast, influencing the response strength of LWCs. In conclusion, among the different stimulus parameters we find the angle α to be the most important factor correlating with object influences on the neuronal responses.

To further quantify the object-induced response changes, we selected two adjacent intersaccadic intervals (No. 13 and 14) with clear object-induced responses. Here, the bee moved to the left side and thus allowed one of the objects to move on the retina in the cells' preferred direction. The object-induced response changes elicited by camouflaged landmarks [cond. 3] are very similar to those induced by the homogeneous landmarks [cond. 2]. For both intersaccades the object led to significant response deviations from zero (Fig. 8). These deviations are similar for the grey background condition (Fig. 8). Notwithstanding, these findings corroborate quantitatively the above conclusion that the objects significantly influence the response of the recorded cells.

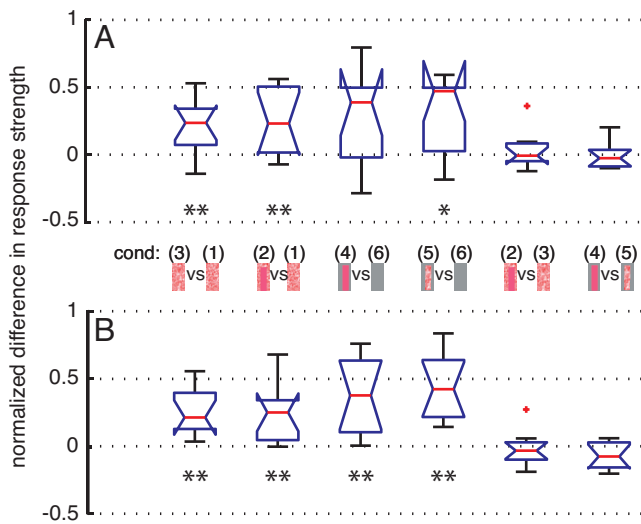


Fig. 8. Normalized differences between responses of LWCs to pairs of stimulus conditions (see pictograms between A und B) during intersaccade No. 13 (subplot A) and No. 14 (subplot B).

Depicted data from LWCs with preferred direction of motion from back-to-front. Number of cells: $N = 11$. Explanation of box symbols: red central horizontal line – median; box edges represent 25th and 75th percentiles; whiskers – most extreme data points that are not outliers ($> 75^{\text{th}}$ percentile + $(1.5 * \text{box size})$ OR $< 25^{\text{th}}$ percentile – $(1.5 * \text{box size})$). Outliers are plotted separately. Notches describe the 95% confidence intervals of the median. Two medians are significantly different at the 5% significance level if the notches do not overlap (McGill and Tukey, 1978). Asterisks indicate statistically significant deviation from zero (two-tailed t-test; * $p < 0.05$, ** $p < 0.01$). Median at zero level means no object influence.

We analysed the role of object texture in shaping the object-induced response changes during the two selected intersaccades by comparing the responses to stimulus conditions with the same background texture but different object textures. We do not find significant deviations from zero, indicating that the texture of objects is not strongly reflected in the neural response, as already suggested by the almost equal strengths of the intersaccadic response profiles for different object textures (Fig. 4).

In summary, these findings further support our conclusion that the object-induced response does not strongly depend on object texture during in the intersaccadic parts of the neuronal responses. This finding is in accordance with the behavioural performance of honeybees (Dittmar et al., 2010).

Texture effects on neuronal responses during saccadic flight phases

The object-induced neuronal responses differ also during saccades (Figs. 4C, 4D, 6C, 6D). Hence, objects do not only affect the intersaccadic neuronal responses. Even the camouflaged objects have an impact on the neuronal response during saccades, although the amount of relative motion is relatively small compared to the fast rotatory retinal movement (Figs. 4C, 4D).

The object-induced differences during saccades are similar to the ones observed during the intersaccades (Figs. 4A, 4B, 6A, 6B) as each intersaccade is followed in time by a saccade. Thus, neighbouring saccades and intersaccades occur at similar locations in the flight arena and might, thus, be affected by the environment in similar ways (as e.g. Fig. 4).

In contrast to the intersaccades, the responses evoked during the saccades are affected by the retinal size of the landmark. We find a positive correlation for back-to-front LWCs between the retinal size of the objects and the saccadic responses when the background was randomly textured (for cond. 2, $R = 0.36$; for cond. 3, $R = 0.28$). These correlations are even stronger when the background was grey and, thus, the neural response was affected exclusively by the objects (for cond. 4: $R = 0.47$; for cond. 5: $R = 0.43$).

The object influence on the saccadic responses depends also slightly on the texture of the objects (Figs. 4C, 4D). With grey background [cond. 4 and 5] the object texture influence is stronger. These effects are also visible for front-to-back LWCs (Fig. 6), although in a less pronounced way.

DISCUSSION

We show that direction-selective motion sensitive wide-field cells in the lobula (LWCs) of bumblebees convey information about nearby landmarks that play a role for local homing in our experimental setup. It is long known that bees use motion cues in a variety of other behaviours like landing and pattern discrimination (Lehrer and Collett, 1994; Srinivasan et al., 2000; Srinivasan and Zhang, 2004; Lehrer and Campan, 2005). In this account we focused on learning flights as fundamental components of navigation behaviour and on what features of objects are actually represented in the bee's visual motion pathway using behaviourally relevant, naturalistic visual stimulation. The temporal profile of responses of LWCs during both intersaccades and saccades depends on the landmark constellation in a characteristic way, indicating that the neuronal responses of LWCs contain information about the spatial layout of the environment.

Similar to other insects like e.g. flies and ants (Hateren and Schilstra, 1999; Land, 1999; Schilstra and Hateren, 1999; Lent et al., 2010) bees separate their locomotion into phases of saccades and intersaccades (Boeddeker and Hemmi, 2010; Boeddeker et al., 2010; Braun et al., 2012). During the intersaccadic phases of translatory motion bees can gather depth information from the environment (Boeddeker et al., 2005; Kern et al., 2005; Egelhaaf et al., 2012). This separation of flight into different phases might also be reflected in the representation of landmarks relevant for navigation in the motion vision pathway. Indeed, we find the activity of LWCs to be modulated by objects during intersaccadic flight phases, but also during saccades. However, whereas during saccades textural differences of objects seem to slightly influence the neuronal responses, there is almost no difference in responses between differently textured objects during intersaccades.

This independence of intersaccadic LWC responses from object texture mirrors the overall performance of bees in local navigation behaviour that was largely unaffected by textural changes of landmarks (Dittmar et al., 2010). Rather than by object texture, response modulations during self-motion of the animal seem to be caused by factors like the relative motion of the object against the background. This is intuitive as bees flying sideways experience close frontal objects as moving faster on the retina than more distant ones. Especially during sideways flight manoeuvres, we therefore find larger neuronal object-induced responses. Independent of the actual mechanism that induces object-driven response changes in the neurons we conclude that during intersaccades the bee might be provided with information related to the geometrical layout of the immediate surroundings in which it is navigating.

How could an animal profit from processing the neuronal responses that are induced by saccades? These signals might be involved in the animal's optomotor response as has already been suggested by an earlier study (DeVoe et al., 1982). Given the slight differences during saccades between both landmark textures, it might also be possible to extract textural information out of the signal conveyed by LWCs. This information could be used to distinguish landmarks carrying different textures. Honeybees are able to use this textural information when it provides positional information in a navigation task (Dittmar et al., 2011).

Even by classifying the recorded LWCs into just two groups according to their preferred direction of motion, we see characteristic correlation between the impact of the landmarks on the neuronal response and the amount of sideways movement in the intersaccadic parts of flight. We find this for LWCs with back-to-front motion as preferred movement direction, which is not surprising as sideways movement provides strong motion input from back-to-front to a cell with a quite frontal receptive field. For both classes of cells, front-to-back and back-to-front LWCs, we could show that landmarks appearing in the receptive field modulate the cells' response and therefore convey information about the animal's surroundings. The transfer of information via graded modulation of the membrane potential or a combination of graded membrane potential changes and spikes is very common in insect neurons. Both graded potential changes as well as mixed potentials were also shown to exist in presynaptic areas of neurons with thick axons and to be transferred to postsynaptic neurons (Warzecha et al., 2003; Beckers et al., 2007, 2009; Rien et al., 2011).

We possibly pooled the data across several cell types with similar but slightly different response properties by using the preferred direction as the main feature for cell classification. Analysing unique cell types individually would potentially have led to even more pronounced effects compared to what we already observe while possibly averaging across a whole class of LWCs. Nevertheless, our results indicate that we describe a global response property of those cells that is not tied to a single cell type. This information could then be used in the context of local homing to compare the current LWC activity profile to a previously stored LWC activity profile – the neural correlate of an optic flow snapshot of a location that is important for the animal to recognize.

We recorded from neurons in the lobula, which is presumably the last visual processing stage before the information is projected into brain areas that are involved in multimodal processing and learning (Hertel and Maronde, 1987; Paulk and Gronenberg, 2008; Paulk et al., 2009; Mota et al., 2011). Most likely, the visual input to the lobula is processed independently of other sensory modalities. Recent studies could show for flies that an active behavioural state of the animal affects the amplitude of neuronal responses and may even somewhat shift their velocity tuning (Maimon et al., 2010; Rosner et al., 2010; Jung et al., 2011). Such effects of an active behavioural state would probably not affect our conclusion that the landmark constellation is reflected in the intersaccadic neural responses. Rather, an increasing gain of the neurons may possibly make it easier for the animal to distinguish objects from background.

It is of great interest to know where the cells we recorded from project to, as a multitude of behavioural studies show that bees store, compare and also combine multisensory cues for navigation. We know that there are projections from LWCs to brain regions like the contralateral lobula (DeVoe et al., 1982) or the mushroom body calyx (Paulk and Gronenberg, 2008) that is known to play an important role for multimodal learning. Additionally, it has been shown recently that visual novelty during learning flights leads to upregulation of the immediate early gene EGR in the mushroom bodies of honeybees (Lutz and Robinson, 2013), which indicates involvement of the mushroom body into visual learning processes. However, the lobula is also connected to the central complex (Ribi and Scheel, 1981; Paulk et al., 2009), an area that may also be involved in multimodal processing (Gronenberg, 1986; Maronde, 1991) and was demonstrated to be involved in processing visual information in bees (Milde, 1988). Additionally, the central complex has recently been shown to be essential for place learning in *Drosophila* (Ofstad et al., 2011).

Due to often very short recording times we decided to not stain the neurons, although this would have allowed us to individually identify them anatomically. The functional properties of the recorded neurons and, in particular, the responses to objects do of course not depend on their anatomical characterization. Still, anatomical evidence could provide further information on possible roles of those neurons and should be obtained in follow up studies. Nonetheless, even without knowing the projection area of these cells, we show that they convey information about the spatial layout of the landmark configuration – information that is crucially relevant in a homing context.

ACKNOWLEDGEMENTS

We thank B.R.H. Geurten, J.P. Lindemann and W. Stuerzl for methodological support and Nicole E. Carey for improving the manuscript.

REFERENCES

- Beckers U, Egelhaaf M, Kurtz R (2007) Synapses in the fly motion-vision pathway: evidence for a broad range of signal amplitudes and dynamics. *J Neurophys* 97:2032–2041.
- Beckers U, Egelhaaf M, Kurtz R (2009) Precise timing in fly motion vision is mediated by fast components of combined graded and spike signals. *Neuroscience* 160:639–650.
- Boeddeker N, Dittmar L, Stürzl W, Egelhaaf M (2010) The fine structure of honeybee head and body yaw movements in a homing task. *Proc R Soc Lond B Biol Sci* 277:1899–1906.
- Boeddeker N, Hemmi JM (2010) Visual gaze control during peering flight manoeuvres in honeybees. *Proc R Soc Lond B Biol Sci* 277:1209–1217.
- Boeddeker N, Lindemann JP, Egelhaaf M, Zeil J (2005) Responses of blowfly motion-sensitive neurons to reconstructed optic flow along outdoor flight paths. *J Comp Physiol* 191:1143–1155.
- Bouget, Jean Y (1999) *Visual methods for three-dimensional modelling*. California: California Institute of Technology Available at: http://www.vision.caltech.edu/bougetj/calib_doc/.
- Braun E, Dittmar L, Boeddeker N, Egelhaaf M (2012) Prototypical components of honeybee homing flight behavior depend on the visual appearance of objects surrounding the goal. *Front Behav Neurosci* 6:1–16.
- Braun E, Lindemann JP (2011) IVtools. Available at: <http://opensource.cit-ec.de/projects/ivtools>.
- Collett T (1978) Peering – a locust behaviour pattern for obtaining motion prallax information. *J Exp Biol* 76:237–241.
- Collett TS, Graham P, Harris RA, Hempel-de-Ibarra N (2006) Navigational memories in ants and bees: memory retrieval when selecting and following routes. In: *Advances in the Study of Behavior*, pp.123–172.
- Collett TS, de Ibarra NH, Riabinina O, Philippides A (2013) Coordinating compass-based and nest-based flight directions during bumblebee learning and return flights. *J Exp Biol* 216:1105–1113.
- DeVoe RD, Kaiser W, Ohm J, Stone LS (1982) Horizontal movement detectors of honeybees: directionally-selective visual neurons in the lobula and brain. *J Comp Physiol* 147:155–170.

Dittmar L, Egelhaaf M, Stürzl W, Boeddeker N (2011) The behavioral relevance of landmark texture for honeybee homing. *Behav Neurosci* 5:1–11.

Dittmar L, Stürzl W, Baird E, Boeddeker N, Egelhaaf M (2010) Goal seeking in honeybees: matching of optic flow snapshots? *J Exp Biol* 213:2913–2923.

Egelhaaf M, Boeddeker N, Kern R, Kurtz R, Lindemann JP (2012) Spatial vision in insects is facilitated by shaping the dynamics of visual input through behavioral action. *Front Neur Circ* 6:108.

Gillner S, Weiss AM, Mallot H (2008) Visual homing in the absence of feature-based landmark information. *Cognition* 109:105–122.

Haag J, Borst A (1997) Encoding of visual motion information and reliability in spiking and graded potential neurons. *J Neurosci* 17:4809–4819.

Hateren J, Schilstra C (1999) Blowfly flight and optic flow. II. Head movements during flight. *J Exp Biol* 202:1491–1500.

Hausen K (1982) Motion Sensitive Interneurons in the Optomotor System of the Fly: I. The Horizontal Cells: Structure and Signals. *Biol Cybern* 156:143–156.

Hempel de Ibarra N, Philippides A, Riabinina O, Collett TS (2009) Preferred viewing directions of bumblebees (*Bombus terrestris* L.) when learning and approaching their nest site. *J Exp Biol* 212:3193–3204.

Hertel BYH, Maronde U (1987) The physiology and morphology of centrally projecting visual interneurons in the honeybee brain. *J Exp Biol* 133:301–315.

Ibbotson M (1991) Wide-field motion-sensitive neurons tuned to horizontal movement in the honeybee, *Apis mellifera*. *J Comp Physiol* 168:91–102.

Jung SN, Borst A, Haag J (2011) Flight activity alters velocity tuning of fly motion-sensitive neurons. *J Neurosci* 31:9231–9237.

Karmeier K, van Hateren JH, Kern R, Egelhaaf M (2006) Encoding of naturalistic optic flow by a population of blowfly motion-sensitive neurons. *J Neurophys* 96:1602–1614.

Kern R, van Hateren JH, Egelhaaf M (2006) Representation of behaviourally relevant information by blowfly motion-sensitive visual interneurons requires precise compensatory head movements. *J Exp Biol* 209:1251–1260.

Kern R, van Hateren JH, Michaelis C, Lindemann JP, Egelhaaf M (2005) Function of a fly motion-sensitive neuron matches eye movements during free flight. *PLoS Biol* 3:1130–1138.

Land MF (1999) Motion and vision: why animals move their eyes. *J Comp Physiol* 185:341–352.

Lehrer M (1993) Why do bees turn back and look? *J Comp Physiol* 172:549–563.

Lent DD, Graham P, Collett TS (2010) Image-matching during ant navigation occurs through saccade-like body turns controlled by learned visual features. *Proc Natl Acad Sci USA* 107:16348–16353.

Lindemann JP, Kern R, Michaelis C, Meyer P, Van Hateren JH, Egelhaaf M (2003) FliMax, a novel stimulus device for panoramic and highspeed presentation of behaviourally generated optic flow. *Vision Res* 43:779–791.

Lutz CC, Robinson GE (2013) Activity-dependent gene expression in honey bee mushroom bodies in response to orientation flight. *J Exp Biol* 216:2031–2038.

Maimon G, Straw AD, Dickinson MH (2010) Active flight increases the gain of visual motion processing in *Drosophila*. *Nature neuroscience* 13:393–399.

Matlab (n.d.) The Mathworks. Available at: <http://www.mathworks.de/help/techdoc/ref/corrcoef.html>.

McGill R, Tukey J (1978) Variations of box plots. *Am Stat* 32:12–16.

Menzel R, Geiger K, Chittka L, Joerges J, Kunze J, Müller U (1996) The knowledge base of bee navigation. *J Exp Biol* 199:141–146.

Milde J (1988) Visual responses of interneurons in the posterior median protocerebrum and the central complex of the honeybee *Apis mellifera*. *J Insect Physiol* 34:427–436.

Mota T, Yamagata N, Giurfa M, Gronenberg W, Sandoz J-C (2011) Neural organization and visual processing in the anterior optic tubercle of the honeybee brain. *J Neurosci* 31:11443–11456.

Ofstad TA, Zuker CS, Reiser MB (2011) Visual place learning in *Drosophila melanogaster*. *Nature* 474:204–207.

Paulk AC, Dacks AM, Phillips-Portillo J, Fellous J-M, Gronenberg W (2009) Visual processing in the central bee brain. *J Neurosci* 29:9987–9999.

Paulk AC, Gronenberg W (2008) Higher order visual input to the mushroom bodies in the bee, *Bombus impatiens*. *Arthropod Struct Dev* 37:443–458.

Paulk AC, Phillips-Portillo J, Dacks AM, Fellous J-M, Gronenberg W (2008) The processing of color, motion, and stimulus timing are anatomically segregated in the bumblebee brain. *J Neurosci* 28:6319–6332.

Philippides A, de Ibarra NH, Riabinina O, Collett TS (2013) Bumblebee calligraphy: the design and control of flight motifs in the learning and return flights of *Bombus terrestris*. *J Exp Biol* 216:1093-1104.

Ribi WA (1976) The first optic ganglion of the bee II. Topographical relationships of the monopolar cells within and between cartridges. *Cell Tissue Res* 373:359–373.

Ribi WA, Scheel M (1981) The second and third optic ganglia of the worker bee. *Cell Tissue Res* 221:17–43.

Rien D, Kern R, Kurtz R (2011) Synaptic transmission of graded membrane potential changes and spikes between identified visual interneurons. *EJN* 34:705–716.

Rosner R, Egelhaaf M, Warzecha A-K (2010) Behavioural state affects motion-sensitive neurones in the fly visual system. *J Exp Biol* 213:331–338.

Schilstra C, Hateren J (1999) Blowfly Flight and Optic Flow - I. Thorax kinematics and flight dynamics. *J Exp Biol* 1490:1481–1490.

Seelig JD, Chiappe ME, Lott GK, Dutta A, Osborne JE, Reiser MB, Jayaraman V (2010) Two-photon calcium imaging from head-fixed *Drosophila* during optomotor walking behavior. *Nature methods* 7:535-540.

Warzecha A, Kurtz R, Egelhaaf M (2003) Synaptic transfer of dynamic motion information between identified neurons in the visual system of the blowfly. *Neuroscience* 119:1103–1112.

Zeil J, Boeddeker N, Stürzl W (2009) Visual homing in insects and robots. In: *Flying Insects and Robots*, pp.87–99.

Zeil J, Kelber A, Voss R (1996) Structure and function of learning flights in bees and wasps. *J Exp Biol* 199:245–252.

3

STRUCTURE AND ODOUR CODING PROPERTIES IN THE BUMBLEBEE ANTENNAL LOBE

The content of this chapter is prepared for publication as: M Mertes, J Carcaud, M Egelhaaf, JC Sandoz: **STRUCTURE AND ODOUR CODING PROPERTIES IN THE BUMBLEBEE ANTENNAL LOBE**

ABSTRACT

Odorants are an important source of information for Hymenoptera. They perceive pheromonal signals from their queen and are able to find food sources based on their sense of smell. Whereas there is a solid knowledge base on the olfactory pathways in honeybees and ants, this knowledge was missing for the bumblebee. In this account we characterized the bumblebee primary center for olfactory processing, the antennal lobe (AL). Via antennal stainings we disentangled the sensory input structure of tract T1 to T4 that allowed attributing single glomeruli to their input tracts. 3D reconstruction of the whole AL revealed that T-tract fibre output patterns are very similar to those of the honeybee. The number of glomeruli found to be 158 ± 4 , which is slightly lower compared to honeybees. After retrogradely staining the I-APT projection neuron pathway of the AL with the calcium indicator Fura-2 dextran, we conducted calcium imaging of the I-APT subunit of the AL. Our odour set comprised 16 aliphatic odours that differed according to their carbon chain length and their functional groups (primary alcohols, secondary alcohols, ketones, aldehydes). The response pattern measured in glomeruli of the I-APT revealed functional group coding as well as carbon chain length coding in the bumblebee AL, similar as in honeybees. High correlation values in neuronal activity patterns between honeybees and bumblebees further underline the high similarity. This study provides deep insight into the bumblebee AL anatomy and depicts for the first time neuronal activity via calcium-imaging in the bumblebee AL.

INTRODUCTION

For several decades, honeybees *Apis mellifera* have been a mainstream model system for research in ethology, neurobiology and animal cognition (Menzel and Muller, 1996; Giurfa et al., 2001; Menzel, 2012). Thanks to their good amenability to behavioural

protocols, these insects are used for studying such diverse cognitive abilities as stimulus generalization (Guerrieri et al., 2005), categorisation (Benard et al., 2006), rule learning (Giurfa et al. 2001; Mota et al. 2011; Avargues Weber et al. 2012) and navigation (Zeil et al., 2009 ; Menzel et al. 2011). In addition, invasive neurobiological techniques like intra- and extracellular electrophysiology (Hammer, 1993; Okada et al., 2007; Brill et al., 2013) or *in vivo* calcium imaging (Joerges et al., 1997; Carcaud et al., 2012) are routinely applied for addressing the neuronal basis of these behaviours.

In recent years, an increasing number of studies have been dedicated to another social Hymenoptera, the bumblebee *Bombus* sp. (e.g. Paulk et al., 2008; Riveros and Gronenberg, 2009a, 2009b; Morawetz and Spaethe, 2012). In comparison to honeybees, bumblebees provide certain advantages, like allowing season-independent sampling or conducting free-flying behavioural experiments indoors, while controlled laboratory conditioning protocols can also be used (Laloi et al., 1999; Riveros and Gronenberg, 2009a). In addition, their natural robustness is beneficial for coupling invasive techniques with conditioning experiments (Riveros and Gronenberg, 2009b).

Recently, some studies have started describing the anatomy of the bumblebee brain (Mares et al., 2005; Paulk and Gronenberg, 2008; Paulk et al., 2009), which appears very similar to honeybees. These studies either performed a general description of neuropil areas, or focused on the visual system. However, apart from the visual modality, olfaction also plays a crucial role in the behaviour of bumblebees, e.g. while searching for food on flowers or in the nest (Dornhaus et al., 2003). While in honeybees many studies have addressed the morphological and functional basis of olfactory coding and processing (Galizia and Menzel, 2001; Sandoz, 2011), little is known in bumblebees, except some early anatomical and electrophysiological data (Fonta and Masson, 1985a, 1987). In insects, odorants are detected by olfactory receptor neurons (ORNs) on the antennae. ORN axons project to a primary processing centre, the antennal lobe (AL), constituted of anatomical and functional units, the glomeruli (~165 in honeybees). Within the AL, local interneurons perform local computations, and projection neurons then convey processed information to higher-order centres (mushroom bodies and lateral horn). While a high morphological similarity appears in the AL of honeybees and bumblebees (Fonta and Masson, 1985a), no data exists on olfactory coding in bumblebees. We thus performed the first *in vivo* optical imaging study of odour coding in the AL of the bumblebee *Bombus terrestris*. Honeybees and bumblebees mostly forage in the same habitats and partly pollinate the same flowers; they are consequently exposed to a similar set of floral volatiles. To compare odour-coding rules in both species, we presented a panel of 16 floral odorants previously used in studies on olfactory processing and perception in honeybees (Guerrieri et al., 2005; Carcaud et al., 2012).

MATERIALS AND METHODS

Bumblebee preparation

Medium-sized bumblebee workers were caught from an indoor hive (Koppert, Berkel en Rodenrijs, The Netherlands) chilled on ice for 5-10 min until they stopped moving. Then, bumblebees were prepared according to the standard preparation to image the AL in honeybees (Joerges et al. 1997, Sachse and Galizia 2002, Carcaud et al. 2012). In summary, the bumblebee's head was inserted and fixed in a plastic chamber with its antennae oriented to the front. Using bee wax, we glued the proboscis at the front end of the holder to avoid movement of the brain during the experiment. Hairs on the top of the bumblebee head were removed and a pool was built with bee wax and pieces of plastic around the rostral part of the head capsule (behind the antennae). The pool was made waterproof with two-component epoxy glue (red Araldite, Bostik Findley, S.A.). Using a microscalpel carrying broken razor blade chips, a small window was then cut in the head cuticle from the bases of the antennae up to the ocelli. Glands as well as parts of the tracheal sheath were removed to expose the antennal lobes and parts of the protocerebrum. Finally, the pool was filled with some ringer solution (in mM: NaCl, 130; KCl, 6; MgCl₂, 4; CaCl₂, 5; sucrose, 160; glucose, 25; Hepes, 10; pH 6.7, 500 mOsmol; all chemicals from Sigma-Aldrich, Lyon, France), to avoid desiccation of the brain surface. Three hours prior to the experiment, a dye mixture was inserted into the brain with a broken borosilicate micropipette, aiming for the tract of I-APT projection neurons, between the α lobe and the border of the optic lobe, rostrally from the lateral horn. The dye mixture consisted of the calcium-indicator Fura-2 dextran (10,000 kDa, Life technologies, France), of tetramethylrhodamine dextran (10,000 kDa, Life technologies, France) for later anatomical observation and of bovine serum albumin (2 %) to dissolve the dye crystals.

Calcium imaging

In vivo optical recordings were performed as described elsewhere (Deisig et al., 2010), with a T.I.L.L. Photonics imaging system (Martinsried, Germany), under an epifluorescence microscope (Olympus BX51WI) with a 10 \times water-immersion objective (Olympus, UMPlanFL; NA 0.3), which was dipped into the ringer solution covering the brain. Only one AL was recorded in each bee. Images were taken with a 640 \times 480 pixels 12-bit monochrome CCD camera (T.I.L.L. Imago) cooled to -12 °C. Fura-2 was alternatively excited with 340 nm and 380 nm monochromatic light (T.I.L.L. Polychrom IV). Each measurement thus consisted of 50 double frames recorded at a rate of 5 Hz (integration time for each frame at 340 nm: 40–80 ms; for 380 nm: 10-20 ms) with 4 \times 4 binning on chip (pixel image size corresponded to 4.8 μ m \times 4.8 μ m). The filter set on the microscope contained a 490 nm dichroic filter and a bandpass (50 nm) 525 nm emission filter.

Odour presentation

A constant clean airstream, into which odour stimuli could be presented, was directed from a distance of 2 cm to the bee's antennae. Odour stimuli (see below) were given at the 15th frame for 1 s (5 frames). Odour sources consisted in exchangeable Pasteur pipettes containing a piece of filter paper (1 cm²) soaked with 5 µl of pure odorant (Sigma Aldrich, France).

We tested 16 different aliphatic odours that are part of floral blends bumblebees encounter while foraging (Knudsen, 1993). The odours differed in carbon chain lengths (between 6 and 9 carbon atoms) and functional groups (primary alcohol, secondary alcohol, aldehyde and ketone). As control stimulus, we used a pipette containing a clean piece of filter paper without odour solution. This stimulus set was also used in a calcium imaging study on the honeybee AL (Carcaud et al., in prep.) allowing the comparison of odour coding in honeybees and bumblebees. We presented the odours in pseudo-randomized order between different bumblebees, and defined the order of the 17 different stimuli pseudo-randomly as we avoided consecutive stimuli to contain the same functional group or the same carbon chain length. Within each bee, the same order was retained until each stimulus had been presented three times.

Anatomical staining

After successful calcium imaging, we dissected out the brains and fixed them in 4 % paraformaldehyde solution for at least 24 h, dehydrated the brains in ascending concentrations of ethanol, and cleared and stored them in methyl salicylate (Sigma-Aldrich, France). We took images of the tetramethylrhodamine-stained glomeruli with a confocal laser scanning microscope (Zeiss, LSM 700) with a W Plan-Apochromat 20x/1.0 objective and a 555 nm excitation wavelength at 2 µm optical section thickness and pixel size of 0.31 µm × 0.31 µm. Recorded stacks of images were adjusted in brightness and contrast using imageJ (Rasband; National Institutes of Health, Bethesda, MD). For antennal stainings of the whole antennal lobe, the scape of the antennae of the bumblebee were carefully opened using a microscalpel, and the antennal nerve was cut with a borosilicate micropipette coated with tetramethylrhodamine dextran. Afterwards, animals were kept in a cool place until the next day to allow the dye to migrate to the antennal lobe, and stain the glomeruli. For brain extraction and microscopy we used the same techniques as described above for imaged animals. Segmentation and anatomical reconstruction of the antennal lobe was performed using Amira (version 4.5.1 Mercury Computer Systems, Merignac, France).

Data processing and analyses

Data were analysed using custom-made software written in IDL 6.0 (Research Systems, Boulder, CO) (see Deisig et al., 2010). Each odour presentation produced a four-dimensional array consisting of the excitation wavelength (340 or 380 nm), two spatial dimensions (x- and y-coordinates) along time (50 frames). We first calculated the fluorescence ratio between excitation wavelengths at each pixel and time point: $R = F_{340 \text{ nm}} / F_{380 \text{ nm}}$. We then computed the relative fluorescence changes

between the recorded odour responses R at each time point compared to the background fluorescence (before any odour presentation) R_0 , defined as the average of the three images before odour stimulus onset (frames 12–14). Relative fluorescence changes were thus calculated as: $\Delta R / R_0 = (R - R_0) / R_0$. We then filtered each of the three dimensions with a median filter of window size 3 pixels to reduce photon noise. Lastly, we corrected for possible irregularities of lamp illumination by subtracting the median pixel value of each frame from each single pixel of the corresponding frame.

The amplitude of the odour-induced response was calculated by subtracting the average of three consecutive frames during the odour presentation (frames 17–19) from the average frames before stimulus onset (frames 12–14).

Activity maps are presented in a false-colour code, from dark blue (no signal) to red (maximum signal), after application of a spatial low-pass filter (Gaussian 7×7). For each bumblebee the mean activity map is based on three presentations of each odour.

As unambiguous identification of identical glomeruli across individual bumblebees was not feasible, activity was analysed over the entire surface of the AL using a pixelwise analysis that avoids any bias due to glomerular misidentification. It was previously shown in honeybees that results based on the pixelwise method lead exactly to the same conclusions as glomerular identification (Carcaud et al., 2012). For each bumblebee, a mask was precisely drawn along the edges of the antennal lobe to limit the measure of odour-evoked responses to the glomerular area. We measured global glomerular activity upon odour stimulation by averaging the intensity values of all pixels within the unmasked area. Evaluation of (dis-)similarity relationships between neural representations was done by calculating pixelwise Euclidian distances for all pairs of the 16 odour stimuli that we used (120 odour pairs).

Statistical analysis

We compared intensity measures among functional groups and chain lengths using ANOVA for repeated measurements, followed by Tukey post-hoc tests for further analysis of statistically significant main effects. Wilcoxon matched-pairs tests were applied to compare Euclidean distances obtained for: 1) different presentations of the same odour vs presentations of different odours; 2) odours with the same or with a different functional group; 3) odours with the same or with a different chain length. For all analyses, average maps for the three presentations of each odorant were used apart from the comparison of same vs. different odour (see Fig. 5), where each single odour presentation was used in the analysis. Note that therefore distance values presented in Fig. 5 A cannot be directly compared with values presented in Fig. 5, B–D. Correlations are expressed using the Pearson correlation coefficient.

In some analyses, the bumblebee data was compared to honeybee data (Carcaud et al., 2012), which were acquired using exactly the same experimental and analytical procedures. Therefore we could directly compare odour-induced intensity and similarity relationships among odours in the AL of these two species. When comparing distance matrices between the two species, a Mantel test was used to control for significant correlation between bumblebee and honey Euclidian distance matrices.

All tests were performed with Statistica (version 5.5, StatSoft, Tulsa, UK), R (www.r-project.org) or Matlab (The Mathworks, Natick, MA, USA). All results are displayed as means \pm SEM.

RESULTS

Antennal lobe anatomy

Using fluorescent tracers, we performed mass stainings of olfactory receptor neurons (ORNs) that are afferents to the antennal lobe of the bumblebee *Bombus terrestris* (Fig. 1Ai to Ax). The tracers migrated along the antennal nerve until the ORNs' axonal endings in the cortex (outer layer) of the glomeruli. There, ORNs synapse onto antennal lobe neurons, i.e. local neurons carrying out local processing and projection neurons, which convey the olfactory information to higher-order brain centres. The afferent antennal system has been well described in another Apinae, the honeybee *Apis mellifera*. It consists of six main fibre bundles, called the T1–T6 tracts, four of which innervate the honeybee antennal lobe forming four different glomerular clusters (T1–T4, Pareto, 1972; Suzuki, 1975; Flanagan and Mercer, 1989; Galizia et al. 1999). The two additional tracts, T5–6, bypass the antennal lobe completely and innervate the dorsal lobe (T5) as well as the subesophageal ganglion and parts of the dorsal protocerebrum (Pareto, 1972).

As previously reported (Fonta and Masson, 1985b), we found a similar arrangement of sensory tracts in the bumblebee antennal lobe as in the honeybee. The most prominent tract, T1, is easily identifiable, crossing the centre of the antennal lobe from the antennal nerve caudally (Fig. 1^{Aiii-iv}, lower part of the picture) to the most ventral and rostral part of the antennal lobe where it innervates many glomeruli (upper part of the picture). The T3 tract is also prominent, leaving the antennal nerve on the caudal side of the antennal lobe, propagating medially on its outskirts and innervating many glomeruli on the dorso-caudal region. T3 divides itself into at least 3 sub-branches, two running medially (T3a,b), innervating many medial glomeruli and one running laterally innervating caudo-lateral glomeruli. Tract T2 is a much smaller tract that goes from the nerve entrance through the medial part of the lobe neuropil at approximately half depth and innervates only a few medial glomeruli (Fig. 1^{Avi-vii}). Tract T4 is another smaller tract, which runs laterally along the outer side of the glomerular region, and innervates a set of tear-shaped glomeruli on the most dorsal part of the antennal lobe, close to the dorsal lobe. Contrary to other glomeruli with a clearly stained cortex, these T4 glomeruli are characterized by a homogeneous staining of sensory neurons (Fig. 1^{Avii-viii}, most rostral glomerulus). A strong proportion of sensory neurons bypasses the antennal lobe completely on its dorso-lateral side (Fig. 1^{Aix-x}) and forms the two tracts innervating the dorsal lobe (T5) and the subesophageal ganglion and dorsal protocerebrum (T6) that transmit mechanosensory and gustatory information. In the following, single glomeruli from the confocal images were reconstructed (Fig. 1B) and the glomeruli counted. We found 158 ± 4 glomeruli in the antennal lobe of middle-sized bumble bees ($n = 4$ bees), a slightly lower number compared to honeybees (~ 160 -166 glomeruli; Galizia et al., 1999; Kelber et al., 2006; Kirschner et al., 2006).

The existence of the 4 ORN tracts in the bumblebee antennal lobe, and their similar location to those observed in the honeybee (Flanagan and Mercer, 1989; Galizia et al., 1999; Kirschner et al., 2006) suggest a strong homology between honeybee and bumblebee olfactory systems. In addition to this similarity in ORN tracts, we observed that in bumblebees, as in honeybees, the outer surface of the antennal lobe consists of a single layer of glomeruli. This arrangement is particularly well amenable to optical measurements of glomerular activity (see below).

Further similarities between honeybee and bumblebee olfactory systems were observed when staining projection neurons. With the classical technique used in honeybees (Sachse and Galizia), we localized the lateral antenno-protocerebral tract (I-APT) of projection neurons (Fig. 1C). By introducing tracers into the protocerebrum at a location lateral to the α -lobe of the mushroom bodies and rostral to the lateral horn, we obtained clear stainings of I-APT PNs (Fig. 1D) in ventrally-positioned glomeruli (Fig. 1B, red glomeruli) of the antennal lobe, as expected from data in honeybees (Pareto, 1972; Suzuki, 1975; Kirschner et al., 2006). In contrast to anterograde staining of ORNs, PN staining was found to be homogeneous in the whole volume of the glomeruli and PN somata could also be resolved out the outskirts of the glomerular area of the AL (Fig 1D). Thus, I-APT PN location and glomerular innervations were highly similar in bumblebees compared to these well-known pathways in the honeybee olfactory system (Fig. 1C,D).

Since I-APT PNs can be selectively stained in bumblebees, we next asked how far these anatomical similarities translate into similar functional properties between these two closely related species. We thus performed *in vivo* calcium imaging measurements in the bumblebee AL using the calcium indicator Fura-2 dextran, and recorded the calcium responses from the dendrites of I-APT PNs in ventral glomeruli (T1 region). Referring to earlier publications on honeybee olfactory coding (Guerrieri et al., 2005; Carcaud et al., 2012) we presented the same set of 16 aliphatic odorants at the same concentration in order to allow comparing odour coding in both species on a physiological level. We obtained clear and reproducible calcium signals in 14 bumble bees (out of 73 imaged animals). Depending on the chemical structure of the presented odorant, specific and different glomerular activity pattern could be measured (Fig. 1E). All odorants in the panel apart from 1-nonanol induced significant activity in the bumblebee antennal lobe compared to pure air as control stimulus (ANOVA followed by Dunnett's test against air control, $p < 0.01$).

Fig. 1

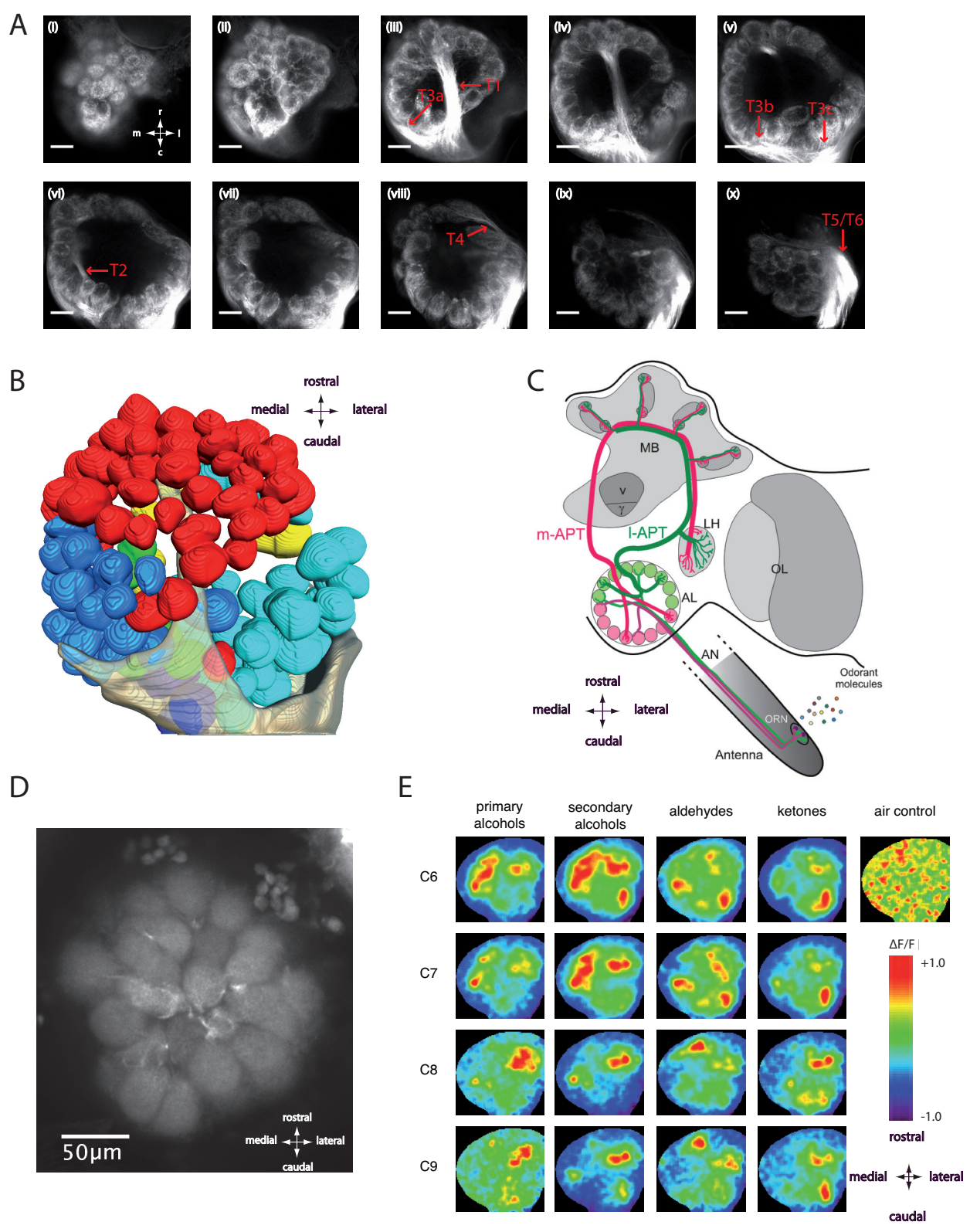


Fig. 1. Anatomy of the bumblebee antennal lobe (AL) and odour-induced calcium signals from glomeruli innervated by the lateral antenno-protocerebral tract (I-APT).

A: Confocal image sequence through a bumblebee antennal lobe (right lobe) obtained by massive anterograde antennal staining (using tetramethylrhodamine dextran). The scale bars indicate a length of 50 μm . The depth along the z-axis of the confocal images is A_i) 6 μm , A_{ii}) 24 μm , A_{iii}) 42 μm , A_{iv}) 60 μm , A_v) 78 μm , A_{vi}) 104 μm , A_{vii}) 114 μm , A_{viii}) 132 μm , A_{ix}) 150 μm , A_x) 166 μm .

B: Three-dimensional reconstruction of the 159 glomeruli in the antennal lobe presented in A. the glomeruli are coloured depending on their input tracts. The numbers of glomeruli per input tracts are: T1 = 60 (red), T2 = 7 (green), T3a = 27 (medium blue), T3b = 16 (dark blue), T3c = 42 (turquoise), and T4 = 7 (yellow) glomeruli. The incoming antennal nerve is shown in semi-transparent colouring.

C: Hymenopteran dual olfactory pathway (adapted from Carcaud et al. 2012 with permission). Odorant molecules are detected by olfactory receptor neurons (ORNs) on the antenna, which form the antennal nerve (AN) and send olfactory information to the primary olfactory centre, the antennal lobe (AL). Then, projection neurons (PNs) convey information to higher-order centres, the mushroom bodies (MB) and the lateral horn (LH), by means of two main tracts, the m-APT (medial- antenna-protocerebral tract, in pink) and the I-APT (lateral APT, green). PNs of the m-APT and I-APT project to distinct areas in the MB and LH. OL, optical lobe. v: vertical lobe.

D: Confocal image (z-projection over 14 μm , from 6 μm till 20 μm depth) of the superior part of the AL after retrograde staining (using tetramethylrhodamine dextran) of I-APT projection neurons. Dendrites of I-APT PNs are clearly visible in all observed glomeruli.

E: Odour-induced calcium signals in the I-APT glomeruli to a panel of odorants varying according to their carbon chain length (C6–C9) and their chemical functional group (primary and secondary alcohols, aldehydes and ketones).

Relative fluorescence changes ($\Delta R/R\%$) are presented in a false-colour code, from dark blue (no response) to red (maximal response). Different odours induce different glomerular activity patterns.

Intensity of odour-induced responses

We evaluated the influence of the odorants' chemical group and carbon chain length on the intensity of calcium responses as measured on the imaged glomerular surface. We find significant odour-evoked responses for all four different chemical groups that we tested (Dunnett's test: $p < 0.0001$, $df = 52$, $n = 14$).

Odorants with different functional groups induced different antennal lobe activity (Fig 2A, ANOVA $F_{3,39} = 12.96$, $p < 0.001$). Among functional groups, the weakest responses were evoked by primary alcohols (Fig 2A), which induced significantly lower responses than the other chemical groups (Tukey HSD test: $p < 0.05$ compared to secondary alcohols and $p < 0.001$ compared to ketones and aldehydes), which did not differ from each other.

Odorants with different chain lengths also induced different antennal lobe activity (Fig 2B, ANOVA $F_{3,39} = 6.95$, $p < 0.001$). Generally, global response intensity decreased with increasing chain length, i.e. odorant molecules with 6 and 7 carbons induced stronger neural activity than odorants with 9 carbons (Fig 2B, Tukey HSD test: $a \neq b$: $p < 0.05$ (C7) and $p < 0.001$ (C6) compared to C9). C8 odorant molecules induced intermediate responses between C6/C7 and C9.

This pattern of results is highly similar to that observed in previous experiments in honeybees (Sachse et al. 1999; Carcaud et al. 2012). A main variable can explain these observations. The individual vapour pressure of an odorant molecule indicates how volatile this molecule is. If we relate the vapour pressure of the presented odorants

to the corresponding calcium response on the ventral AL surface, we find a strong positive correlation with the log of the vapour pressure (Fig. 2C, $R^2 = 0.88$, $p < 0.0001$). We provided odorants as a given volume of pure substance on filter paper. The more volatile the odorant (i.e. the larger its vapour pressure), the more molecules were present in headspace in the sample and the larger was the recorded AL response to this odorant. In the presented odorant panel, alcohols and molecules with large carbon chain possess lower volatility and logically induce lower responses.

Fig. 2

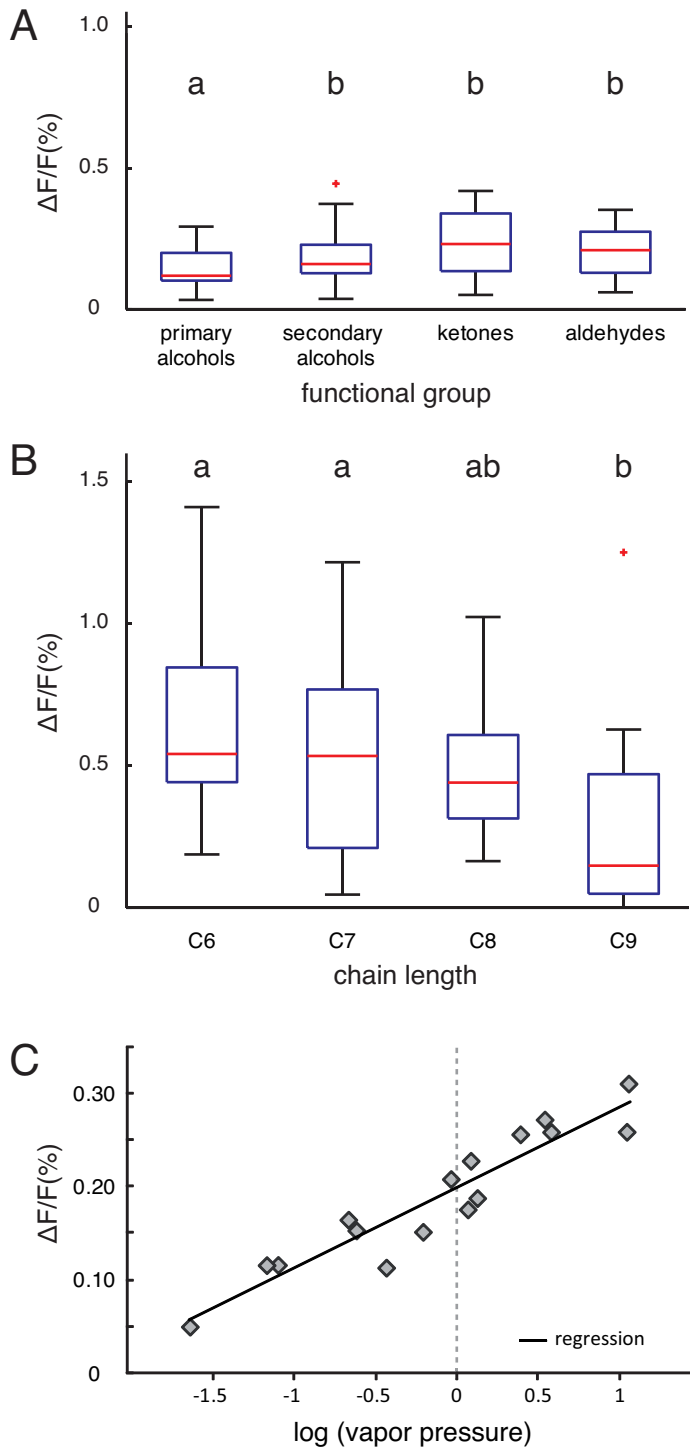


Fig. 2. Odour quantity coding: intensity of calcium response to 16 aliphatic odorants.

A: Amplitude of calcium responses ($\Delta R/R\%$) recorded in I-APT PNs to different odours according to their functional group (primary and secondary alcohols, aldehydes, and ketones). Primary alcohols induce weaker activation than other functional groups ($n = 14$). Explanation of box symbols: red line: median; box edges: 25th and 75th percentiles; whiskers; most extreme data points that are not outliers ($> 75^{\text{th}}$ percentile + $(1.5 * \text{box size})$ or $< 25^{\text{th}}$ percentile - $(1.5 * \text{box size})$). Outliers are plotted separately.

B: Amplitude of calcium responses ($\Delta R/R\%$) in relation to odorants' carbon chain length (6, 7, 8, and 9 carbons). Odorants with the longest carbon chain (C9) induce weaker activation than odorants with a short carbon chain ($n = 14$). Box symbols are the same as in A.

C: Amplitude of calcium responses ($\Delta R / R\%$) induced by each of the 16 aliphatic odorants as a function of their vapour pressure. The linear regression shows a significant correlation ($R^2 = 0,88$; $p < 0.001$).

Similarity among odour response maps

Until now we compared the chemical properties (functional group and carbon chain length) of odorants and observed that these properties affect the strength of AL neuronal activity. We now evaluated how these properties affect similarity relationships among odour response maps. We thus calculated pixelwise Euclidian distances between response maps for all possible pairs of the 16 tested odorants (e.g. Fig. 1E). Based on these 120 odour combinations we generated a Euclidian distance matrix, which provided an overview of similarity relationships among these odorants (Fig. 3). The more similar odour responses between two odorants, the smaller are the Euclidian distances and the more intense is the colour in the matrix. Scrutinizing the matrix reveals a strong effect of the odourant's carbon chain length on similarity relationships, as shown by the red diagonal lines in the matrix (e.g. for primary alcohols vs. secondary alcohols). Generally, distances between any two odorants of the same carbon chain length were smaller than distances between odorants with different carbon chain lengths. Moreover, distances between odorants appear larger with a larger difference in carbon chain length. The matrix also suggests that odour pairs with longer carbon chains (C8 vs. C9, C9 vs. C8) evoke more similar activation patterns (i.e. smaller Euclidian distances in Fig. 3) than odour pairs with shorter carbon chain length (C6 vs. C7, C7 vs. C6). This more pronounced similarity is also visible in single recordings, as for example that shown in Fig. 1E, where a distinct change in the glomerular activity map can be seen between e.g. C7 and C8 odorants, but not between C6 and C7 or C8 and C9 molecules.

Odorants' functional group also played a role in similarity relationships, although these effects are less easily visible in the matrix. Usually, for two odorants within the same functional group, a high similarity was found for odorants with one or less carbon atoms, an effect, which was less pronounced, when comparing odorants from two different functional groups (compare values for odourant pairs close to the main diagonal of the matrix with similar values in other parts of the matrix). In addition, some pairs of functional groups showed higher similarity than others, as most primary and secondary alcohols showed a high similarity (low distance).

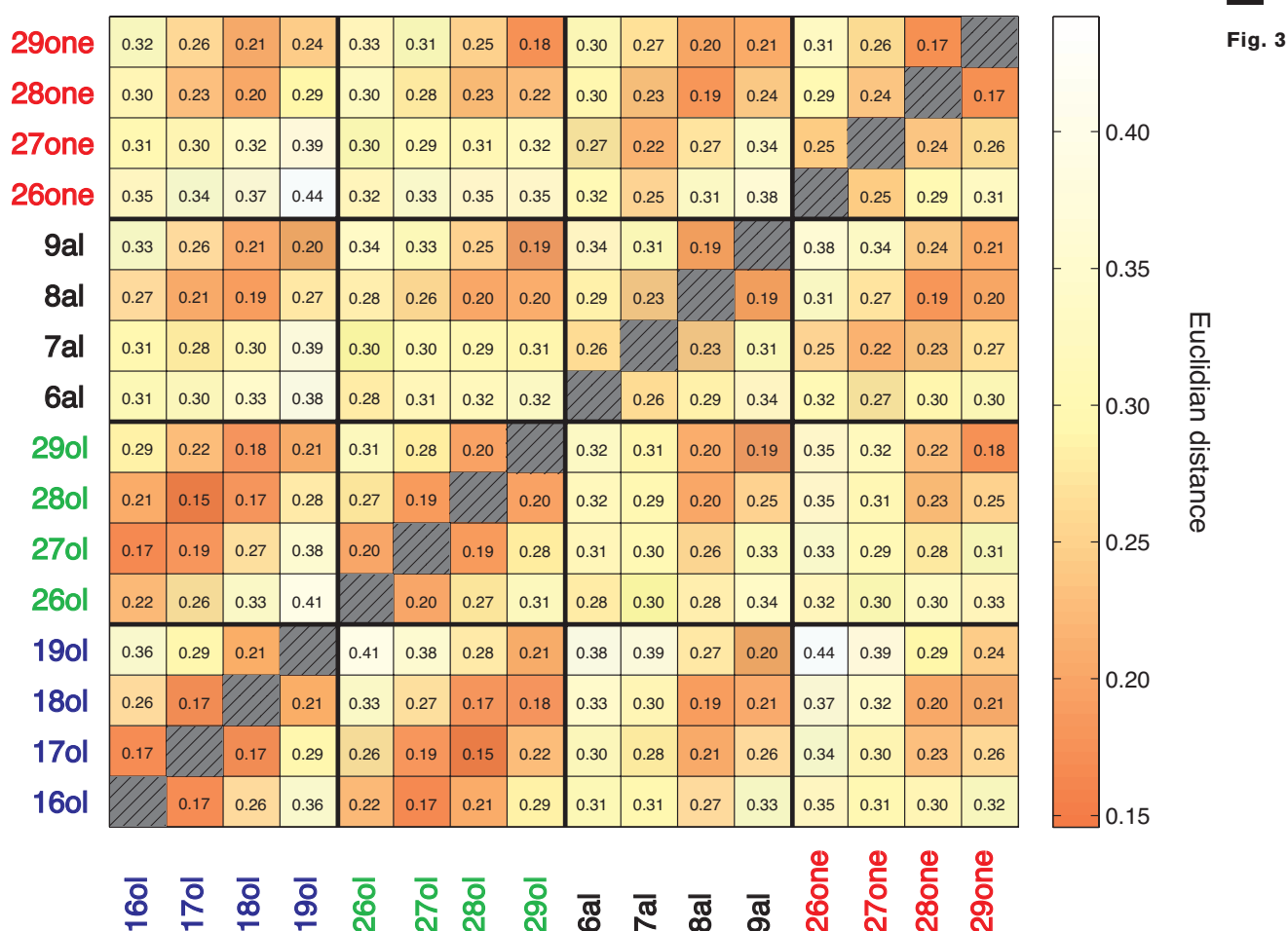


Fig. 3. Odour quality coding: similarity relationships between odour response maps.

Similarity among the 16 odourants is represented in a false-colour matrix, containing the Euclidean distances between the 120 odourant pairs recorded at the level of I-APT projection neurons. Higher similarity (shorter distances, D_{\min}) is represented in red, while lower similarity (longer distances, D_{\max}) is shown in lighter colours. Distances between same odours are represented by the hatched areas and would correspond to a distance of 0.

The matrix shows significantly smaller distances between odour pairs with carbon chain length C8 and C9 (e.g. 8al vs. 29one or 9al vs. 8ol) compared to the corresponding odour pair combinations within shorter chain lengths, i.e. C6 and C7. Short Euclidean distances are also found between primary and secondary alcohols (lower left side of the matrix).

We confirmed these observations by performing multidimensional analyses using these Euclidean distance measures (Fig. 4). We first performed a cluster analysis using Ward's classification method. The odourants in our stimulus set are segregated in two main clusters (Fig. 4A). The upper branch predominantly groups odourants with short carbon chain lengths (C6 and C7). Within this branch, odourants are grouped according to their functional groups, with primary and secondary alcohols in one subgroup (-OH function) and aldehydes and ketones in the other (=O function). The lower branch exclusively contains odours with larger carbon chain lengths (C8 and C9). Within this

branch, the odours are widely distributed independently of their functional group, with only the two long-chain ketones grouped in a separate branchlet of the dendrogram. This suggests, as can be seen from the matrix (Fig. 3) as well as from individual recordings (Fig. 1E), that long-chain molecules evoke highly similar activity patterns, which are less dependent on the functional group than shorter-chain molecules.

We next performed a proximity analysis (multidimensional scaling) on the basis of the Euclidian distances we obtained to attempt to understand the most meaningful dimensions that underlie these similarity relationships among odorants. The first three dimensions explain about 2/3 of overall variance (dimension 1: 34 %; dimension 2: 22.5 %; dimension 3: 9.7 %). Dimension 1 mostly provides information about odorants' carbon chain length, as dimension 1 coordinates increase monotonically with decreasing carbon chain length for all functional groups. Dimension 2 contains both functional group and chain length information. Primary and secondary alcohols are not separated from each other, but they are separated from both ketones and aldehydes. Aldehydes are basically separated from other groups, except for heptanal which deviated from other aldehydes. Dimension 2 also contains carbon chain length information for primary and secondary alcohols, as coordinates increase with increasing carbon chain length. Lastly, dimension 3 clearly separates ketones from aldehydes, with primary and secondary alcohols falling in between. To summarize, the proximity analysis generated three main dimensions, which first represents odorants chain length, then functional group information, distinguishing alcohols, ketones and aldehydes from each other.

The observations made on the distance matrix (Fig. 3) and the multidimensional analyses (Fig. 4) are supported by statistical analyses. First, odour-specific coding is demonstrated by the fact that odour response maps for presentations of the same odour are more similar (show smaller Euclidian distances) than odour response maps for presentations of two different odorants (Fig. 5A; (Wilcoxon matched pairs test same vs. different odour : $Z = 3.30$, $p < 0.001$). Second, odorants with the same functional group induced significantly more similar odour response maps compared to odorants with different functional groups (Wilcoxon matched pairs test same vs. different funct. group: $Z = 3.30$, $p < 0.001$; Fig. 5B). Lastly, odorants with the same carbon chain length induce more similar response maps than odorants with different carbon chain lengths (Wilcoxon matched pairs test same vs. different chain length: $Z = 3.30$, $p < 0.001$; Fig. 5C). This effect increases with the difference in the number of carbon atoms between the odorant molecules. In Fig 5D, the Euclidean distance between any two odorants is represented as a function of the difference in their numbers of carbon atoms. The difference between odour maps is stronger when they differ by at least 2 carbons, i.e. C6 vs. C8 or C6 vs. C9. These analyses thus demonstrate that odour coding in the bumblebee antennal lobe relies on odorants' chain length and functional group.

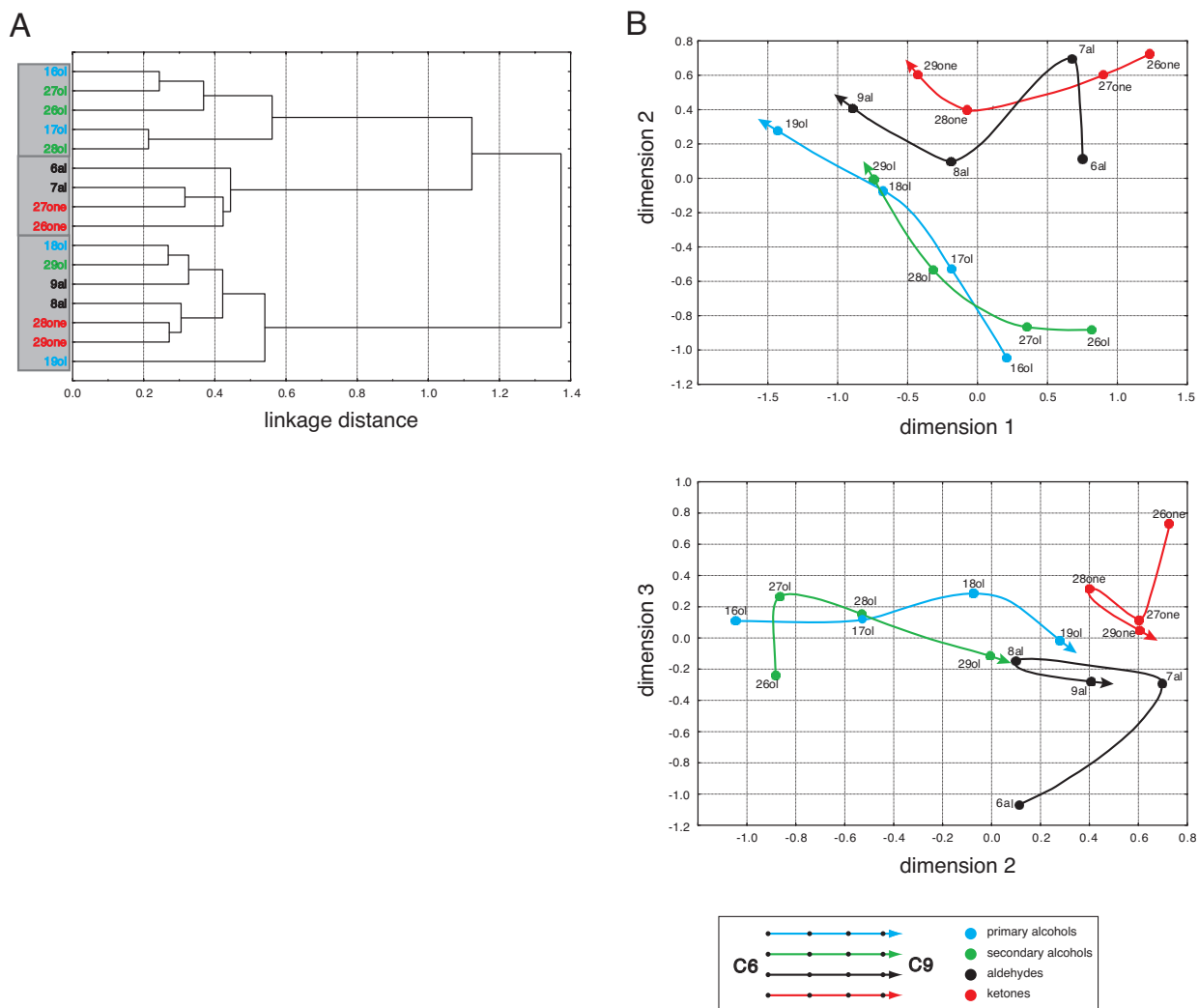


Fig. 4. Odour quality coding: cluster and proximity analyses.

A: Cluster analysis showing similarity relationships among odorants at the level of I-APT projection neurons ($n=14$; Ward's classification method). Short linkage distance between branches indicates odorants with similar response maps. The four different functional groups are shown in colour: primary alcohols in blue, secondary alcohols in green, aldehydes in black, and ketones in red. The dendrogram clearly shows a separation between odorants with short and long carbon chain lengths. Odorants with a short carbon chain are subdivided into alcohols (primary and secondary) and ketones/aldehydes, while longer carbon chain molecules are not further subdivided.

B: Proximity analysis using Euclidean distances obtained for the 120 odorant pairs. The first dimension (upper plot) explains 34% of overall variance and generally orders molecules according to their chain length from short (on the right) to long (on the left). The second dimension explains 22.5% of variance and quite distinctly separates alcohols (blue, green) from ketones (red) and aldehydes (black). The third dimension (lower plot) explains 9.7% of variance and separates aldehydes (black) from ketones (red), with alcohols in between. Thus, odorants' chain length as well as functional group represent main dimensions of odour-induced activity in I-APT projection neurons.

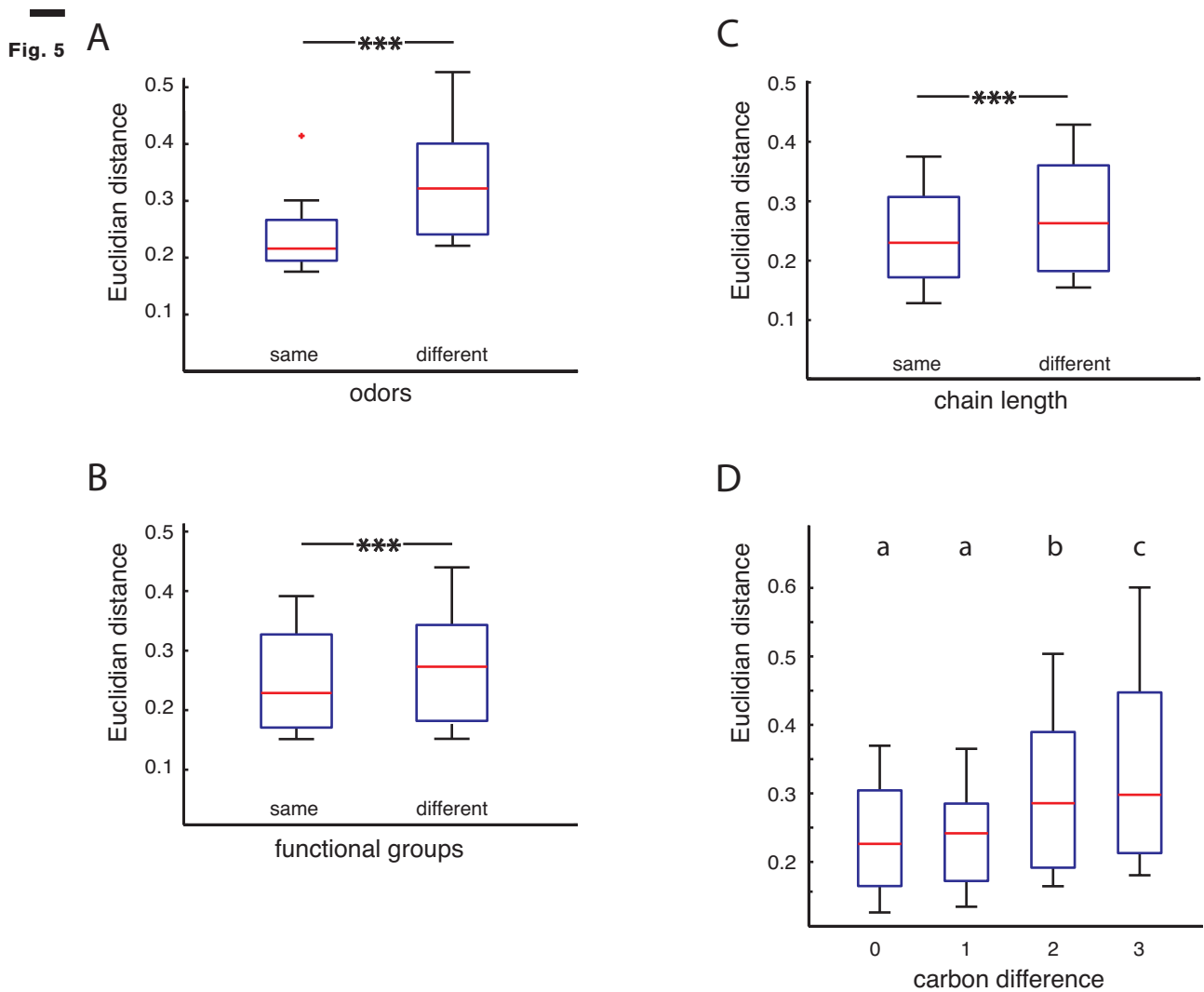


Fig. 5. Odour quality coding in I-APT projection neurons.

Similarity depending on functional group or carbon chain length.

A: Similarity between presentations of the same or of different odorants. Activity maps are more similar when the same odorant is presented, showing specific odour coding in I-APT projection neurons (Wilcoxon matched pairs test: $p < 0.001$).

B: Similarity between odorants with the same or different functional groups. Odorants with the same functional group induce more similar glomerular activity patterns than odorants with different functional groups ($p < 0.001$).

C: Similarity between odorants with the same or different carbon chain lengths. Odorants with the same chain length induce more similar glomerular activity patterns than odorants with different chain lengths ($p < 0.001$).

D: Similarity between odorants depending on the difference in their number of carbon atoms. Euclidean distances increase (i.e. response maps are more dissimilar) with increasing difference in the number of carbons (ANOVA, with tukey HSD post-hoc tests).

Comparison of honeybee and bumblebee data

The results we have described so far for bumblebees are generally very similar to the data obtained when imaging the homologous region of the honeybee antennal lobe (Sachse et al. 1999; Carcaud et al., 2012), although with a staining technique emphasizing ORN activity (bath applied Ca-Green). More recent experiments (Carcaud et al. in prep) imaged I-APT projection neuron activity evoked by the same odorants under

the same experimental conditions as in the current study. Although these data will be presented in a separate account, we took advantage of these joint studies to assess the similarity of odour coding in bumblebees and honeybees.

We thus performed a linear regression analysis between response intensity and similarity measures in bumblebees and honeybees (Fig. 6). Response intensities measured for the 16 odourants were highly correlated ($R^2 = 0.57$; $p < 0.001$) showing that odourants inducing strong responses in bumblebees also induced strong activity in honeybees. Similarly, Euclidian distances between odour response maps for the 120 odour pairs were also strongly correlated between honeybees and bumblebees ($R^2 = 0.55$; $p < 0.001$) indicating that odours inducing similar activity patterns in the honeybee AL also induce similar activity patterns in the bumblebee AL.

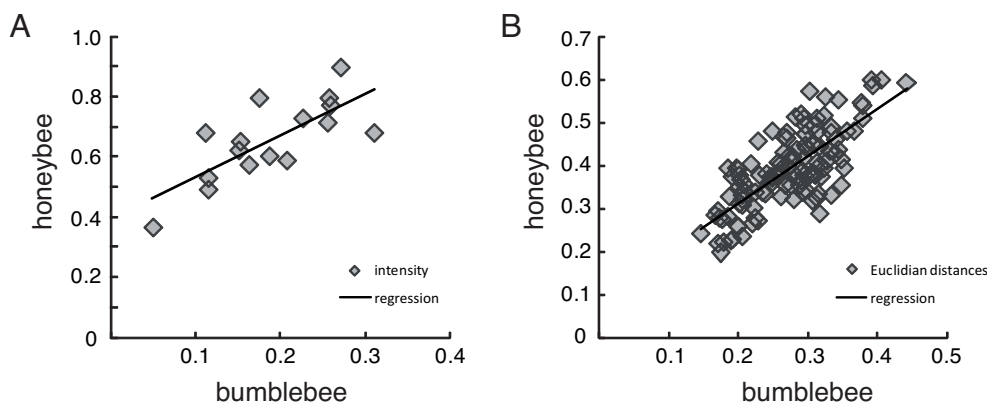


Fig. 6

Fig. 6. Correlation between bumblebee and honeybee neuronal activity measures in the I-system of the antennal lobe.

A: Correlation between bumblebee ($n = 14$) and honeybee ($n = 10$) measures of response intensity for each of the 16 presented odours, corresponding to the increase in antennal lobe neural activity upon olfactory stimulation. A high and significant correlation is observed ($R^2 = 0.57$; $p < 0.001$).

B: Correlation of Euclidian distances between odour response maps for the 120 odour pairs (see also Fig. 3) obtained in bumblebees and honeybees. A high and significant correlation is also observed ($R^2 = 0.55$; $p < 0.001$) Honeybee data from Carcaud et al., (in preparation).

We have seen that odour responses are quite similar between honeybees and bumblebees, both in terms of intensity and similarity relationships. As the number of glomeruli in the bumblebee AL (see Fig. 1) is certainly not identical to a honeybee AL, it is meaningful to ask to what extent the characteristic distribution of glomeruli as described for honeybees (Galizia et al., 1999) is conserved in the bumblebee brain.

DISCUSSION

This study shows that the bumblebee is a suitable model organism for studying olfactory coding and processing using optical imaging. Neuroanatomical staining and 3D reconstructions indicated that the structure of the bumblebee antennal lobe greatly resembles that of the honeybee. We retrogradely stained the ventral glomeruli of the bumblebee AL via the lateral projection neuron pathway (I-APT), which is a common pathway in all Hymenoptera (Rössler and Zube, 2011). Using *in vivo* optical recordings, we demonstrate that a panel of 16 aliphatic odorants evokes consistent neuronal activity in the glomeruli of the bumblebee antennal lobe. Each odorant evokes a different glomerular activity pattern, which depends both on the molecules' carbon chain length and functional group. These chemical features are strong encoding dimensions as shown by proximity analyses. These findings are in accordance with previous data on honeybees, underlining the close relationship of these two Apinae species, which evolved separately since about 70–90 million years.

Body size differences within bumblebees and comparison to honeybees

In contrast to honeybee workers, whose intraspecific size variance is quite low, there are considerable anatomical and behavioural differences between small and large workers within single bumblebee colonies (Mares et al., 2005). On the one hand, these differences influence the behaviour of the bumblebees as small bumblebees rather remain within the hive and care for the brood, whereas the largest bumblebee workers forage more frequently outside of the colony. This size-dependent division of labour is organised as a continuum, so that medium-sized workers care for the brood or manage the temperature of the colony, but also go out foraging (Goulson, 2010). Additionally, body size also influences brain anatomy. Mares and colleagues (Mares et al., 2005) found for instance that the central body and the mushroom body lobes of larger bumblebees are smaller (relative to the whole brain volume) than in smaller workers. However, in both honeybees and bumblebees, brain volumes are correlated to body weight and body size. But the size of the antennal lobes is not correlated to the body size in both species. Although these size dependent differences do not seem to influence antennal lobe size, we particularly chose medium-sized bumblebee for the experiments to minimize size-dependent effects for our study.

Earlier findings point to a body size dependent variation in the number of olfactory sensilla that affected the animals' individual odour sensitivity (Fonta and Masson, 1987; Spaethe et al., 2007), which was a further reason to restrict in our experiments the body size variation to a minimum.

Antennal lobe morphology

Morphologically, the bumblebee AL is similar to that of the honeybee (Flanagan and Mercer, 1989; Galizia et al., 1999). Both consist of a single layer of glomeruli around

an inner coarse neuropil characterized by the presence of numerous local interneurons and projection neurons (see Fig. 1). Restricted innervation of the glomerular cortex by olfactory receptor neurons (ORN) is also similar to that in the honeybee (except for a few most dorsal glomeruli in both species), AL glomeruli are innervated by four ORN tracts (Fig. 1A), which reside at very similar positions in both species (Kirschner et al., 2006). The most prominent T1 tract innervates a large proportion of glomeruli on the ventral surface of the AL (Fig. 1B), which are directly accessible when opening the brain capsule. As in honeybees, these glomeruli could be stained retrogradely by placing dye crystals on the I-APT tract of projection neurons. We are thus confident that the group of glomeruli that we imaged in bumblebees is structurally homologous to the glomeruli usually imaged in honeybees with the ventral preparation (Joerges et al., 1997; Sachse et al., 1999; Sachse and Galizia, 2002).

The number of glomeruli that we found for bumblebees in our sample reconstructions ($n = 153\text{--}162$) was however slightly lower than the typical number of glomeruli found in honeybees ($\sim 160\text{--}165$; Flanagan and Mercer, 1989; Galizia et al., 1999). As only medium-sized bumblebees were examined here, one possibility is that smaller bumblebees also have a lower number of glomeruli than larger ones. This possibility arises from the observation that the number of olfactory sensilla on the antenna was shown to increase with body size in bumblebees (Spaethe et al., 2007). Thus, larger workers may have a glomerulus number in the range of the honeybee's AL (Flanagan and Mercer, 1989; Galizia et al., 1999). Future work should specifically address possible differences among differently-sized bumblebee workers. Whatever the case, the numbers of glomeruli were only slightly lower in bumblebees compared to honeybees. This leads to the question, whether glomeruli that can be identified in the honeybee can be found in the bumblebee at similar positions.

Currently, it is assumed that each ORN expresses one type of odour-specific receptor, while all ORNs carrying the same receptor project to the same glomerulus in the AL (Vosshall et al., 2000). This hypothesis is especially appealing as in honeybees the number of olfactory receptor genes largely coincides with the number of glomeruli in the AL (163 vs. ~ 165 ; Robertson and Wanner, 2006). One may then ask, how quickly olfactory receptor genes evolve. Recent evidence in different species of the genus *Drosophila* suggests that the number of olfactory receptor genes has remained quite similar for the entire period of *Drosophila* evolution (63 million years; Tamura et al., 2004), but that frequent gains and losses of genes occurred in each evolutionary lineage (Nozawa and Nei, 2007). This may have changed the sequence of olfactory receptor neurons leading to different glomerular wiring patterns. The oldest common ancestors of honeybees and bumblebees are estimated to have lived between 70 and 90 million years ago (Michener and Grimaldi, 1988; Schultz et al., 2001; Ramírez et al., 2010). This long time of separate evolution suggests that profound changes could also have taken place in the sequence of olfactory receptor genes in both species, which may have led to a complete change of each receptor's sensitivity spectrum to odorant molecules, as well as their localization in the AL. Only a direct comparison of OR sequences between bumblebees and honeybees may reveal the amount of conservation in their OR repertoires.

Functional comparison of the glomerular activity

Despite the possible divergent evolution of OR sequences in bumblebees and honeybees, we found a high similarity of general coding principles at the neural population level. First, the intensity of odour-induced activity was similar in both species. Primary alcohols induced significantly lower activity than secondary alcohols, ketones and aldehydes. Furthermore, a chain length effect of the odorants was observed, with short chain molecules activating glomeruli more strongly than molecules with longer chain lengths (Fig. 2). All in all, this similarity of both species could be explained by the strong correlation found between glomerular activity and the vapour pressure of odorants (honeybees: Sachse et al., 1999; Carcaud et al., 2012). As a population, ORNs in both species respond gradually depending on the number of molecules in headspace.

Moreover, we found clear homologies in the similarity relationships observed between odorant molecules. The cluster analyses in bumblebees indicated a primary separation of long chain length molecules from short chain length molecules and also a branching pattern that separates the two different functional groups of alcohols from ketones and aldehydes (Fig. 4 A). This differentiation is also apparent in the multidimensional scaling analyses arranging odorants based on chain length and separating ketones, aldehydes, and alcohols. Here, primary and secondary alcohols could not be distinguished on the basis of these glomerular activity patterns (Fig. 4B). All these results are fully in agreement with previous findings in honeybees, in which I-APT glomeruli primarily classify odorants based on chain length, with functional group acting as a secondary feature (Carcaud et al., 2012).

The responses evoked by different odour stimuli that were found for bumblebees seem to be quite robust as a strong correlation between honeybee and bumblebee responses was measured (Fig. 6). This indicates a strong similarity in the antennal lobe processing mechanisms that underlie primary olfactory sensation.

Possible pheromone effects of odour stimuli

Although the odorants used in this study frequently occur in floral volatile emissions (Knudsen et al., 1993), some can also act as pheromones. For instance, honeybees produce 2-heptanone in their mandibular glands to mark flowers that have been visited recently, and this compound was also shown to affect honeybee guards (Vallet et al., 1991; Giurfa and Núñez, 1992). Interestingly, 2-heptanone induced activity in the honeybee AL that was slightly different compared to other odours of the same group or with the same or similar chain length (Sachse et al., 1999; Carcaud et al., 2012). In multidimensional analyses, it appeared slightly separated from other molecules with a closely similar chemical structure. 2-heptanone is also abundant in bumblebee colonies (Graham et al., 2012) and has been found in their mandibular gland (Cederberg, 1977). Although bumblebees are not actively placing scent marks for foraging (Wilms and Eltz, 2008; Leadbeater and Chittka, 2011), it is not reported that 2-heptanone acts as a pheromone for bumblebees meaning that the odour response should differ considerably from the response that would be expected purely from the chemical identity. At least, the recorded neural responses in this study do not indicate a different response compared to other odours of the same functional group.

However, abundant in honeybees hives, but absent in bumblebee hives is heptanal (Graham et al., 2012). This odorant was very remarkable as it was the only one from the tested 16 aliphatic odours that induced an odour response that deviated from the predicted odour response in the multidimensional scaling analysis (Fig. 4, dimension 2). Clearly, heptanal did not follow the same curve of increasing chain lengths as other aldehydes in our panel. This observation is very similar to what was observed with 2-heptanone in honeybees. It is still unknown whether heptanal serves as a pheromone in bumblebees. Only a few studies have dealt with pheromone communication in bumblebees up to now, but there is some information on pheromone blends that induce behavioural changes. It has been described that recruiting bumblebees release a pheromone that induces non-foraging workers to leave the nest in search for food (Dornhaus et al., 2003), and which was later found to be mainly Eucalyptol (Granero et al., 2005). In addition to foraging-related pheromones there exist a number of studies that focussed on sex pheromones in bumblebee males and queens (van Honk et al., 1978; Röseler et al., 1981; Krieger et al., 2006). Now that monitoring olfactory coding in the antennal lobe of bumblebees is established it would be possible to study the representation of known pheromones in the bumblebee antennal lobe.

Conclusion

This study underlines the high similarity in primary olfactory processing between bumblebees and honeybees. Nevertheless it is not clear, whether honeybees can be fully replaced by bumblebees to address research questions that have been developed on the basis of findings in honeybees. Certainly, this study shows a large amount of general similarity between those two species. However, strong similarities in morphological structures or neuronal coding mechanisms cannot automatically be attributed to an identically wired nervous system. Future studies will have to elucidate similarities in even more specific functions in the bumblebee olfactory pathway to allow equalizing the coding mechanisms in both species.

ACKNOWLEDGEMENTS

We would like to thank Antoine Couto and Manon Lefèvre-Houard for their help in the anatomical reconstruction. The study was supported by the Deutsche Forschungsgemeinschaft (DFG).

REFERENCES

- Benard J, Stach S, Giurfa M (2006) Categorization of visual stimuli in the honeybee *Apis mellifera*. *Animal cognition* 9:257–270.
- Brill MF, Rosenbaum T, Reus I, Kleineidam CJ, Nawrot MP, Rössler W (2013) Parallel processing via a dual olfactory pathway in the honeybee. *J Neurosci* 33:2443–2456.
- Carcaud J, Hill T, Giurfa M, Sandoz J-C (2012) Differential coding by two olfactory subsystems in the honeybee brain. *J Neurophys* 108:1106–1121.
- Cederberg GB (1977) Chemical basis for defense in bumblebees. *Proc 8th Int Congr I USSI* 77.
- Collett TS, Graham P, Harris RA, Hempel-de-Ibarra N (2006) Navigational memories in ants and bees: memory retrieval when selecting and following routes. In: *Advances in the Study of Behavior*, pp.123–172.
- Dornhaus a, Brockmann A, Chittka L (2003) Bumble bees alert to food with pheromone from tergal gland. *J Comp Physiol* 189:47–51.
- Flanagan D, Mercer AR (1989) An atlas and 3-D reconstruction of the antennal lobes in the worker honey bee, *Apis mellifera* L. (Hymenoptera : Apidae). *International Journal of Insect Morphology and Embryology* 18:145–159.
- Fonta C, Masson C (1985a) Organisation neuroanatomique de la voie afférente antennaire chez les Bourdons mâles et femelles (*Bombus* sp.). *Comptes rendus des séances de l'Académie des sciences Série 3, Sciences de la vie* 300:437–442.
- Fonta C, Masson C (1985b) Fonta and Masson 1985.pdf. *Comptes rendus des séances de l'Académie des sciences Série 3, Sciences de la vie* 300:437–442.
- Fonta C, Masson C (1987) Structural and functional studies of the peripheral olfactory nervous system of male and female bumble-bees (*Bombus hypnorum* and *Bombus terrestris*). *Chemical Senses* 12:53–69.
- Galizia CG, McIlwrath SL, Menzel R (1999) A digital three-dimensional atlas of the honeybee antennal lobe based on optical sections acquired by confocal microscopy. *Cell and tissue research* 295:383–394.
- Giurfa M, Núñez JA (1992) Honeybees mark with scent and reject recently visited flowers. *Oecologia* 89:113–117.

Giurfa M, Sandoz J-C (2012) Invertebrate learning and memory: Fifty years of olfactory conditioning of the proboscis extension response in honeybees. *Learning & memory* (Cold Spring Harbor, NY) 19:54–66.

Giurfa M, Zhang S, Jenett A, Menzel R, Srinivasan M V (2001) The concepts of “sameness” and “difference” in an insect. *Nature* 410:930–933.

Goulson D (2010) *Bumblebees - behaviour, ecology, and conservation*. New York: Oxford University Press.

Graham JR, Carroll MJ, Teal PE a., Ellis JD (2012) A scientific note on the comparison of airborne volatiles produced by commercial bumble bee (*Bombus impatiens*) and honey bee (*Apis mellifera*) colonies. *Apidologie* 44:110–112.

Granero AM, Sanz JMG, Gonzalez FJE, Vidal JLM, Dornhaus A, Ghani J, Serrano AR, Chittka L (2005) Chemical compounds of the foraging recruitment pheromone in bumblebees. *Die Naturwissenschaften* 92:371–374.

Guerrieri F, Schubert M, Sandoz J-C, Giurfa M (2005) Perceptual and neural olfactory similarity in honeybees. *PLoS biology* 3:e60.

Hammer M (1993) An identified neuron mediates the unconditioned stimulus in associative olfactory learning in honeybees. *Nature* 366:59–63.

Van Honk C, Velthuis H, Röseler P (1978) A sex pheromone from the mandibular glands in bumblebee queens. *Experientia* 34:838–839.

Joerges J, Küttner A, Galizia CG, Menzel R (1997) Representations of odours and odour mixtures visualized in thoneybee brain. *Nature* 387:285–288.

Kelber C, Rössler W, Kleineidam CJ (2006) Multiple olfactory receptor neurons and their axonal projections in the antennal lobe of the honeybee *Apis mellifera*. *J Comp Neurol* 496:395–405.

Kirschner S, Kleineidam CJ, Rybak R, Gru B, Zube C (2006) Dual olfactory pathway in the honeybee, *Apis mellifera*. *Comparative and General Pharmacology*:933–952.

Knudsen JT, Tollsten L, Bergström LG (1993) Floral Scents – A checklist of volatile compounds by head-space techniques. *Phytochemistry* 33:253–280.

Krieger GM, Duchateau M-J, Van Doorn A, Ibarra F, Francke W, Ayasse M (2006) Identification of queen sex pheromone components of the bumblebee *Bombus terrestris*. *Journal of chemical ecology* 32:453–471.

Laloi D, Sandoz JC, Picard-Nizou AL, Marchesi A, Pouvreau A, Tasei JN, Poppy G, Pham-delegue MH (1999) Olfactory conditioning of the proboscis extension in bumble bees. *Entomologia Experimentalis et Applicata* 90:123–129.

Leadbeater E, Chittka L (2011) Do inexperienced bumblebee foragers use scent marks as social information? *Animal cognition* 14:915–919.

Mares S, Ash L, Gronenberg W (2005) Brain allometry in bumblebee and honey bee workers. *Brain, behavior and evolution* 66:50–61.

Menzel R (2012) The honeybee as a model for understanding the basis of cognition. *Nature reviews Neurosci* 13:758–768.

Menzel R, Muller U (1996) Learning and memory in honeybees: from behavior to neural substrates. *Annual review of neuroscience* 19:379–404.

Michener CD, Grimaldi D a (1988) The oldest fossil bee: Apoid history, evolutionary stasis, and antiquity of social behavior. *Proc Natl Acad Sci* 85:6424–6426.

Morawetz L, Spaethe J (2012) Visual attention in a complex search task differs between honeybees and bumblebees. *J Exp Biol* 215:2515–2523.

Nozawa M, Nei M (2007) Evolutionary dynamics of olfactory receptor genes in *Drosophila* species. *Proc Natl Acad Sci* 104:7122–7127.

Okada R, Rybak J, Manz G, Menzel R (2007) Learning-related plasticity in PE1 and other mushroom body-extrinsic neurons in the honeybee brain. *J Neurosci* 27:11736–11747.

Pareto A (1972) Die zentrale Verteilung der Fühlerafferenz bei Arbeiterinnen der Honigbiene, *Apis mellifera* L. *Zellforschung* 131:109–140.

Paulk AC, Dacks AM, Phillips-Portillo J, Fellous J-M, Gronenberg W (2009) Visual processing in the central bee brain. *J Neurosci* 29:9987–9999.

Paulk AC, Gronenberg W (2008) Higher order visual input to the mushroom bodies in the bee, *Bombus impatiens*. *Arthropod Struct Dev* 37:443–458.

Paulk AC, Phillips-Portillo J, Dacks AM, Fellous J-M, Gronenberg W (2008) The processing of color, motion, and stimulus timing are anatomically segregated in the bumblebee brain. *J Neurosci* 28:6319–6332.

- Ramírez SR, Nieh JC, Quental TB, Roubik DW, Imperatriz-Fonseca VL, Pierce NE (2010) A molecular phylogeny of the stingless bee genus *Melipona* (Hymenoptera: Apidae). *Molecular phylogenetics and evolution* 56:519–525.
- Riveros AJ, Gronenberg W (2009a) Olfactory learning and memory in the bumblebee *Bombus occidentalis*. *Die Naturwissenschaften* 96:851–856.
- Riveros AJ, Gronenberg W (2009b) Learning from learning and memory in bumblebees. *Die Naturwissenschaften* 96:437–440.
- Robertson HM, Wanner KW (2006) The chemoreceptor superfamily in the honey bee, *Apis mellifera*: Expansion of the odorant, but not gustatory, receptor family. *Genome Research* 16:1395–1403.
- Röseler P, Röseler I, van Honk C (1981) Evidence for inhibition of corpora allata activity in workers of *Bombus terrestris* by a pheromone from the queen's mandibular glands. *Experientia* 37:348–351.
- Rössler W, Zube C (2011) Dual olfactory pathway in Hymenoptera: Evolutionary insights from comparative studies. *Arthropod structure & development* 40:349–357.
- Sachse S, Galizia CG (2002) Role of inhibition for temporal and spatial odor representation in olfactory output neurons : A calcium imaging study. *J Neurophys* 87:1106–1117.
- Sachse S, Rappert A, Galizia CG (1999) The spatial representation of chemical structures in the antennal lobe of honeybees : steps towards the olfactory code. *EJN* 11:3970–3982.
- Schultz TR., Engel MS., Aschier JS. (2001) Evidence for the origin of eusociality in the corbiculate bees (Hymenoptera : Apidae). *Journal of the Kansas Entomological Society* 74:10–16.
- Spaethe J, Brockmann A, Halbig C, Tautz J (2007) Size determines antennal sensitivity and behavioral threshold to odors in bumblebee workers. *Die Naturwissenschaften* 94:733–739.
- Suzuki H (1975) Antennal movements induced by odour and central projection of the antennal neurones in the honey-bee. *J Insect Physiol* 21:831–847.
- Tamura K, Subramanian S, Kumar S (2004) Temporal patterns of fruit fly (*Drosophila*) evolution revealed by mutation clocks. *Molecular biology and evolution* 21:36–44.
- Vallet A, Cassiert P, Lensky Y (1991) Ontogeny of the fine structure of the mandibular glands of the honeybee (*Apis Mellifera* L.) workers and the pheromonal activity of 2-Heptanone. *J Insect Physiol* 37:789–804.

Vosshall LB, Wong AM, Axel R (2000) An olfactory sensory map in the fly brain. *Cell* 102:147–159.

Wilms J, Eltz T (2008) Foraging scent marks of bumblebees: footprint cues rather than pheromone signals. *Die Naturwissenschaften* 95:149–153.

Zeil J, Boeddeker N, Stürzl W (2009) Visual homing in insects and robots. In: *Flying Insects and Robots*, pp.87–99.

ERKLÄRUNG

Ich versichere, dass ich diese Arbeit selbständig und ohne unzulässige Hilfe verfasst habe, keine anderen als die angegebenen Quellen und Hilfsmittel benutzt und Zitate kenntlich gemacht habe.

Marcel Mertes

DANKSAGUNG

Ich möchte mich zuerst bei meinen beiden Betreuern, Prof. Dr. Martin Egelhaaf und Dr. Norbert Boeddeker bedanken, die sich immer für meine Belange Zeit genommen haben und mich jederzeit unterstützt und geholfen haben meine Pläne voran zu treiben. Auf euch war immer Verlass!

Mein Dank gilt außerdem allen Kollegen des Lehrstuhls für Neurobiologie, die mir in meinen großen und kleinen Anliegen immer geholfen haben sowie durch Kommentare und Anmerkungen zur Qualität meiner Arbeit entscheidend beigetragen haben. Besonders herausheben möchte ich Daniel Kress und Dr. Laura Dittmar. Die lange Zeit, die ihr mich auf meinem Weg zum Dokortitel begleitet habt, war sehr schön für mich. Ich danke euch auch dafür, dass ihr mich bei Bedarf immer wieder eingeordnet habt und mich auch ein Stück weit zu dem Menschen habt werden lassen, der ich heute bin.

Nicht unerwähnt bleiben dürfen Dr. Jean-Christophe und Dr. Julie Carcaud, denen ich für die fruchtbare Zusammenarbeit während meines Olfaktorik-projekts am CNRS in Gif-sur-Yvette danken will. Ich wurde von euch und der gesamten Arbeitsgruppe mit offenen Armen empfangen und habe mich jederzeit sehr wohl gefühlt.

Ich möchte Sarah Scheffen danken, dass sie meine schwankenden Launen zumeist mit stoischer Ruhe ertragen hat und mir immer genügend Freiraum gewährt hat. Du hast mich jederzeit ermutigt meinen Weg zu gehen. Danke für die tägliche Unterstützung und Deine kritischen Töne zur rechten Zeit! Ich weiß, dass Du es mit mir nicht immer leicht hast und weiß daher die Zeit umso mehr zu schätzen, die Du mit mir verbringst.

Zuletzt danke ich meinen Eltern Gudrun und Ralph Mertes. Solange ich mich erinnern kann, habt ihr mir mehr gegeben als man überhaupt verlangen kann. Mir hat es nie an etwas gefehlt. Ich weiß, dass ich ohne eure Unterstützung und Fürsorge nie im Leben dort angekommen wäre, wo ich heute bin. Meine guten Eigenschaften habe ich allesamt von euch beiden mitbekommen und doch hätte ich viel weniger daraus machen können, wenn unser Zuhause nicht immer so ein Ruhepol für mich gewesen wäre. Danke für alles!